

CHAPTER III

RESULTS AND DISCUSSION

The new PNA systems in this research are designed based on a modification of the original *aeg*PNA by replacing the deoxyribose of DNA with a pyrrolidine ring. In this type of pyrrolidine derivatives bearing nucleobases at the C-4 position, there are four possible diastereomers resulting from different configurations of stereogenic centers at C-2 and C-4 namely *2R,4R* (*cis*-D), *2R,4S* (*trans*-D), *2S,4R* (*trans*-L) and *2S,4S* (*cis*-L) isomers. The phosphate group of DNA was replaced by β -amino acid spacers which may be categorized into 3 groups, namely 1) acyclic β -amino acid, 2) cyclic β -amino acid with one chiral center and 3) cyclic β -amino acid with two chiral centers.

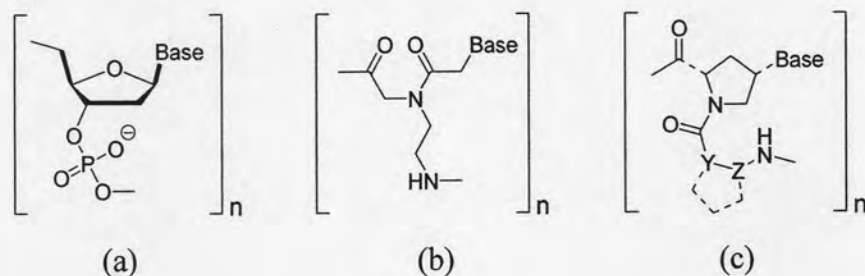


Figure 3.1 Core structures of (a) DNA (b) Nielsen's *aeg*PNA and (c) pyrrolidine-PNA with β -amino acid spacer.

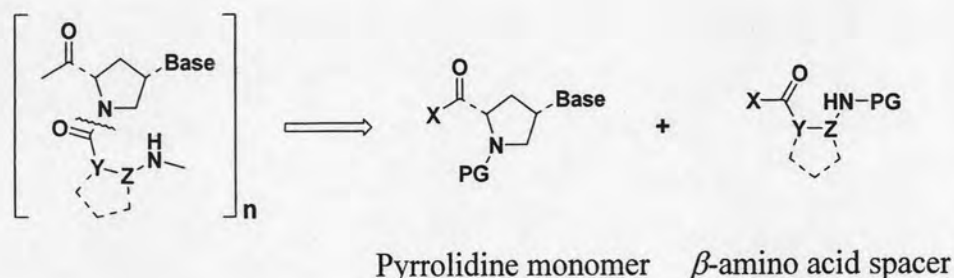
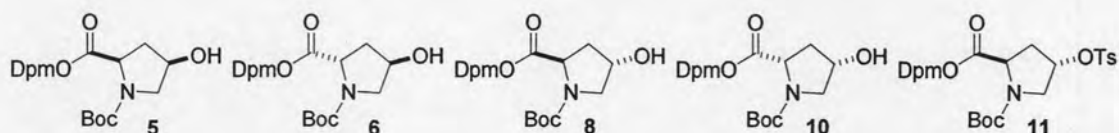


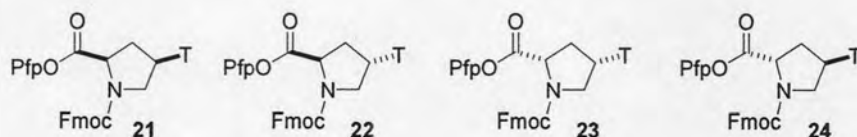
Figure 3.2 Retrosynthetic analyses for synthesis of PNA.

Synthesis of all four diastereomers of thymine pyrrolidinyll monomers started from the same set of intermediates (**Section 3.1.1**) whereby thymine was attached in a stereocontrolled fashion (**Section 3.1.2**). For other bases (adenine, cytosine and guanine) only the pyrrolidinyll monomers with *cis*-D configuration which are identical to natural DNA were studied (**Section 3.1.3**). Details of the synthesis will be described in the details in the next topic.

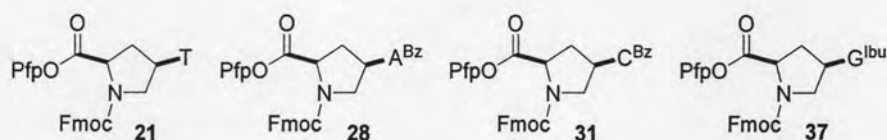
Section 3.1.1 Synthesis of Intermediates



Section 3.1.2 Synthesis of all four diastereomers of thymine pyrrolidinyll monomers

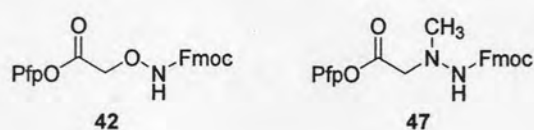


Section 3.1.3 Synthesis of *cis*-D pyrrolidinyll monomers with bases A, C and G

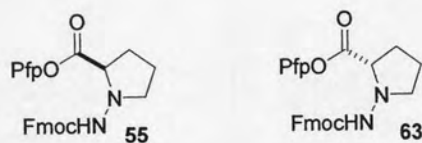


β -Amino acid spacers selected as spacers based on their high potential to pre-organize into well-defined and easily folded to secondary structure [35-39]. Synthesis of these β -amino acid spacers will be described in **Section 3.2.1**, **3.2.2** and **3.2.3**.

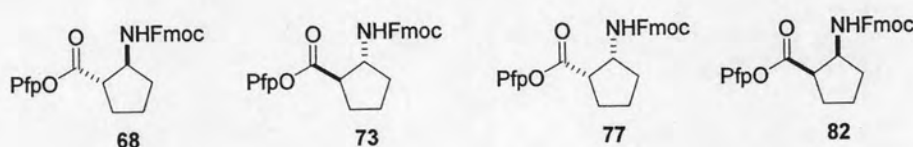
Section 3.2.1 Synthesis of acyclic β -amino acid spacers



Section 3.2.2 Synthesis of cyclic β -amino acid spacers containing one stereogenic center



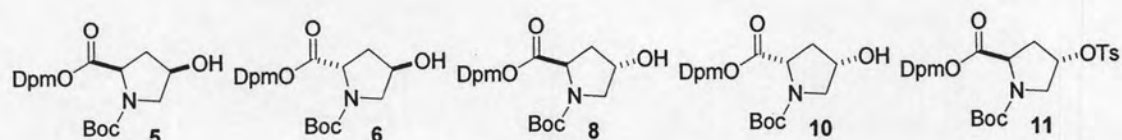
Section 3.2.3 Synthesis of cyclic β -amino acid spacers containing two stereogenic centers



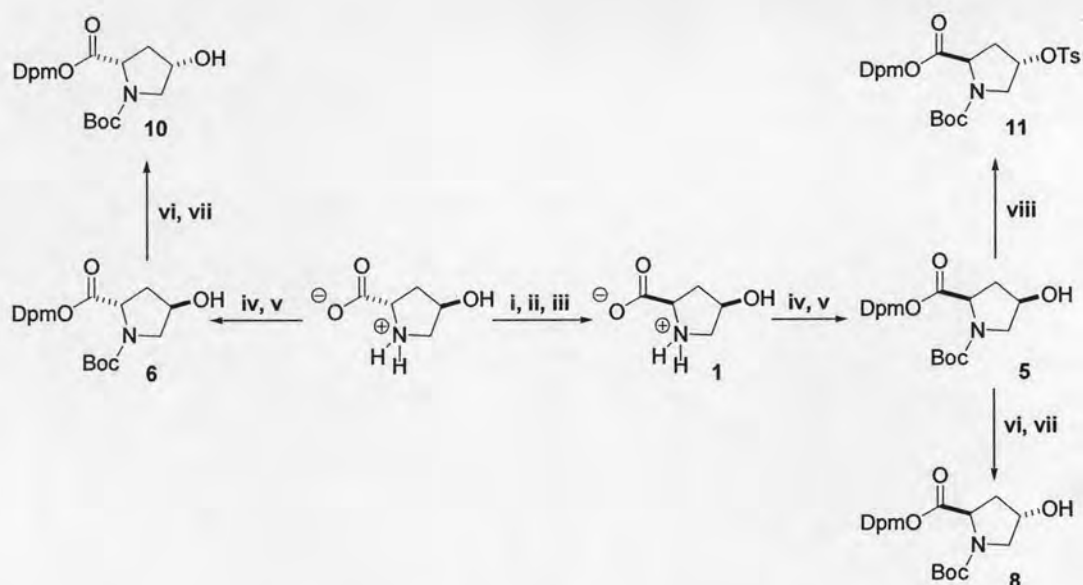
Syntheses of all pyrrolidine monomers and β -amino acid spacers will be discussed in details below. Then oligomerization of these monomers on solid phase will be discussed. The last topic involves biophysical studies of interaction between the PNA and DNA.

3.1 Synthesis of pyrrolidinyl monomers

3.1.1 Synthesis of intermediates



The Boc-protected monomers **5**, **6**, **8**, **10** and **11** reported earlier by Vilaivan *et al.* [80] (**Figure 3.3**) were the starting points for the synthesis of all pyrrolidine monomers.



Reagents and conditions: i. Ac_2O , heat 90°C 16 h; ii. 2 M HCl, reflux 5 h; iii. propylene oxide, MeOH; iv. Boc_2O , $t\text{BuOH}$, NaOH (aq), 8 h; v. Ph_2CN_2 , EtOAc, 8 h; vi. HCO_2H , Ph_3P , DIAD, THF, 8 h; vii. NH_3 , MeOH, 2 h; viii. MeOTs, Ph_3P , DIAD, THF, 8 h.

Figure 3.3 A synthetic scheme for the intermediate proline derivative 5, 6, 8, 10 and 11 according to Vilaivan *et al.*

The literature method to synthesize compounds 5, 6, 8, 10 and 11 were adopted essentially without modifications. Syntheses of the *trans*-L and *cis*-L thymine pyrrolidinyll monomers started from the commercially available *trans*-4-hydroxy-L-proline. Syntheses of the *cis*-D and *trans*-D thymine pyrrolidinyll monomers required *cis*-4-hydroxy-D-proline. This compound was easily prepared by epimerization at α -position of *trans*-4-hydroxy-L-proline using acetic anhydride in reflux condition followed by hydrolysis to give a 2:1 ratio mixture of *cis*-D and *trans*-L hydroxy proline hydrochloride salt [99]. The resulting mixture of hydroxyproline epimers were separated by fractional recrystallization [100]. However the hydrochloride salt was more difficult to precipitate than the free amino acid, therefore the hydrochloride salt was converted to the free amino acid by stirring the crude mixed amino acid containing both epimers with propylene oxide and methanol to afford a mixture of free hydroxyprolines as a brown solid. The 2-chloro-1-propanol by-product can be removed easily by filtration and washing (**Figure 3.4**). This method of HCl removal

provided better recovery of the free amino acid was simpler to operate compared to the earlier method which used Et_3N to neutralize the HCl [101].

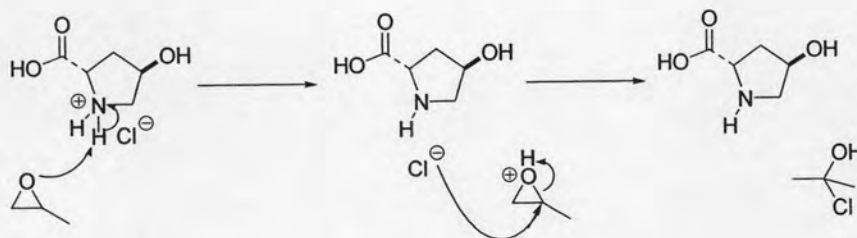


Figure 3.4 Removal hydrochloride salt from hydroxy proline with propylene oxide in methanol.

The crude mixture of *cis*-D and *trans*-L isomer was recrystallized from methanol-water to give the pure *cis*-D epimer as colorless needles up to 64 % from starting material. The ^1H NMR spectra of the *cis*-D and *trans*-L forms are quite different hence both can be distinguished by NMR as shown in **Figure 3.5**.

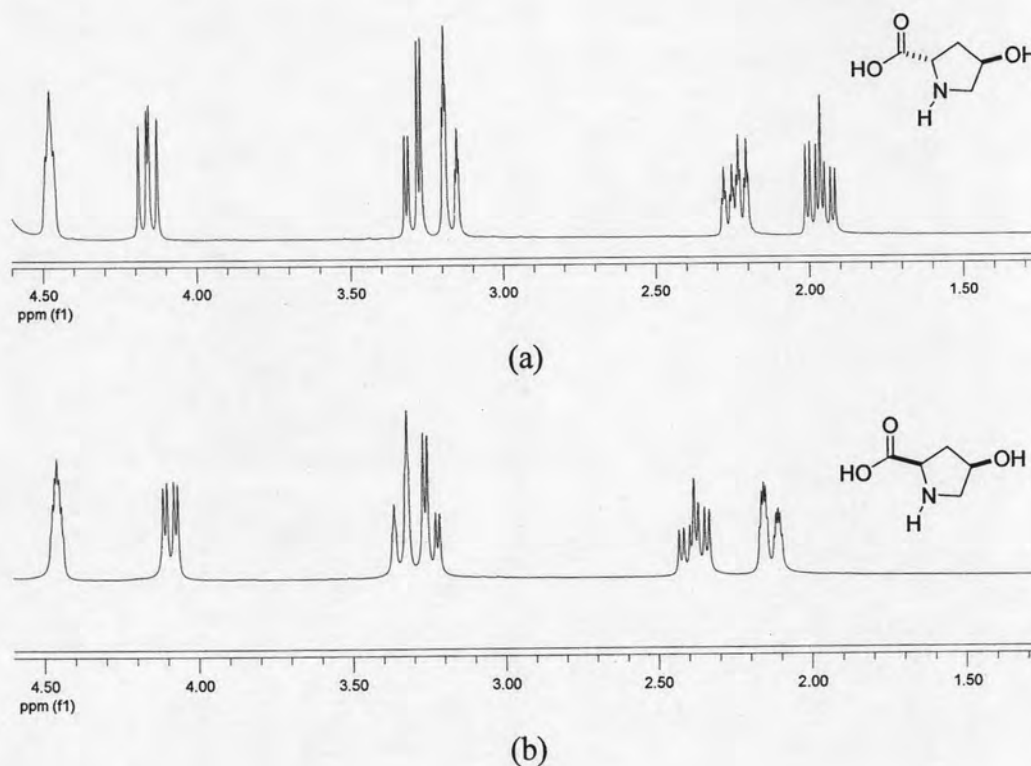


Figure 3.5 Comparison of ^1H NMR spectra (D_2O , 400 MHz) between (a) *trans*-4-hydroxy-L-proline and (b) *cis*-4-hydroxy-D-proline

The mechanism of epimerization from *trans*-L to *cis*-D proceeded via enolization at the α -carbon of the mixed anhydride intermediate as shown in **Figure 3.6**. According to the literature [78], the presence of an *N*-acyl group allowed facile formation of an intermediate bicyclic mesoionic compound (**3.6a**). Finally, the lactone intermediate (**3.6b**) decomposed through a mixed anhydride intermediate (**3.6c**) deriving from the intermolecular attack of the acetate anion on the carbonyl group.

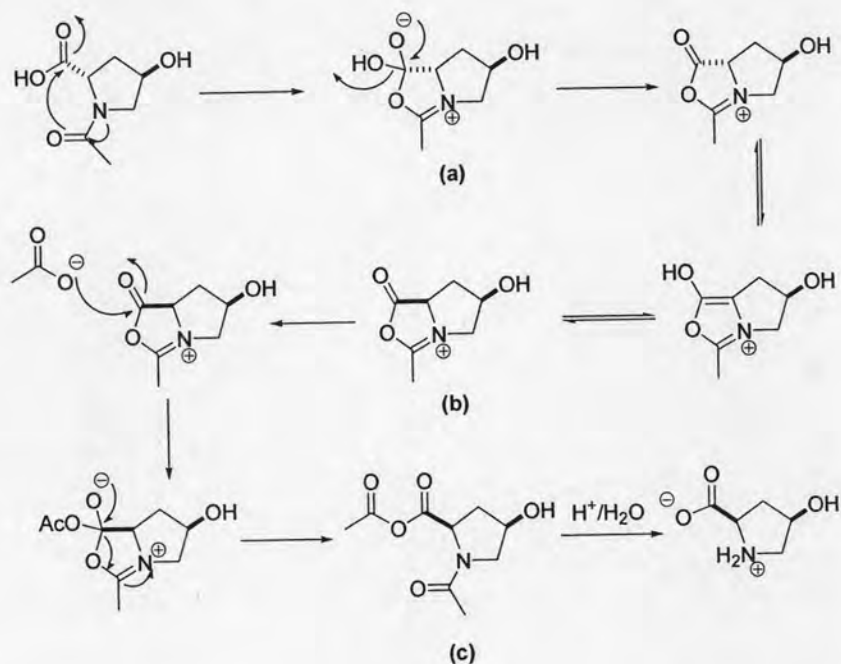


Figure 3.6 Epimerization from *trans*-4-hydroxy-L-proline to *cis*-4-hydroxy-D-proline via enolization mechanism

After the *cis*-4-hydroxy-D-proline was obtained, the reactive amino and carboxylic groups of the compound were protected in order to avoid undesired side reactions during subsequent nucleophilic displacement steps to attach the thymine or other nucleobases. The acid labile but nucleophilically stable *tert*-butoxycarbonyl (Boc) group and diphenylmethyl (Dpm) group were chosen as the protecting groups for the amino and carboxylic groups respectively. The reaction between *cis*-4-hydroxy-D-proline (**1**) and di-*tert*-butyl dicarbonate (Boc_2O) in aqueous sodium hydroxide/*tert*-butanol gave *N*-*tert*-butoxycarbonyl-*cis*-4-hydroxy-D-proline sodium salt, carbon dioxide and *tert*-butanol as by-products. The crude reaction was worked up by acidification followed by extraction and evaporation to afford the desired

product *N*-*tert*-butoxycarbonyl-*cis*-4-hydroxy-D-proline as a mixture of rotamers (2). The structure of which was confirmed by ^1H NMR [101].

For protection of the carboxyl group, diphenylmethyl (Dpm) protecting group was chosen according to previous experiences in this group [79]. The crystalline Boc/Dpm protected intermediate 5 was synthesized from *N*-*tert*-butoxycarbonyl-*cis*-4-hydroxy-D-proline (2) by treatment with diphenyldiazomethane (4) which provided the desired product, *N*-*tert*-butoxycarbonyl-*cis*-4-hydroxy-D-proline diphenylmethyl ester (5), in good yield (90%) together with nitrogen gas as the only by-product (Figure 3.7). The diphenyldiazomethane was freshly prepared by oxidation of benzophenone hydrazone with yellow mercury (II) oxide in the presence of ethanolic potassium hydroxide as catalyst [83]. Because diphenyldiazomethane might decompose under photolytic and thermal conditions, light and heat must be avoided and the product must be used immediately. The crude protected hydroxyproline (5) was easily obtained as white crystalline solid by trituration with hexanes.

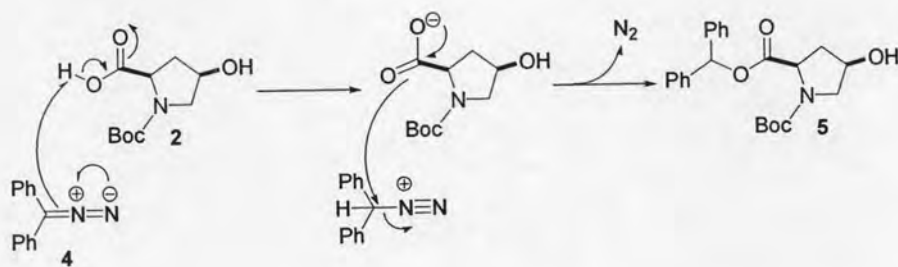


Figure 3.7 The reaction mechanism of protecting the carbonyl group by diphenyl diazomethane.

The use of a new protecting group at carboxylic end had also been attempted. Benzyl group was chosen to be alternative of acid stable protecting group due to its simple preparation. The reaction of protected Boc hydroxyproline (2) with benzyl bromide and K_2CO_3 in DMF, afforded two products in equal amounts which were identified as *mono*-substituted and *di*-substituted benzylated products. The maximum reaction yield was only 52 %, therefore Dpm group appeared to be the better choice for carboxyl protection.

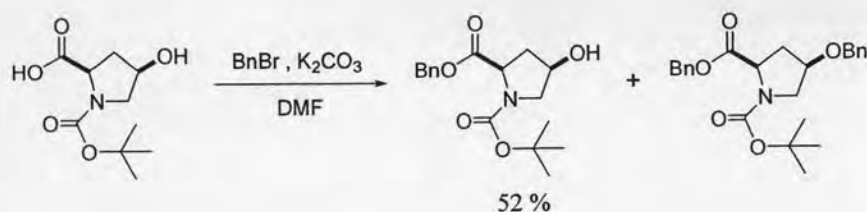


Figure 3.8 The reaction of protecting the carbonyl group by benzyl group.

Protection of *trans*-4-hydroxy-L-proline at the amino group by Boc and carboxyl group by Dpm has also been performed using the same method described for *cis*-4-hydroxy-D-proline above to give the intermediate *N*-*tert*-butoxycarbonyl-*trans*-4-hydroxy-L-proline diphenylmethyl ester (**6**). *N*-*tert*-Butoxycarbonyl-*trans*-4-hydroxy-D-proline diphenylmethyl ester (**8**) and *N*-*tert*-Butoxycarbonyl-*cis*-4-hydroxy-L-proline diphenylmethyl ester (**10**) were also synthesized in the same way by inverting the configuration of the OH group at the C-4 position of the protected Boc/Dpm *cis*-D (**5**) and the protected Boc/Dpm *trans*-L (**6**) respectively. These were accomplished by using the Mitsunobu reaction under the conditions shown in **Figure 3.9**. The protected hydroxyprolines were first reacted with formic acid to give formate esters with inverted configurations by Mitsunobu reaction. After ammonolysis of the formate esters, the protected Boc/Dpm *trans*-D (**8**) and *cis*-L (**10**) hydroxyprolines were obtained. The mechanism involves activation of the hydroxyl group at C-4 position of compound (**5**) by PPh₃-DIAD complex to give an alkoxyphosphonium compound. Subsequent S_N² attack of the alkoxy phosphonium salt by the formate anion gave the compound *N*-*tert*-butoxycarbonyl-*trans*-4-formyloxy-D-proline diphenylmethyl ester (**7**) and by products (triphenylphosphine oxide and diisopropyl hydrazinedicarboxylate) which were separated by column chromatography to give (**7**) as the desired product (**Figure 3.9**). Ammonolysis of this compound afforded the hydroxy compound **8** with the inverted C4-OH group compared to compound **5**.

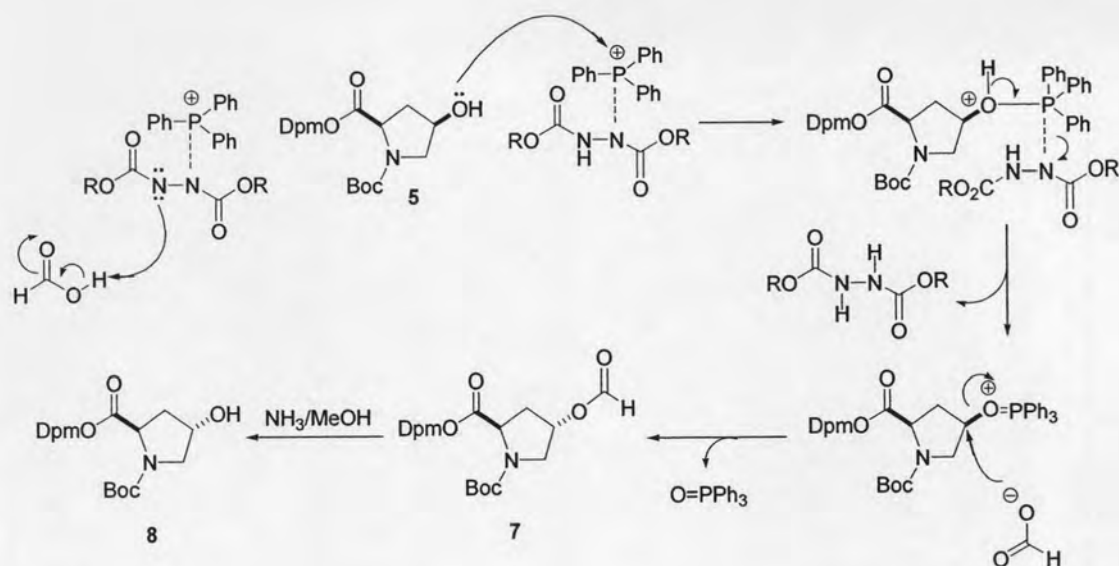
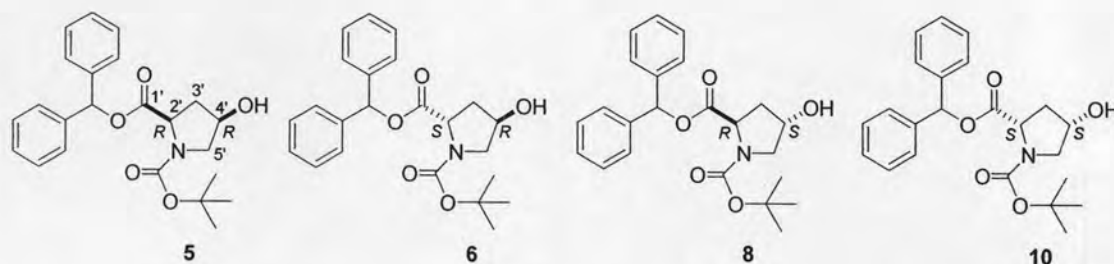


Figure 3.9 Mitsunobu reaction of *N*-*tert*-butoxycarbonyl-*cis*-4-hydroxy-D-proline diphenylmethyl ester (5) to form *N*-*tert*-butoxycarbonyl-*trans*-4-formyl-D-proline diphenylmethyl ester (7) and its hydrolysis to *N*-*tert*-butoxycarbonyl-*trans*-4-hydroxy-D-proline diphenylmethyl ester (8)

The structure of the intermediate compound 5, 6, 8 and 10 were confirmed by ¹H NMR, ¹³C NMR and also optical rotation as shown in **Table 3.1**.

It should be noted that compounds 5 and 10 are enantiomers pair, as well as compounds 6 and 8, therefore they should have identical ¹H and ¹³C NMR spectra to each others. On the other hand, compound 5 and 6 with compound 8 and 10 are diastereomers and therefore their NMR are slightly different. For example, CH(2') of pyrrolidine ring for *cis*-D and *cis*-L show double doublet at 4.34, 4.40 ppm and 4.45, 4.57 respectively, while CH(2') of pyrrolidine ring for *trans*-D and *trans*-L show double triplet at 4.56, 4.63 ppm and 4.56, 4.63 respectively. ¹H and ¹³C NMR spectra of all four isomers were shown in **Figure 3.10**.

Table 3.1 ^1H NMR, ^{13}C NMR optical rotation and percent yield of protected monomers **5**, **6**, **8** and **10**.



Position	Chemical Shift (ppm)							
	5 (<i>cis</i> -D)		10 (<i>cis</i> -L)		6 (<i>trans</i> -L)		8 (<i>trans</i> -D)	
	^1H	^{13}C	^1H	^{13}C	^1H	^{13}C	^1H	^{13}C
1'	-	173.6	-	173.3	-	171.8	-	171.9
2'	4.34	58.0	4.45	58.1	4.56	57.8	4.56	57.9
	4.40		4.57		4.63		4.63	
3'	1.98	37.7	2.09	37.7	2.06	38.2	2.03	38.2
	2.24		2.28		2.31		2.25	
4'	4.24	70.0	4.35	69.9	4.48	69.3	4.44	69.2
5'	3.51	55.3	3.64	55.2	3.63	54.6	3.62	54.7
$\underline{\text{CO}}$ Boc	-	153.8	-	153.8	-	154.1	-	154.2
$\underline{\text{CCH}_3}$ Boc	-	77.9	-	77.9	-	80.2	-	80.6
CH_3 Boc	1.17	28.4	1.27	28.0	1.25	28.0	1.25	28.1
	1.39		1.49		1.48		1.48	
$\underline{\text{CH}}$ Dpm	6.81	80.3	6.91	80.2	6.91	80.5	6.91	77.2
	6.88		6.99		6.96		6.96	
Ph Dpm	7.25	127.0	7.36	126.9	7.35	126.7	7.35	126.9
$[\alpha]_D^{25}$ ^a	+15.0		-14.6 ^b		-49.0		+48.8	
% yield ^c	57		78		79		45	

a an optical rotation was operated in chloroform ($c=1.00$ g/100 mL).

b an optical rotation was operated in chloroform ($c=3.29$ g/100 mL).

c percent yield was calculated from starting material *trans*-4-hydroxy-L-proline.

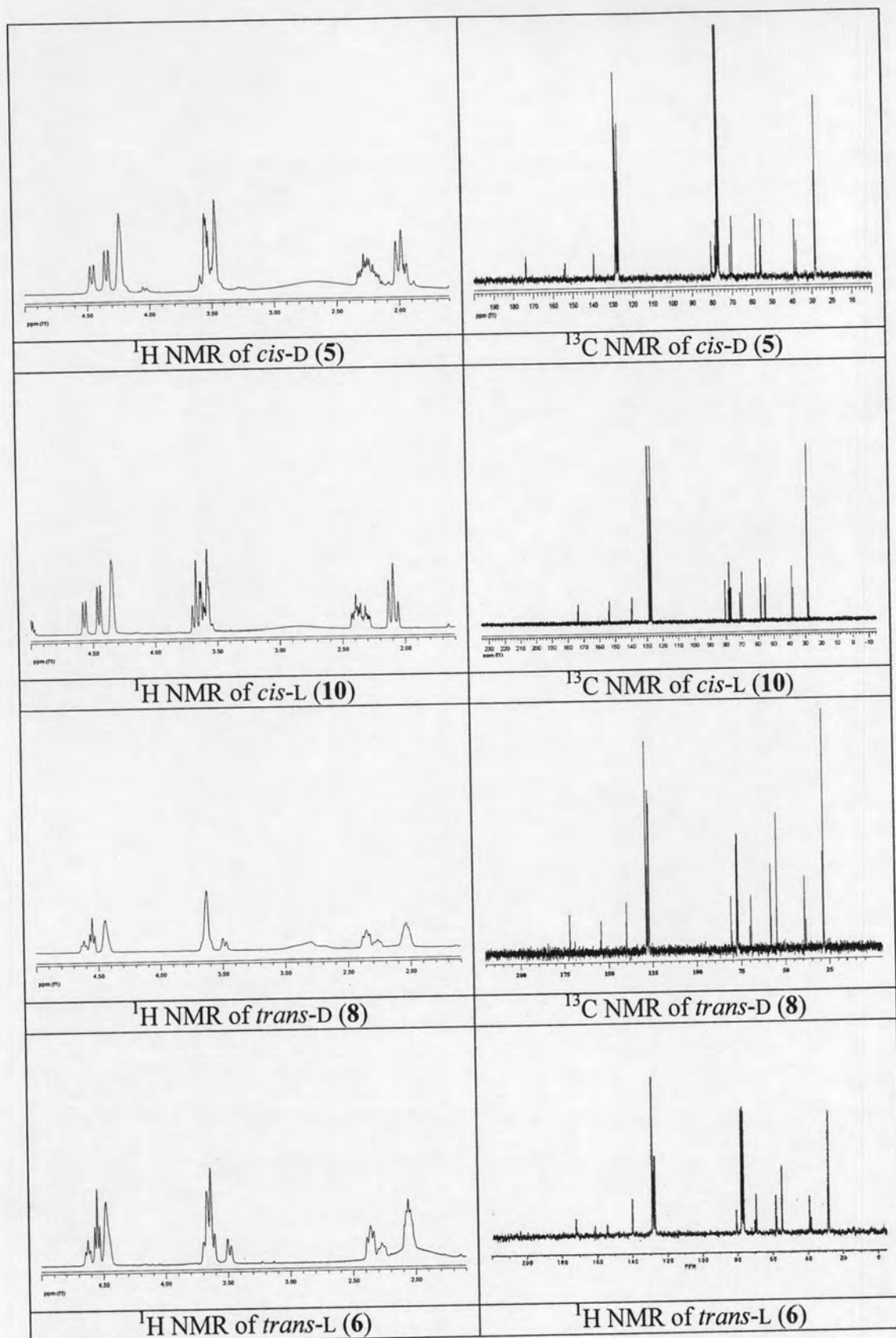


Figure 3.10 Comparison of ^1H and ^{13}C NMR spectrum of intermediate *cis*-D (5), *cis*-L (10), *trans*-D (8) and *trans*-L (6).

While direct substitutions of the C4-OH group in the protected hydroxyprolines by the bases thymine and guanine have been carried out efficiently using Mitsunobu reaction, the same reactions with the base adenine and cytosine did not work well. The problem was solved in the literature [79] by first converting the OH group into tosyl which is a good leaving group. Since in this work, only the *cis*-D diastereomer will be investigated with all four nucleobases, another important intermediate for the syntheses of (2*R*,4*R*)-adenine and (2*R*,4*R*)-cytosine should be *N*-*tert*-butoxycarbonyl-*trans*-4-tosyl-D-proline diphenylmethyl ester (**11**). This compound has been previously prepared by Mitsunobu reaction of the Boc/Dpm protected *cis*-D proline (**5**) using methyl tosylate (MeOTs) as the nucleophile (**Figure 3.11**) [85]. The tosylate ester was an important intermediate for S_N² displacement reaction with the nucleobases adenine and cytosine. The mechanism is similar to that described in **Figure 3.9**. The proline hydroxyl group was activated by S_N² displacement of the tosylate ion to give the tosylate ester (**11**) with inverted configuration.

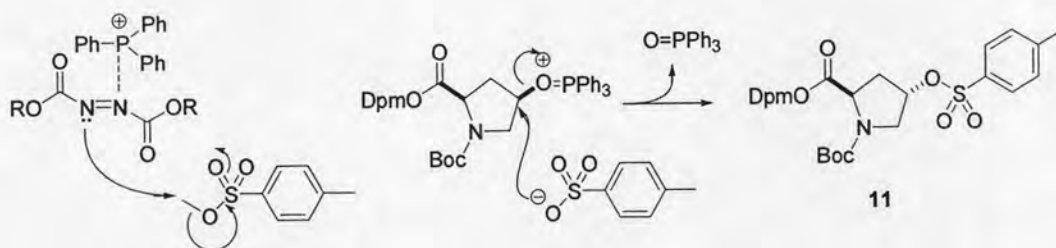
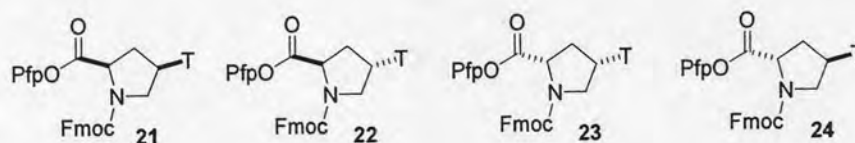


Figure 3.11 Mitsunobu reaction mechanism of *N*-*tert*-Butoxycarbonyl-*trans*-4-tosyl-D-proline diphenylmethyl ester (**11**).

3.1.2 Synthesis of all four diastereomers of thymine pyrrolidiny monomers



The nucleobase thymine was initially selected as a model to preliminary biological study for PNA. The four diastereomeric Boc/Dpm-protected pyrrolidine

monomers (13), (14), (15) and (16) with thymine attached at the C-4 position had been synthesized. The starting materials were the four protected hydroxyproline intermediates described earlier (Section 3.1.1). The thymine was incorporated by using Mitsunobu reaction as described in the literature [101]. In order to avoid the regioselectivity problem of N^1/N^3 alkylation of thymine nitrogen, thymine was first protected as the N^3 -benzoyl derivative according to the literature [84]. Reaction between thymine with excess benzoyl chloride in anhydrous pyridine for 4 h gave a mixture of N^3 -monobenzoylate and N^1,N^3 -dibenzoylate adduct as indicated by TLC analysis. The dibenzoylate adduct lose the N^1 -benzoyl group easily under mild alkaline hydrolysis (0.25 M potassium carbonate in aqueous dioxane at 70 °C for 45 min). After removal of the benzoic acid by-product by aqueous washing, the N^3 -benzoylthymine (12) was obtained and used in the Mitsunobu reaction (Figure 3.12).

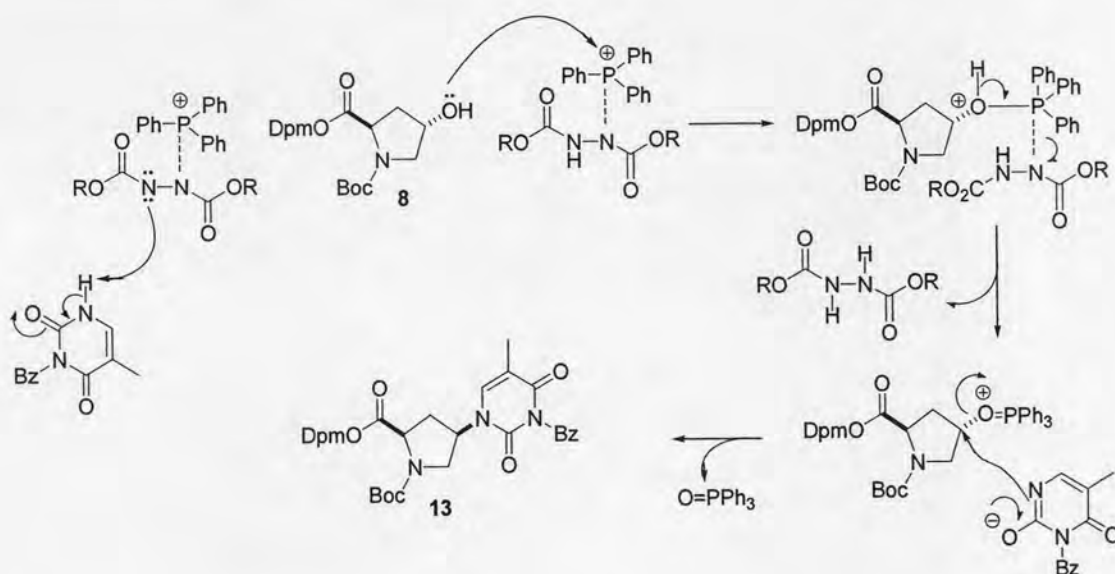


Figure 3.12 Mitsunobu reaction mechanisms of *N*-*tert*-Butoxycarbonyl-*cis*-4-(N^3 -benzoylthymine-1-yl)-*D*-proline diphenylmethyl ester (13)

It should be noted that incorporation of thymine into the pyrrolidine ring via this S_N^2 -type substitution was accompanied by inversion of the configuration of the C4-OH group therefore the product 13 resulting from substitution of the protected *trans*-*D* proline (8) possessed *cis*-*D* configuration.

In the literature, the product 13 was isolated by column chromatography, which was not practical for large scale syntheses because several by-products (Ph_3PO

and DIAD) were quite difficult to remove. In an attempt to improve the product isolation, it was unexpectedly discovered that the product **13** was only slightly soluble in methanol while other by-products (diisopropylhydrazinedi carboxylate and triphenylphosphine oxide) were very soluble. Consequently, purification of the protected *cis*-D thymine intermediate (**13**) could be simplified by recrystallization of the crude product mixture (after evaporation of the reaction solvent) from methanol. This is a significant improvement to the literature method because the same yield of the pure product was obtained without the need for extensive chromatography. Other thymine monomers including *trans*-D (**14**), *cis*-L (**15**) and *trans*-L (**16**) were prepared similarly starting from compounds **5**, **6** and **10** respectively under the same reaction conditions described for the *cis*-D isomer (**13**) except for the purification step which employed column chromatography since it provided better recovery of the products prepared in small scales.

After all thymine pyrrolidinyl monomers were prepared, these PNA monomers must be activated in order to use in solid-phase synthesis of oligo-PNA. Previous experiences in this research group [81] suggested that Fmoc chemistry had a number of advantages over Boc chemistry. This is mainly due to the mild conditions for deprotecting *N*-Fmoc group (20% piperidine in DMF) which results in a simpler design of equipment that is capable of handling small-scale synthesis. To obtain the Fmoc-protected monomers, the Boc-protecting group must be removed and replaced by a fluorenylmethoxycarbonyl (Fmoc) group. The Boc group in compound **13** can be removed by treat with *p*-toluenesulfonic acid monohydrate (*p*-TsOH) in anhydrous acetonitrile at 30 °C for 1.5 h (monitored by TLC analysis) [80]. Then acetonitrile, diisopropylethylamine and 9-fluoronylmethylchloroformate (FmocCl) were added sequentially. The solution was stirred for a further one hour then the solvent was removed by rotary evaporation, diluted with dichloromethane, and extracted with 5% HCl. The organic layer was washed with water and evaporated to dryness. The residue was chromatographed on silica gel and the pure fraction was triturated with hexane to give (**3.13a**) as a white solid as shown in **Figure 3.13**.

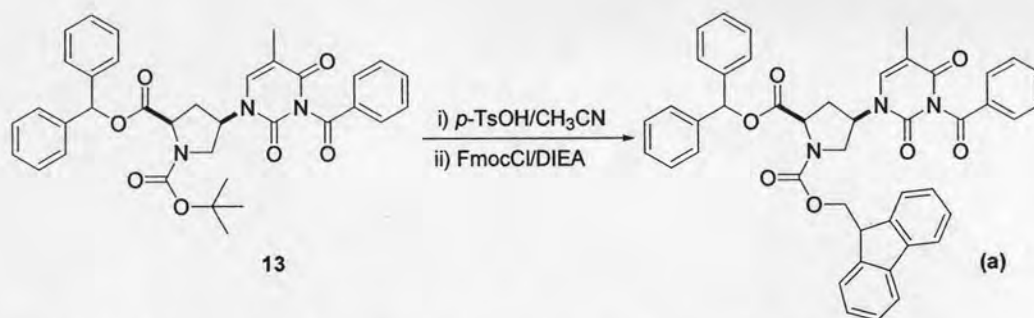


Figure 3.13 Deprotection Boc group and protection Fmoc group.

Next, the diphenylmethyl group in the Fmoc/Dpm protected intermediate (**3.13a**) was changed to the more reactive pentafluorophenyl ester (**Figure 3.14**). Removal of the Dpm group was achieved by treating with TFA/anisole at room temperature for 3-4 h. The volatiles were removed by flushing with a nitrogen stream and the residue was treated with diethyl ether which caused precipitation of the Fmoc-free acid as an off white solid. The ^1H NMR of the product suggested that the benzoyl protecting group of thymine was also cleaved under acidic condition as shown in **Figure 3.15**. However, the presence of unprotected thymine was shown to have no effect on the subsequent peptide coupling steps [101] because the nucleophilicity of thymine N^3 was not very high due to the resonance shown in **Figure 3.15**.

The role of anisole was to function as a scavenger for the highly electrophilic diphenylmethyl and *tert*-butyl cations released from deprotection of the diphenyl methyl and Boc group [89]. The crude TFA salts were used for the next step without further purification and characterization.

The free carboxylic acid was then activated with pentafluorophenol (PfpOH) and dicyclohexylcarbodiimide (DCC) to get the Fmoc-protected PNA active ester thymine monomer (**21**) suitable for the use in solid-phase synthesis.

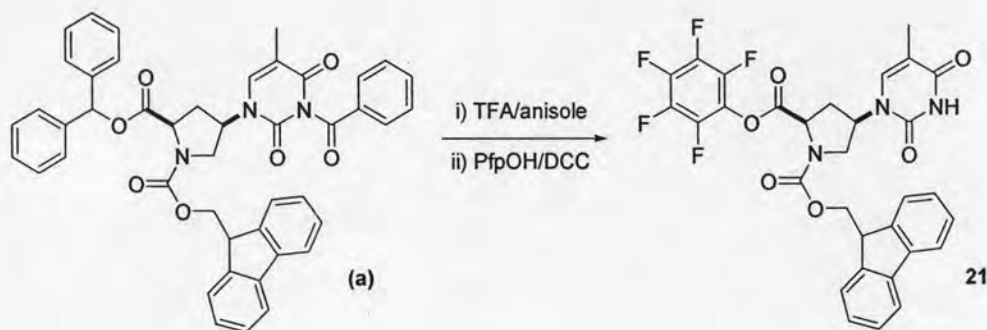


Figure 3.14 Deprotection Dpm group and activation Pfp group.

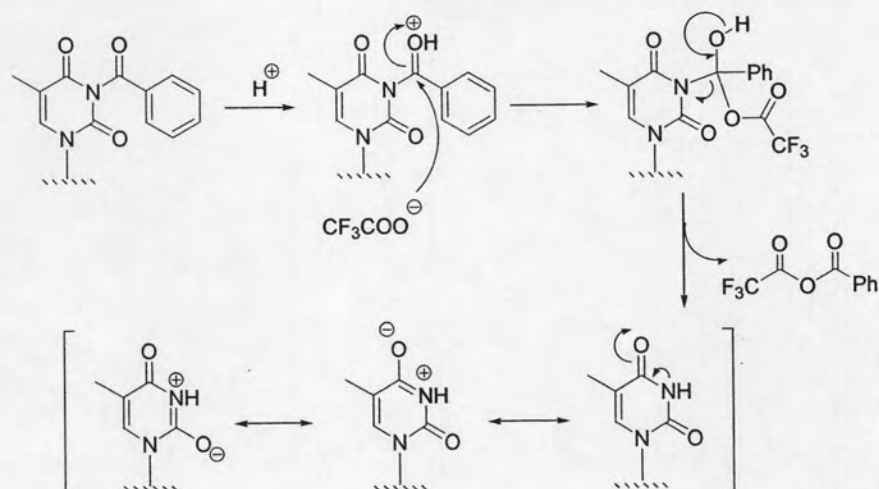


Figure 3.15 Deprotection benzoyl protecting group of *N-tert*-butoxycarbonyl-*cis*-4-(*N*³-benzoylthymine-1-yl)-*D*-proline diphenylmethyl ester (**13**) and resonance form of thymine moiety.

In a modified procedure which has not been previously reported, it was founded that Boc and Dpm groups, both being acid labile, can be cleaved simultaneously under acidic conditions. Hence, when the Boc/Dpm intermediate proline compounds **13**, **14**, **15** and **16** were treated with TFA in the presence of anisole at 30 °C for 24 h to give the free acids in the form of TFA salts (**Figure 3.16**).

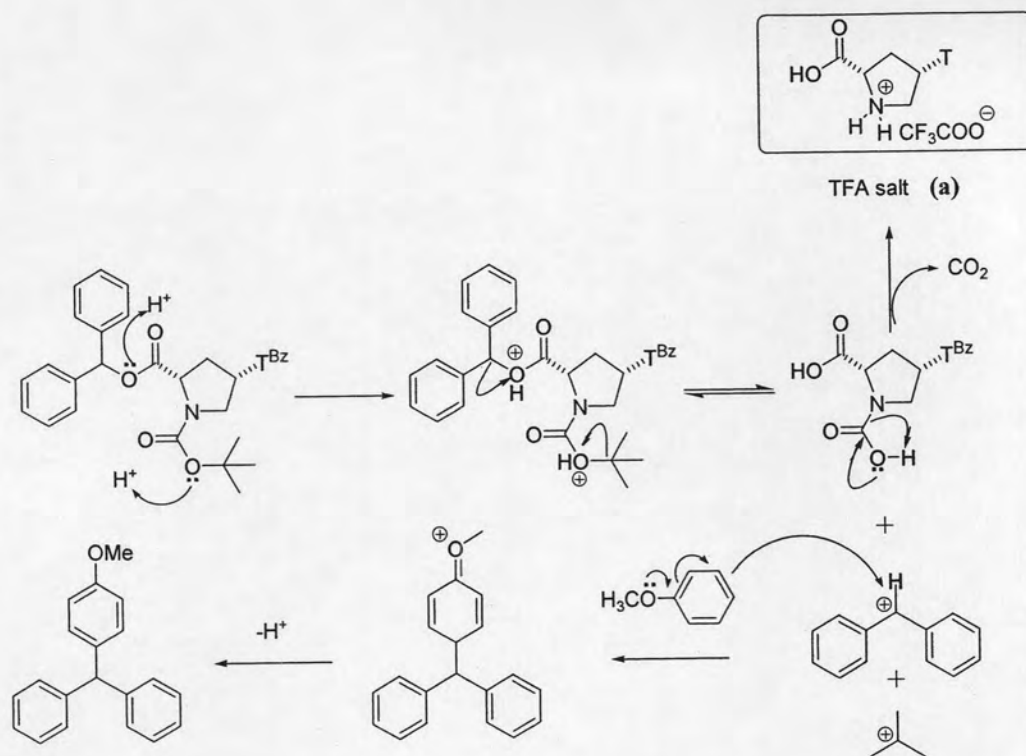


Figure 3.16 Mechanism for deprotection of Boc/Dpm protecting group in the presence of TFA and anisole.

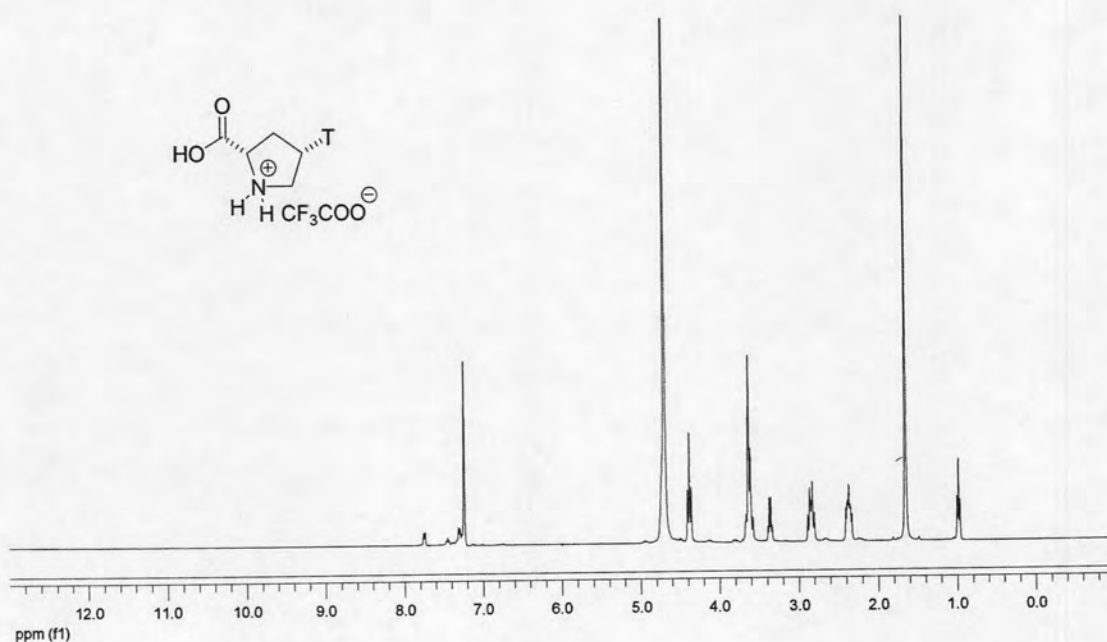


Figure 3.17 ¹H NMR spectrum of TFA salt of the thymine monomer.

In the next step, the free amino group was protected with Fmoc by reacting with 9-fluorenyl succinimidyl carbonate (FmocOSu) under basic conditions (**Figure**

3.18). FmocOSu was used instead of FmocCl in the previous report because FmocCl was too reactive and may cause undesirable reactions such as dipeptide formation [110]. Furthermore, FmocOSu was also more soluble and more stable in aqueous-organic solvents, the condition that the protection was performed, than FmocCl. In all cases, the Fmoc protection took place smoothly at room temperature. The Fmoc amino acids were easily isolated by first extraction of the reaction mixture with diethyl ether to remove the excess FmocOSu followed by acidification with aqueous HCl. The Fmoc-acids **17**, **18**, **19**, **20**, **27**, **30** and **36** were precipitated as white solid which were collected by filtration and dried under vacuum. Since these Fmoc-acids were stable solid compared to the rather labile Pfp esters, this is the preferred form for long term storage.

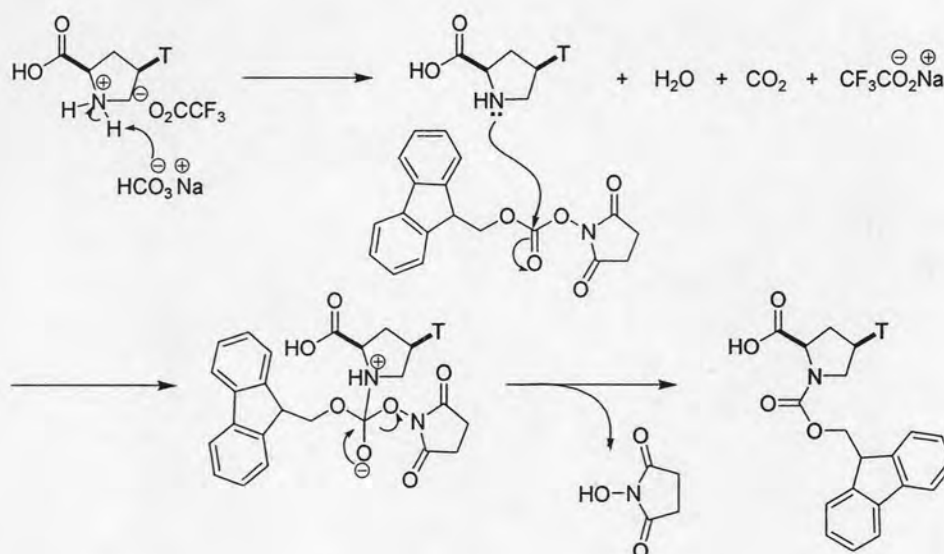


Figure 3.18 Mechanism for the protection of *N* atom with Fmoc group.

^1H NMR spectra of all Fmoc-acid monomers showed two sets of signals due to protons and carbons on the proline ring in approximately 1:1 ratio as shown in **Figure 3.19**. This can be explained by the formation of two rotamers due to the slow rotation of the Fmoc group similar to the corresponding Boc derivative as previously described [101].

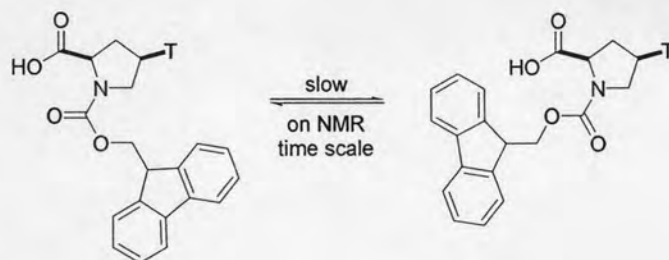
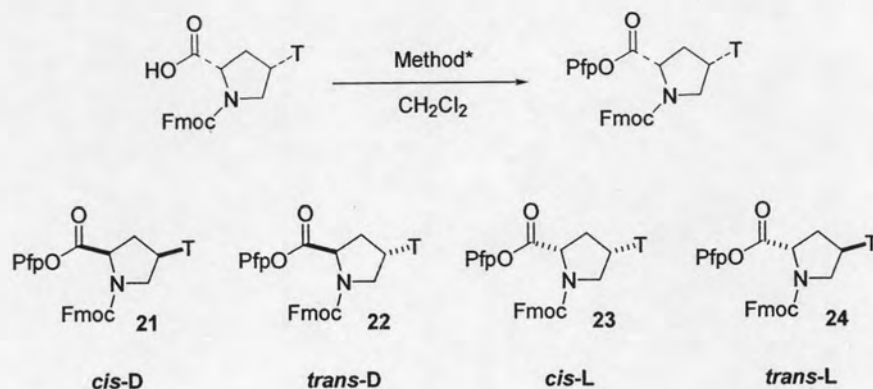


Figure 3.19 Rotamer of the Fmoc free acids.

The Fmoc free acids **17**, **18**, **19** and **20** were converted into the corresponding Pfp esters by reacting with *N*-(3-dimethylaminopropyl)-*N'*-ethyl-carbodiimide hydrochloride (EDC·HCl) and pentafluorophenol (PfpOH) in dichloromethane. This new method was more convenient to perform and provided a good yield as shown in **Table 3.2**, therefore it is preferred over the literature methods [101] which used either PfpOH/DCC or PfpOTfa/DIEA. The reactions with PfpOH/DCC provided a dicyclohexyl urea as by product which was difficult to remove from the product, while the reaction with PfpOTfa/DIEA gave good results but PfpOTfa was rather expensive and unstable. The reactions were usually completed within 1 h at room temperature as judged by TLC analysis. The crude reaction products were purified by flash column chromatography. The chromatographic purification must be performed quickly to avoid decomposition of the product on the silica column. In all cases the Fmoc-protected Pfp-activated thymine monomers **21**, **22**, **23** and **24** were obtained as white solids which may be stored in a freezer for at least a few months.

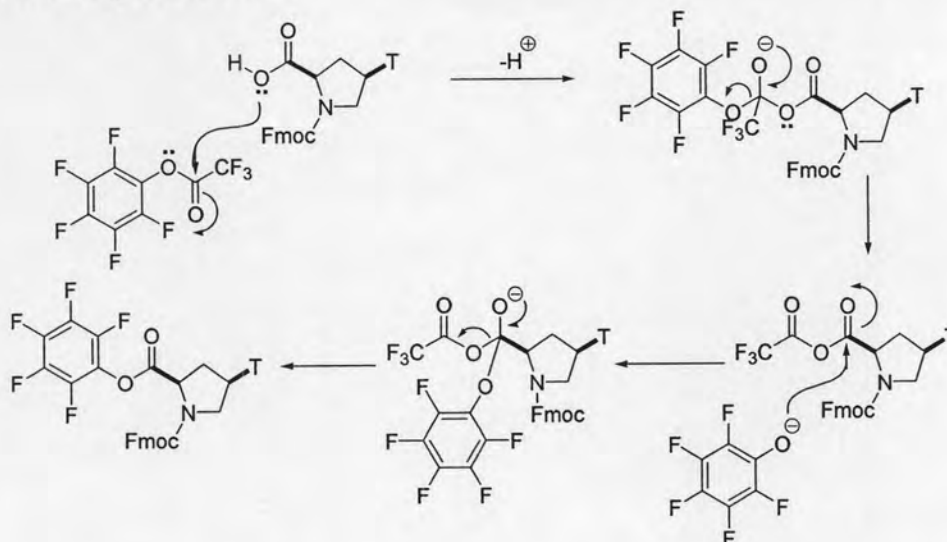
Table 3.2 Comparison between activation of the Fmoc acids of all thymine monomer by formation of Pfp ester in various methods.



Free acid derivatives	Isomer	Pfp ester derivatives	Method	% yield
17	(<i>cis</i> -D)	21	PfpOTfa/DIEA	79
17	(<i>cis</i> -D)	21	PfpOH/DCC	40
17	(<i>cis</i> -D)	21	PfpOH/EDC·HCl	85
18	(<i>trans</i> -D)	22	PfpOTfa/DIEA	75
19	(<i>cis</i> -L)	23	PfpOTfa/DIEA	44
20	(<i>trans</i> -L)	24	PfpOTfa/DIEA	50

The reaction mechanisms for the Pfp-ester formation of both PfpOH/EDC·HCl and PfpOTfa/DIEA methods are illustrated in **Figure 3.20**. The mechanism of activation by PfpOH/DCC is similar to that of PfpOH/EDC·HCl.

Method I - PfpOTf/DIEA



Method II - PfpOH/EDC·HCl

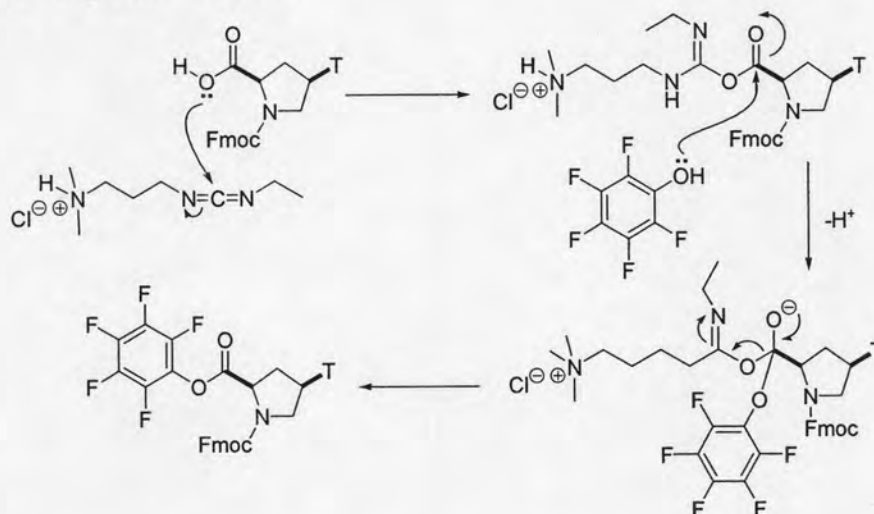
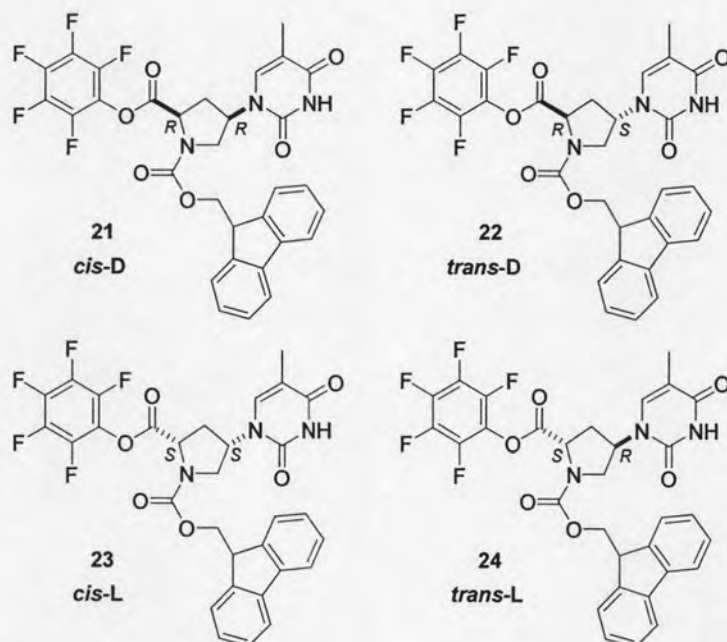


Figure 3.20 Reaction mechanisms for the activation of an Fmoc free acid with Pfp.

The structures and purities of the Pfp-ester thymine-monomers **21**, **22**, **23** and **24** were confirmed by 1H NMR, ^{13}C NMR, optical rotation and elemental analysis (characterization of these compounds are presented in Chapter II). NMR chemical shifts of the monomers were assigned as shown in **Table 3.3**. The values are fully consistent with the expected structures, indicating that the reactions were successful. For enantiomeric/diastereomeric relationships of the four compounds, the compound **21** and **23** were the enantiomer pair, which afforded the optical rotation values of -

2.20 and -0.69 respectively. Similarly, compounds **22** and **24** which were also enantiomers showed $[\alpha]_D^{25}$ at +26.6 and -28.7 respectively.

Table 3.3 ^{13}C NMR, optical rotation and percent yield of protected monomers **21**, **22**, **23** and **24**.



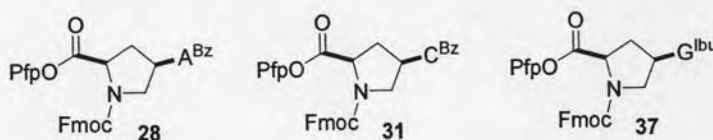
Position	Chemical shifts (ppm)			
	(<i>cis</i> -D) (21)	(<i>trans</i> -D) (22)	(<i>cis</i> -L) (23)	(<i>trans</i> -L) (24)
2 Thymine	151.4	150.7	151.1	150.5
4 Thymine	164.2	163.9	163.8	163.5
5 Thymine	109.5, 109.6	112.1, 112.2	111.9, 112.3	112.3
6 Thymine	138.3	136.4, 136.5	135.7, 135.9	136.2
2' Proline	57.4, 57.8	57.3, 57.6	56.8, 57.2	57.3, 57.5
3' Proline	33.5, 34.9	33.5, 34.9	34.2, 35.7	33.6, 35.0
4' Proline	52.7, 53.3	54.0, 54.8	52.4, 52.8	53.9, 54.7
5' Proline	48.8, 49.4	49.1, 49.2	48.9, 49.2	49.0, 49.2
CH_3 Thymine	12.6	12.6	12.5	12.6
Fmoc CH	47.1	46.9	47.0	46.9
Fmoc CH_2	67.4, 67.7	68.1, 68.4	68.1, 68.5	68.1, 68.4

Position	Chemical shifts (ppm)			
	(<i>cis</i> -D) (21)	(<i>trans</i> -D) (22)	(<i>cis</i> -L) (23)	(<i>trans</i> -L) (24)
Fmoc Ar <u>CH</u>	120.6, 125.6, 127.7, 128.2	120.0, 124.8, 127.0, 127.7	120.0, 124.8, 127.1, 127.8	120.0, 124.8, 127.1, 127.8
Fmoc Ar <u>C</u>	141.2, 144.1	143.0, 143.4 143.5, 143.8	143.0, 143.3 143.5, 143.8	141.2, 143.5
Fmoc <u>CO</u>	154.4	153.7, 154.4	153.9, 154.4	153.6, 154.3
Proline <u>CO</u>	173.1, 173.7	167.8	168.1	167.8
$[\alpha]_D^{25}$ ^a	-2.20	+26.6	-0.69	-28.7
% yields ^b	26 %	17 %	15 %	22 %

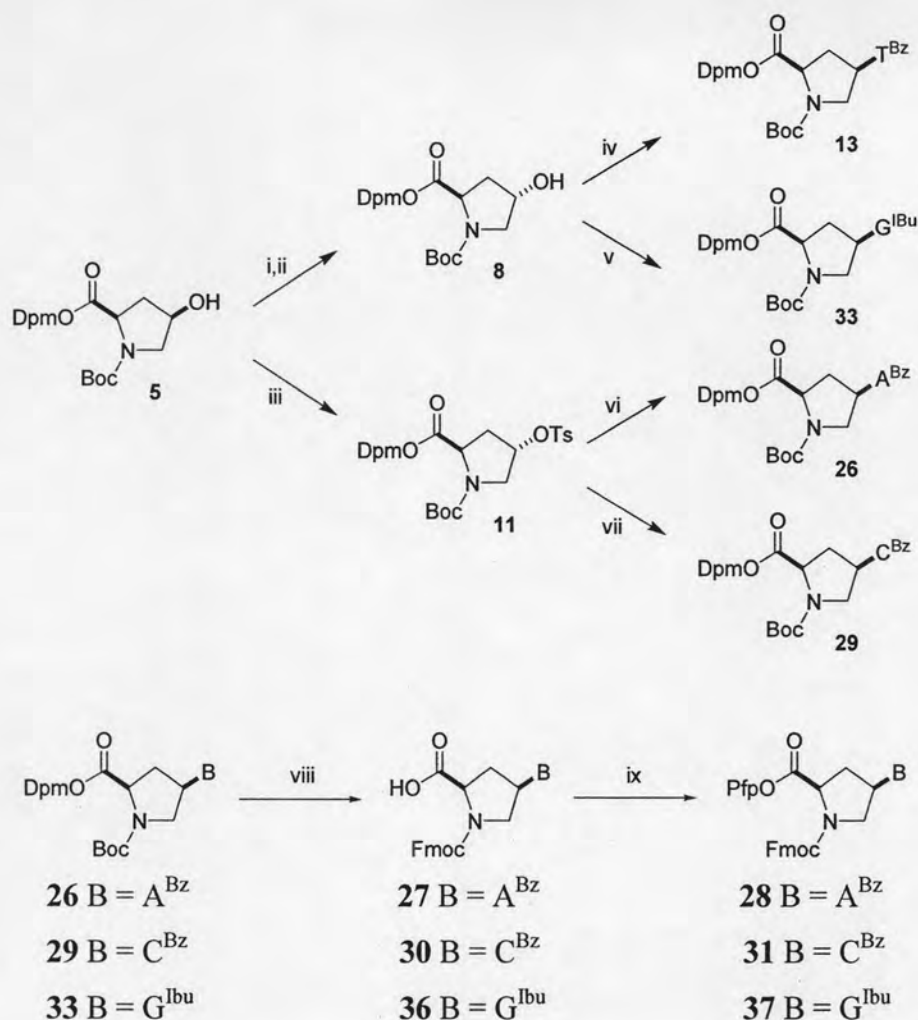
a an optical rotation was operated in chloroform (c=1.0 g/100 mL)

b percent yield was calculated from starting material *trans*-4-hydroxy-L-proline.

3.1.3 Synthesis of *cis*-D pyrrolidinyl monomers with bases A, C and G



Only the *cis*-D pyrrolidinyl monomers with other nucleobases apart from thymine were chosen for further investigation. Literature work indicated that the Boc/Dpm-protected of the guanine monomer may be synthesized from the protected hydroxyl compound **8** in the same way as for thymine monomers. However, as mentioned earlier (Section 3.1.1), synthesis of the Boc/Dpm protected adenine and cytosine monomers required a *trans*-D tosylate (**11**) intermediate *via* substitution S_N² reaction as shown in Figure 3.21.



Reagents and conditions: i. HCO_2H , Ph_3P , DIAD, THF, 8 h; ii. NH_3 , MeOH, 2 h; iii. MeOTs, Ph_3P , DIAD, THF, 8 h; iv. $N^3\text{-BzT}$, Ph_3P , DIAD, THF, 8 h; v. a) $N^2\text{-IbuG(ONpe)}$, Ph_3P , DIAD, dioxane, 8 h; b) DBU, pyridine 2 h; vi. $N^6\text{-BzA}$, K_2CO_3 , DMF, 90 °C 6 h; vii. $N^4\text{-BzC}$, K_2CO_3 , DMF, 90 °C 6 h; viii. a) TFA, anisole; b) FmocOSu, NaHCO_3 , H_2O , MeCN; ix. PfpOH, EDC·HCl, CH_2Cl_2 .

Figure 3.21 A synthetic scheme for the intermediate with various nucleobases derivative 13, 26, 29 and 33.

The tosylate intermediate was then reacted with the nucleobases by S_{N}^2 displacement with inversion at the C-4 position. The reactions were successful for both protected adenine and cytosine. The yields were comparable to those reported in the literature [101].

The adenine monomer was prepared starting from tosylate (**11**), *N*⁶-benzoyladenine [80], anhydrous K₂CO₃ and a catalytic amount of 18-crown-6 in dry DMF and stirred under nitrogen at 80 °C overnight. Addition of 18-crown-6 was initially believed to improve the yield by phase transfer mechanism. However it was later addition of crown ether did not improve the yield. When 18-crown-6 was not added, the percent yield of desired product was 40% but the same reaction with the crown ether afforded only 30%, so no crown ether was added in subsequent reactions.

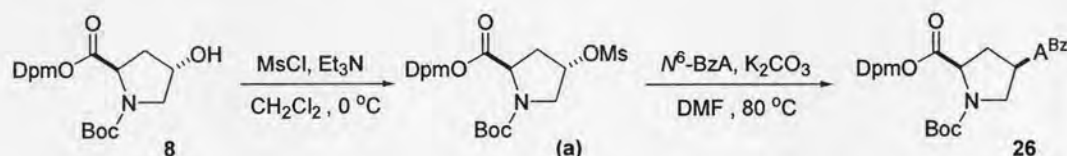


Figure 3.22 The other synthetic scheme for adenine monomer.

When the tosylate group was replaced by a more reactive mesylate (OMs), it was expected that the yield would increase due to the better leaving ability of OMs group. The mesylate (**3.22a**) was prepared in 74 % yield from the reaction of compound **8** with mesyl chloride (MsCl) in the presence of triethylamine (Et₃N) and dichloromethane at 0 °C [102]. The substitution reaction with *N*⁶-benzoyladenine was accomplished in the same way as described earlier giving the product **26** in only 27% yield. Therefore the mesylate was not better than tosylate leaving group for this type of reaction. The adenine intermediate **26** was protected by Fmoc group after removal of the protecting groups with TFA/anisole followed by reacting with FmocOSu under basic conditions as described earlier for the thymine monomers. The free acid was converted into the corresponding Pfp ester by reaction with PfpOH and EDC·HCl in dichloromethane to give the product **28** in 68 % yield.

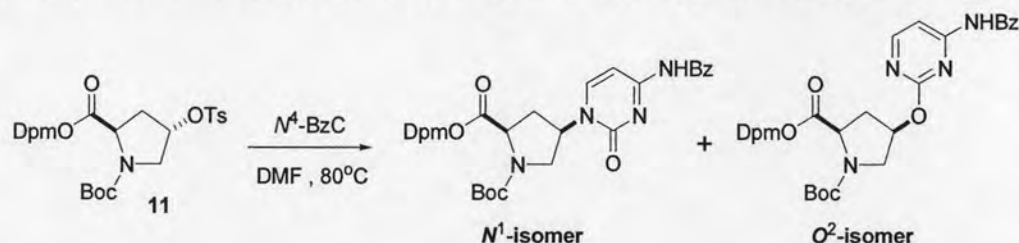
In case of cytosine, the intermediate **29** was prepared analogously to the adenine monomer. The reaction of *trans*-D tosylate (**11**) with *N*⁴-benzoylcytosine [90] in the presence of anhydrous K₂CO₃/18-crown-6 in dry DMF afford the desired *N*¹-isomer **29** along with the less polar *O*²-isomer (**Figure 3.23**) which could be readily separated by chromatography on silica gel.



Figure 3.23 Structure of N^1 -isomer and O^2 -isomer cytosine intermediate.

It is known that O^2 -alkylation of cytosine is the major side reaction in alkylation of cytosine [103-105]. Many experimental conditions were explored to improve the yield and the ratio between N^1 -isomer and O^2 -isomer. The reactions with and without catalytic amount of 18-crown-6 were also investigated. Some other PTC such as tetrabutylammonium hydrogen sulfate (Bu_4NHSO_4), triethylbenzylammonium chloride (BnEt_3NCl) and tetrabutylammonium hydroxide (Bu_4NOH) were tried in place of 18-crown-6 [101]. Furthermore, inorganic base potassium carbonate was converted to a stronger base cesium carbonate (Cs_2CO_3) to enhance the reactivity, the results were summarized in **Table 3.4**.

Table 3.4 Substitution reactions with cytosine to the pyrrolidine ring



Entry	Condition ^a	% yield ^b of N^1 -isomer	% yield ^b of O^2 -isomer
1	K_2CO_3 , 18-Crown-6	25	63
2	K_2CO_3	26	70
3	K_2CO_3 (THF as solvent)	7	75
4	Cs_2CO_3	13	70
5	K_2CO_3 , Bu_4NHSO_4 0.1 equiv	19	62
6	K_2CO_3 , Bu_4NHSO_4 0.2 equiv	11	80
7	K_2CO_3 , Bu_4NHSO_4 1.0 equiv	28	69
8	K_2CO_3 , BnEt_3NCl 0.1 equiv	15	76

Entry	Condition ^a	% yield ^b of <i>N</i> ¹ -isomer	% yield ^b of <i>O</i> ² -isomer
9	Bu ₄ NOH 0.1 equiv	16	65
10	Mitsunobu reaction ^c	-	-

^a All reactions were performed in DMF, except for entries 3 and 10.

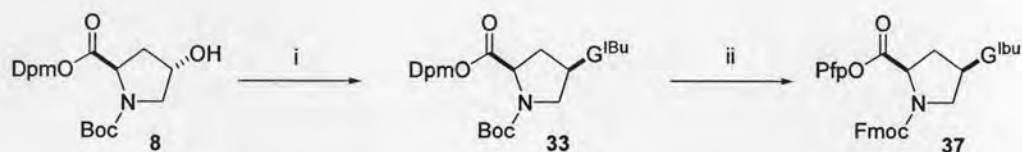
^b The reactions were performed in 0.5 mmol scale and isolated yield by column chromatography on silica gel.

^c This reaction was performed using PPh₃, DIAD in THF at 0 °C

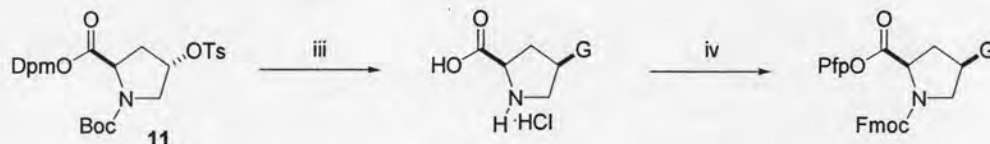
From the **Table 3.4**, the reaction with and without 18-crown-6 gave similar results (25% and 26% yield of *N*₁-isomer respectively). When aprotic polar solvent (THF) was used instead of DMF, less yield of the desired product was obtained. When the base was changed to Cs₂CO₃, a lower yield was also obtained (entry 1-4). Interestingly, Bu₄NHSO₄ as PTC at 0.1 equiv provided 19 % yield of the *N*¹-isomer and 62 % yield of the *O*²-isomer. However, when the Bu₄NHSO₄ was added in higher amounts (0.2 equiv and stoichiometric amount), the yields for the *N*¹ isomer were 11 % and 28 % respectively which was not better than when K₂CO₃ was used alone (entry 6-7). Other PTC catalysts BnEt₃NCl and Bu₄NHSO₄ also gave low yields (entry 8-9). As a result, the condition in entry 2 was used for the synthesis cytosine intermediate. The cytosine intermediate **29** was treated with TFA/anisole to remove the protecting groups and reacting with FmocOSu under basic conditions to afford the free acid **30**. This was converted to the corresponding Pfp esters by reaction with PfpOH and EDC·HCl in dichloromethane using the same method described for the thymine monomers to give the product **31** in 85% yield.

In a literature method for the synthesis of the guanine monomer, the Mitsunobu reaction using *N*²-isobutyryl-*O*⁶-(4-nitrophenylethyl)-guanine gives *N*-*tert*-butyloxycarbonyl)-*cis*-4-(*N*²-isobutylguanin-9-yl)-D-proline diphenylmethyl ester (**33**) after removal of the nitrophenylethyl group with 1,8-diazabicyclo [5.4.0]undec-7-ene (DBU) in pyridine [101]. An alternative method starting with tosylate (**11**) in the presence of 2-chloro-6-aminopurine and K₂CO₃ in DMF via S_N² reaction was also explored as shown in **Figure 3.21**.

Method I



Method II



Reagents and conditions: i. a) N^2 -G^{Ibu}(ONpe), PPh₃, DIAD, dioxane; b) DBU, pyr; ii. a) TFA/anisole; b) FmocOSu, NaHCO₃, H₂O, MeCN; c) PfpOH, EDC·HCl, CH₂Cl₂; iii. a) 2-amino-6-chloropurine, K₂CO₃, DMF, 70 °C; b) TFA/anisole; c) 2 N HCl, reflux; iv. a) FmocOSu, NaHCO₃, H₂O, MeCN; b) PfpOH, EDC·HCl, CH₂Cl₂.

Figure 3.24 A synthetic scheme for the guanine monomer **37**.

The first method was performed according to Vilaivan [80] starting from *N*-tert-Butoxycarbonyl-*trans*-4-tosyl-D-proline diphenylmethyl ester (**8**), N^2 -isobutyryl- O^6 -(4-nitrophenylethyl)-guanine and PPh₃/DIAD in dry dioxane. The isobutyl group (Ibu) was selected to protect the N^2 -position of guanine because it can be removed by aqueous ammonia at a comparable rate to the benzoyl protecting groups of adenine and cytosine [106]. The N^2 protecting group can also enhance the solubility of the compound in organic solvent. In addition, O^6 -position of G^{Ibu} was protected with a bulky substituent such as nitrophenylethyl group to avoid the undesired O^6 and N^7 substitution during the Mitsunobu reaction. G^{Ibu}(ONpe) was prepared from N^2 -isobutyrylguanine by temporary protection of N^7/N^9 by treatment with acetic anhydride followed by Mitsunobu reaction with 2-(4'-nitrophenyl)ethanol according to Benner [107]. This group can be cleaved under basic conditions using DBU at room temperature. The reaction of G^{Ibu}(ONpe) with compound **8** in the presence of PPh₃ and DIAD followed by treatment with DBU in pyridine gave the intermediate **33** (Figure 3.24:Method I) After that, this intermediate was protected with Fmoc and

converted into the corresponding Pfp esters similar to others monomers to give the product **37** in 66% yield.

Another method to synthesize the guanine monomer (**Figure 3.24:Method II**) was also explored. Substituents at C^6 of the 2-aminopurine systems were shown to have a pronounced effect on the ratio of N^7/N^9 -substitution [108]. It would therefore be interesting to use other commercially available 2-aminopurine derivatives such as 2-amino-6-chloropurine as a precursor of guanine monomer instead of the rather difficult to make $G^{tBu}(ONpe)$. The reaction of 2-amino-6-chloropurine with tosylate **11** and K_2CO_3 in DMF at 70 °C gave (*N*-*tert*-butyloxycarbonyl)-*cis*-4-(6-chloro guanin-9-yl)-D-proline diphenylmethyl ester (**34**) in 65% yield. 1H NMR and ^{13}C NMR suggested that product contain both guanine and the proline ring system as shown in **Figure 3.25**. The chloro group at C^6 of intermediate was transformed to the oxo group (C=O) in order to make the guanine monomer. This was first attempted by treating with 3-hydroxypropionitrile and sodium hydride in THF [109] as shown in **Figure 3.26**.

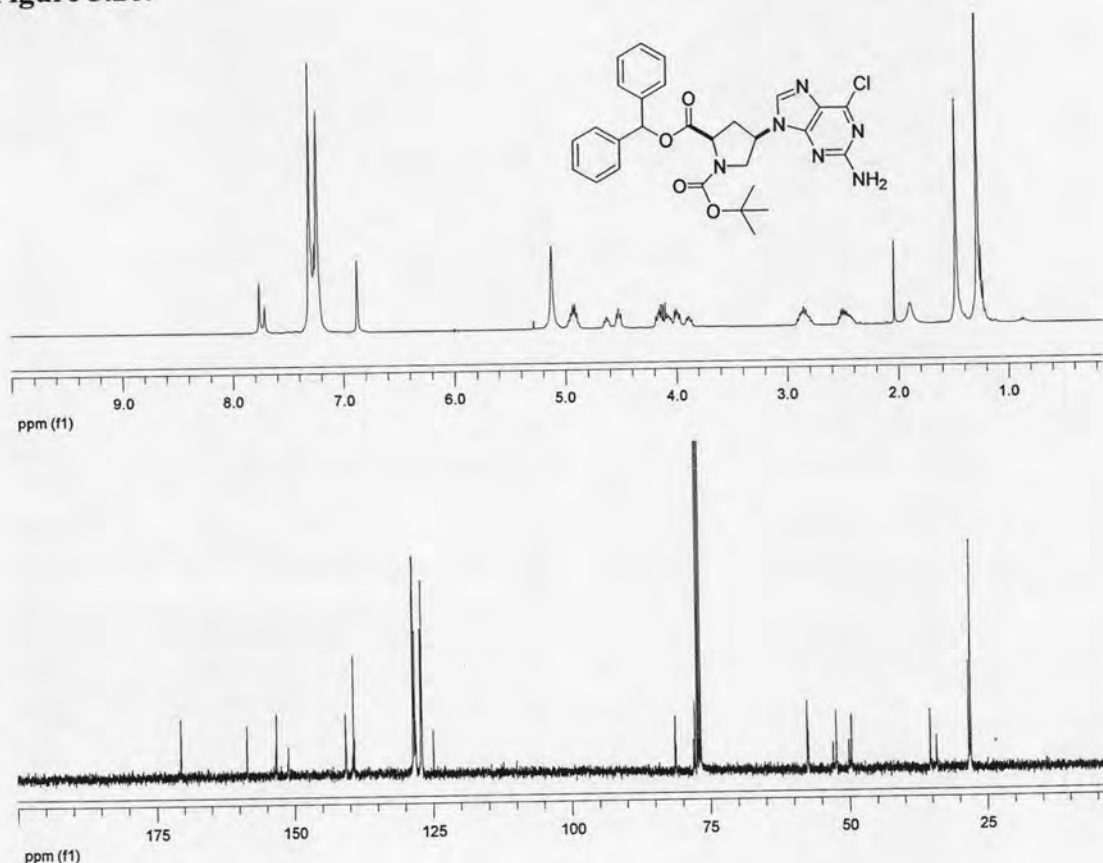


Figure 3.25 1H and ^{13}C NMR spectrum of (*N*-*tert*-butyloxycarbonyl)-*cis*-4-(6-chloro guanin-9-yl)-D-proline diphenylmethyl ester (**34**).

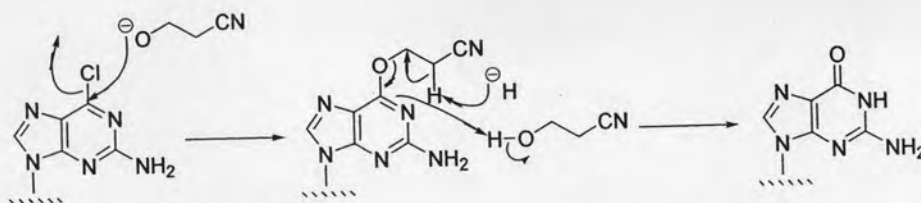
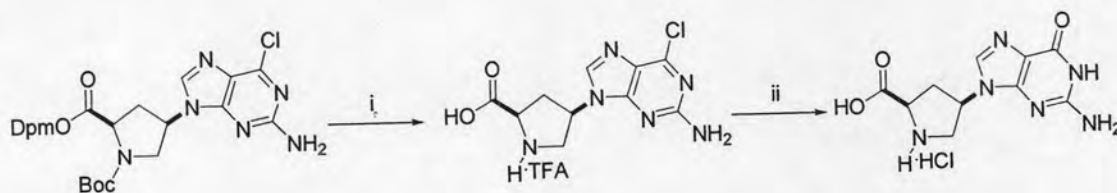


Figure 3.26 A reaction mechanism for turning 2-amino-6-chloropurine to guanine

Nevertheless, the reaction with 3-hydroxypropionitrile gave no products containing guanine according to TLC analysis. It was proposed that cleavage of the Dpm group may be involved in this reaction resulting in the free carboxylic acid. In a different approach, TFA/anisole was used to remove Boc and Dpm groups to give a TFA salt first. Acid hydrolysis of the TFA salt with 1 N HCl gave a quantitative yield of the guanine amino acid [85] as shown in **Figure 3.27**. This intermediate was then protected Fmoc as the same method described for the thymine monomers to give the product **35** in 54% yield.



Reagents and conditions : i. TFA/anisole; ii. 1 N HCl, reflux.

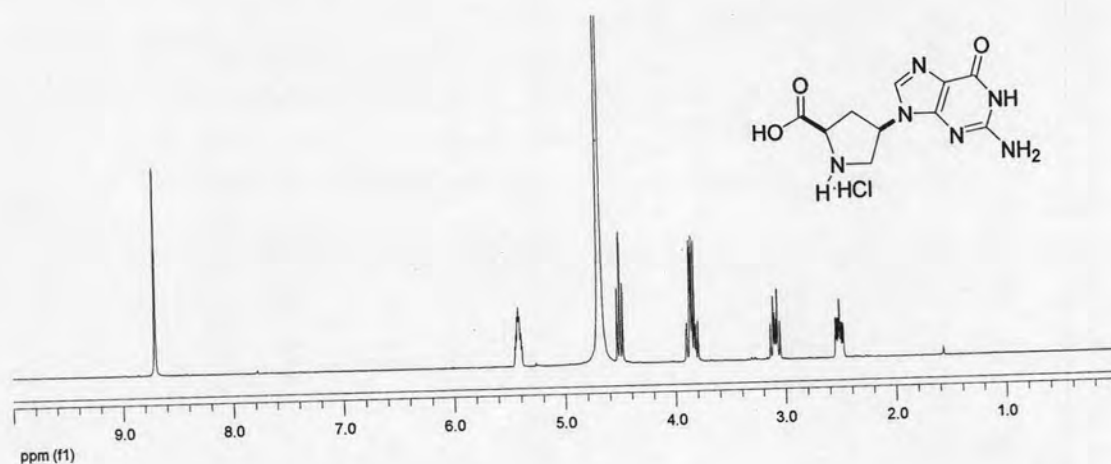


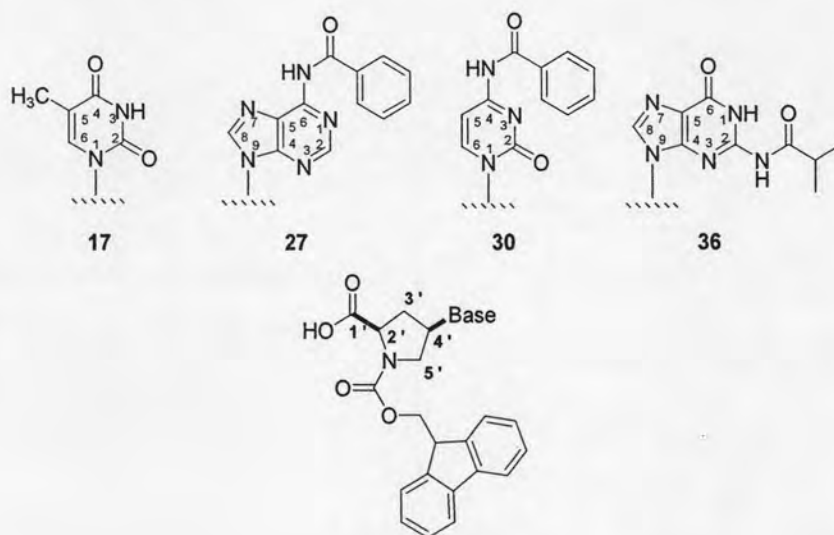
Figure 3.27 A synthetic scheme for guanine amino acid intermediate and ^1H NMR spectrum.

Both methods were considered by comparing percent yield from first attachment of guanine to the pyrrolidine ring to Fmoc protection. The first method involved more steps and required preparation of the protected guanine derivative [$G^{Ibu}(ONpe)$] and it provided less overall yield (9%) than the second method (35%). However, 2-amino-6-chloropurine is a rather expensive compound compare with guanine (over 10 times) and the product required another step for introducing N^2 -guanine protection, the first method was therefore chosen to prepare the guanine monomer in this research.

In summary, all four nucleoside analogues derived from a proline derivative had been successfully prepared in protected form either by starting from reactions of *N*-Boc-*trans*-4-hydroxyproline diphenylmethyl ester (**8**) or *N*-Boc-*trans*-4-tosyl-D-proline diphenylmethyl ester (**11**) with nucleobases under Mitsunobu reaction conditions or *via* S_N^2 displacement of the analogous tosylate.

In addition, ^{13}C NMR chemical shifts and percent yield of all Fmoc-protected monomers **17**, **27**, **30** and **36** were assigned as summarized in **Table 3.5**. The values are fully consistent with the expected structures, indicating that the reactions were successful.

Table 3.5 ^{13}C NMR of Fmoc-protected monomers **17**, **27**, **30** and **36**.



Position	Chemical Shift (ppm)			
	17	27	30	36
2	151.4	152.9	155.4	149.1
4	164.2	150.7	163.1	155.3
5	109.5, 109.6	126.2	96.6	120.5
6	138.3	151.8	147.9	148.2
8	-	141.1	-	138.3
1'	173.1, 173.7	173.0, 173.5	173.2, 173.8	173.0, 173.6
2'	57.4, 57.8	57.7, 58.0	57.7, 58.0	57.8, 58.2
3'	33.5, 34.9	34.0, 35.2	33.5, 33.6	34.8, 35.6
4'	52.7, 53.3	52.4, 53.0	55.5, 56.1	52.1, 52.9
5'	48.8, 49.4	50.0, 50.5	49.2, 49.8	50.5, 51.1
<u>CH</u> ₃	12.6	-	-	19.3
<u>CH</u> (CH ₃) ₂	-	-	-	35.1
Benzoyl <u>C</u>	-	132.9	133.1	-
Benzoyl <u>CH</u>	-	126.2, 127.6, 133.8	128.2, 128.8, 133.6	-
Benzoyl <u>CO</u>	-	166.0	167.9	-
Ibu <u>CO</u>	-	-	-	180.6
Fmoc <u>CH</u>	47.1	47.1	47.1	47.0
Fmoc <u>CH</u> ₂	67.4, 67.7	67.5, 67.8	67.4, 67.7	67.4, 67.7
Fmoc Ar <u>CH</u>	120.6, 125.6, 127.7, 128.2	120.6, 125.8, 128.2, 128.9	120.6, 125.7, 127.6, 128.9	120.2, 125.8, 127.6, 128.1
Fmoc Ar <u>C</u>	141.2, 144.1	143.7, 144.1	141.1, 144.2	141.0, 144.1
Fmoc <u>CO</u>	154.4	154.3	154.4	154.4
[α] _D ²⁵ ^a	-3.85	+7.40	-7.04	-65.96 ^b
% yields ^c	26	14	8	3

a an optical rotation was operated in DMF (c=1.0 g/100 mL).

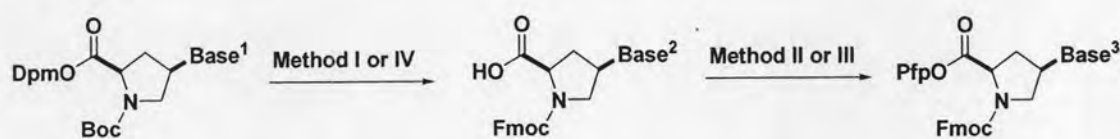
b an optical rotation was operated in DMF (c=0.6 g/100 mL).

c percent yield was calculated from starting material *trans*-4-hydroxy-L-proline.

The identity of the compounds was further confirmed by High Resolution Mass Spectrometry (HRMS) analysis. The results have already been presented by a member of this research group [111].

The Fmoc free acid of the four nucleobase adducts were all converted into the corresponding pentafluorophenyl esters by various methods which were summarized in **Table 3.6**. In all cases the PNA monomers **21**, **28**, **31** and **37** were obtained as white solid which may be stored in a freezer for at least a few months. According to the NMR and TLC analysis the activated monomers were sufficiently pure for the solid phase reactions. The success of the synthesis was also confirmed by HRMS analyses which have also been reported by a member of this research group [111].

Table 3.6 Fmoc protection and Pfp activation of PNA monomers



Method I : i) TFA/anisole; ii) FmocOSu/NaHCO₃/H₂O/MeCN

Method II : PfpOTfa/DIEA/CH₂Cl₂

Method III : PfpOH/EDC·HCl/CH₂Cl₂

Method IV : i) TFA/anisole; ii) 2N HCl; iii) FmocOSu/NaHCO₃/H₂O/MeCN

Monomer	Base ¹	Base ²	Base ³	Method [*]	% yield
T	T ^{Bz}	T		I	78
		T		II	79
		T		III	85
A		A ^{Bz}		I	91
		A ^{Bz}		II	68
		A ^{Bz}		III	81
C		C ^{Bz}		I	83
		C ^{Bz}		II	85
		C ^{Bz}		III	76



Monomer	Base ¹	Base ²	Base ³	Method*	% yield
G	G ^{Ibu}			I	49
	G ^{Cl}	G		IV	54
	G ^{Ibu}			III	66

¹H NMR spectra of the Pfp esters and their parent acids were quite similar (Table 3.5). However, the major difference between the free acid and Pfp ester derivatives was their polarity and can be easily observed by TLC analysis. In general, the esters were significantly less polar than the free acid. ¹³C NMR spectra of the Pfp esters and the free acid were also similar. Nevertheless, the Pfp esters have additional peaks of Pfp carbon-fluorine which were not well determined due to high relaxation ¹³C-¹⁹F couplings. In addition, the ¹³C CO peak of the proline moiety shifted upfield by 5-6 ppm upon formation of the Pfp ester. Comparison of the spectra of cytosine Pfp ester (31) and the cytosine free acid (30) was shown in Figure 3.28.

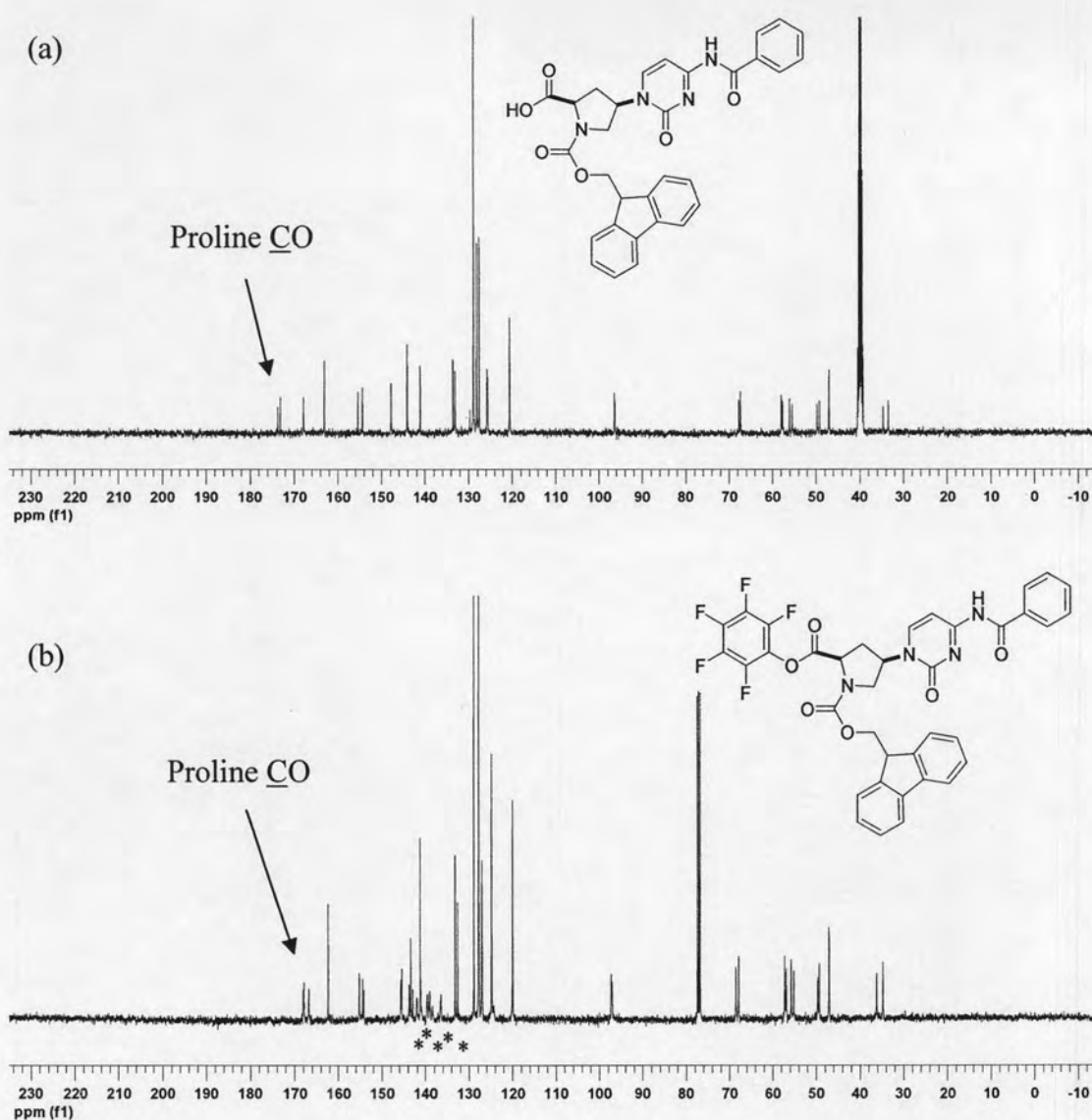
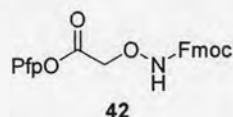


Figure 3.28 Comparison of ^{13}C NMR spectra between (a) (*N*-Fluoren-9-ylmethoxy carbonyl)-*cis*-4-(*N*⁴-benzoylcytosin-1-yl)-D-proline (**30**) and (b) (*N*-Fluoren-9-ylmethoxycarbonyl)-*cis*-4-(*N*⁴-benzoylcytosin-1-yl)-D-proline pentafluorophenyl ester (**31**).

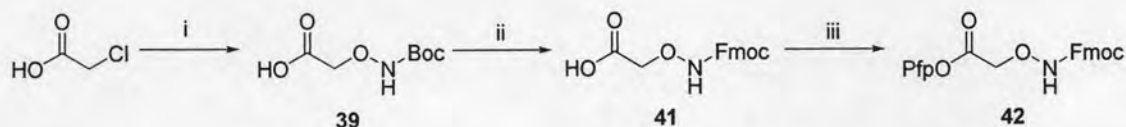
The Pfp ester derivatives **21**, **22**, **23**, **24**, **28**, **31** and **37** were used as monomers in oligomerization *via* solid-phase peptide synthesis which will be discussed in the next section.

3.2 Synthesis of β -amino acid spacers

3.2.1 Synthesis of *O*-spacer



The first group of spacers used in this study was acyclic β -amino acid. Two types of acyclic spacer, namely the *O*-spacer and *N*-spacer, were included to study the effect of flexible structure and positive charge on the spacer, although the acyclic spacer would be expected to increase entropy loss on DNA binding. The monomer for the *O*-spacer is (*N'*-Fluorenylmethoxycarbonyl)-amino-oxy acetic acid pentafluorophenyl ester (**42**). This compound was prepared from protected chloroacetic acid and hydroxylamine as outlined in **Figure 3.29**.



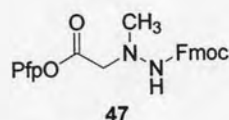
Reagents and conditions : i. BocNHOH, NaOH, EtOH, reflux; ii. (a) conc. HCl, MeOH; (b) FmocCl, NaHCO₃, H₂O, MeCN; iii. PfpOTfa, DIEA, CH₂Cl₂.

Figure 3.29 A synthetic scheme for *O*-spacer.

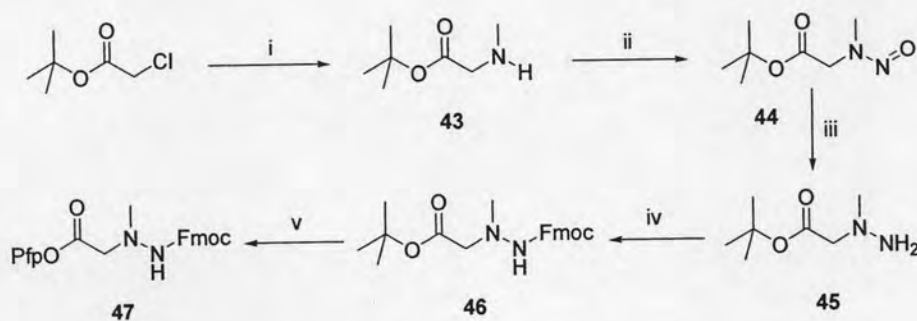
Hydroxylamine hydrochloride was reacted with Boc₂O in the presence of triethylamine in methanol. ¹H and ¹³C NMR spectra indicated that Boc group was successfully attached. Reactions of the BocNHOH with methyl bromoacetate in the presence of K₂CO₃ in refluxing acetonitrile or with chloroacetic acid with sodium hydroxide in refluxing ethanol [91] were not successful. However, when chloroacetic acid was used as the limiting agent, the product *N*-*tert*-Butoxycarbonyl amino-oxy-acetic acid (**39**) can be obtained pure after normal aqueous work-up in a good yield (62%).

The Boc protecting group in compound **39** was changed to Fmoc by treatment with conc. HCl in methanol. The free amino amino-oxy-acetic acid was then reacted with FmocCl in the presence of NaHCO₃. The *N*-Fmoc β -amino acid (**41**) was then activated as Pfp ester using PfpOTfa and DIEA in dichloromethane to afford (*N'*-Fluoren-9-ylmethoxycarbonyl)-amino-oxy acetic acid pentafluorophenyl ester (**42**) as a white solid in 71% yield (25% overall yield).

3.2.2 Synthesis of *N*-spacer



The next acyclic β -amino acid "*N*-spacer" [(*N'*-Fluoren-9-ylmethoxycarbonyl)-(*N*-amino)-*N*-methyl glycine pentafluorophenyl ester] (**47**) was synthesized as outlined in **Figure 3.30** [112].



Reagents and conditions : i. 40 % MeNH₂, KI, H₂O; ii. NaNO₂, 50 % AcOH, 0 °C; iii. Zn, 50 % AcOH, 0 °C; iv. FmocCl, DIEA, CH₂Cl₂; v. a) TFA, CH₂Cl₂; b) PfpOTfa, DIEA, CH₂Cl₂.

Figure 3.30 A synthetic scheme for *N*-spacer.

The *N*-methyl glycine *tert*-butyl ester (**43**) was synthesized in 91% yield by reacting *tert*-butylchloroacetate with 40% methylamine solution and potassium iodide in water. Potassium iodide acted as a nucleophilic catalyst to firstly replace the

chlorine atom and the resulting iodide became a better alkylating agent, which was attacked by the methylamine to afford the product **43**. Nitrosation of the secondary amino group of the compound **43** was achieved under mild conditions using sodium nitrite in 50% acetic acid at 0 °C [94]. The unstable (*N*-nitroso)-*N*-methyl glycine *tert*-butyl ester (**44**) was obtained in 87% yield. The ^1H NMR spectrum of the nitroso compound **44** showed two sets of signals due to the presence of rotameric forms, for example, the proton of methyl at nitrogen (CH_3N) appeared at 3.07 and 3.85 ppm and the proton at α -position appeared as two sets of singlet at 4.10 and 4.82 (Figure 3.31).

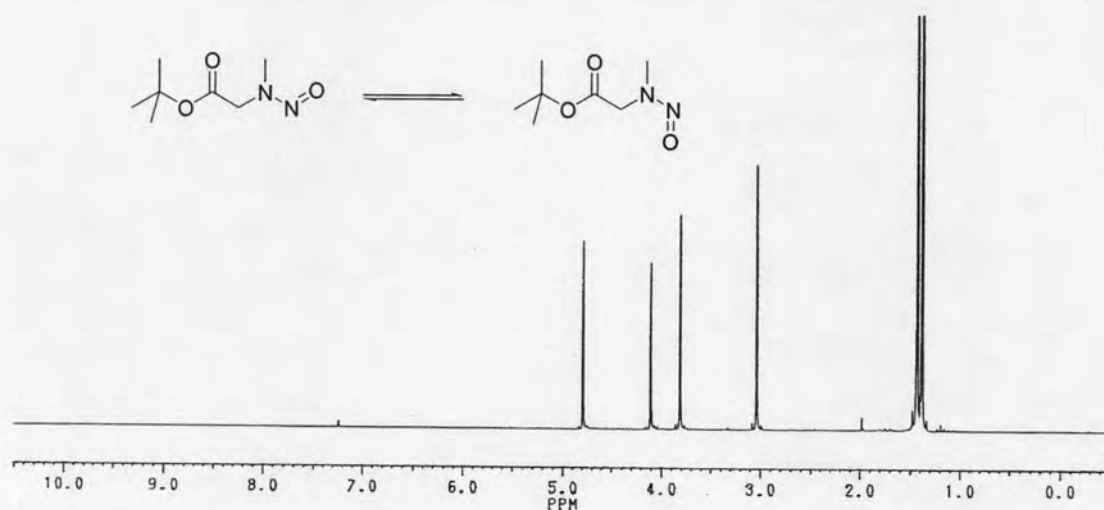


Figure 3.31 ^1H NMR spectrum of (*N*-Nitroso)-*N*-methyl glycine *tert*-butyl ester (**44**).

The partial double bond character of the *N-N* bonds gives rise to a high rotational barrier and this restricted rotation resulted in a slow rotation on the NMR time scale at room temperature similar to what observed in amides.

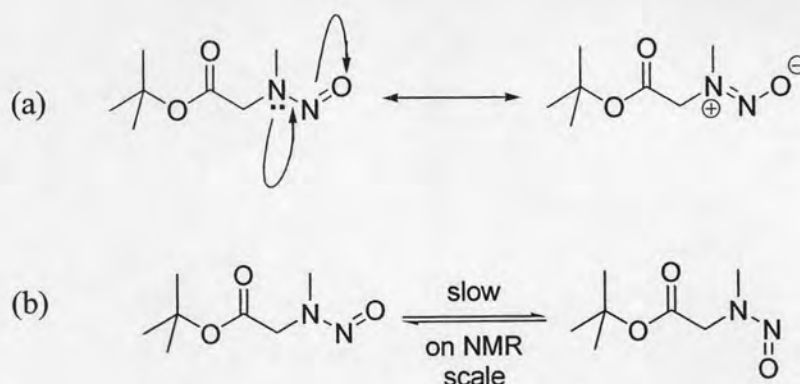


Figure 3.32 (a) The resonance structure of nitroso compound (44) (b) Restricted rotation of around *N-N* bond in (*N*-Nitroso)-*N*-methyl glycine *tert*-butyl ester (44).

The next reaction was the reduction of nitroso group to amino group using zinc metal under acidic conditions at 0 °C. The zinc powder was activated with 10% HCl before use. The progress of the reaction was monitored by TLC. The reaction time was optimized to get a high yield of the hydrazine product **45** with minimal over-reduction, resulting in cleavage of the *N-N* bond. During the work up step, the excess zinc was filtered off and concentrated aqueous ammonia was added to the solution until the solution was strongly basic. This assisted the work-up process because the ammonia formed a zinc-ammine complex, which was water-soluble. Then the product was extracted with dichloromethane and concentrated under reduced pressure afforded a yellow oil, this was shown to be a mixture of the desired hydrazine compound **45** and approximately 20% of the over-reduction product **43** by ^1H NMR spectrum (**Figure 3.33**). The crude hydrazine product could not be purified by chromatography because of its high polarity and instability. However the mixture was used for the next Fmoc protection without further purification.

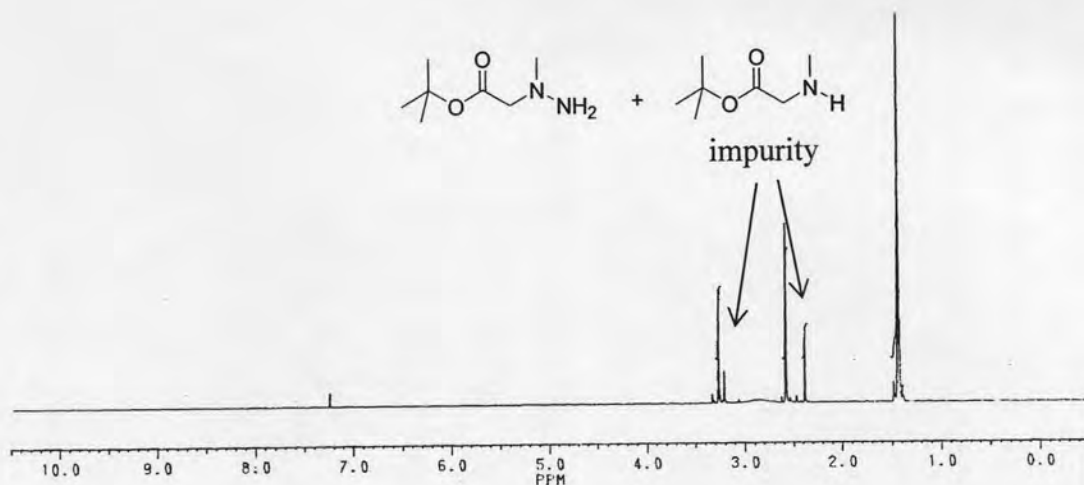


Figure 3.33 The ^1H NMR spectrum of the mixture product of the reduction reaction.

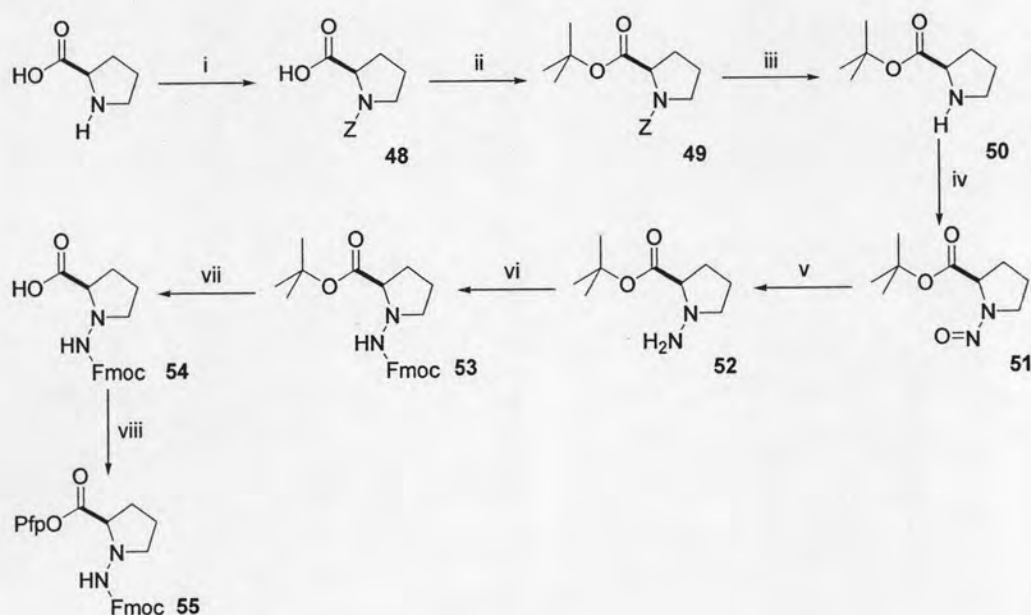
The compound **45** was reacted with FmocCl and DIEA in dichloromethane, the *N*-Fmoc protected β -amino ester was purified by column chromatography (hexanes:ethyl acetate 3:1) to provide the *N*-protected β -amino acid (**46**) as a yellow oil. The compound **46** was treated with TFA/ CH_2Cl_2 to cleave the *tert*-butyl ester to afford the free carboxylic acid. The free acid was immediately activated as the Pfp ester (**47**) using PfpOTfa/DIEA in dichloromethane in the same manner as other monomers.

3.2.3 Synthesis of D-APC spacer and L-APC spacer



The central hypothesis of this work is that it should be possible to enhance further the binding of PNA to the complementary oligonucleotides by replacing the glycine residue of Nielsen's *aeg*PNA with an alternative spacer and an appropriate conformational rigidity [30-33]. However, introducing rigidity will also complicate the synthesis since there would be several possible stereoisomers. The next simplest spacers would be cyclic β -amino acids bearing one chiral stereogenic center. Consequently, (*N'*-fluoren-9-ylmethoxycarbonyl)-*N*-amino-D-pyrrolidinecarboxylic

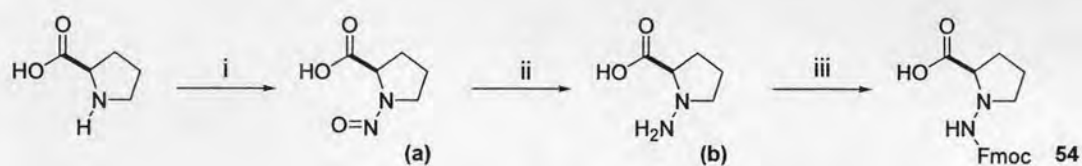
acid pentafluorophenyl ester (**55**) (D-APC) and (*N'*-fluoren-9-ylmethoxycarbonyl)-*N*-amino-L-pyrrolidine carboxylic acid pentafluorophenyl ester (**63**) (L-APC) were chosen to find out the proper configuration of the α -carbon of the spacer. These monomers were synthesized in an identical manner starting from D-proline and L-proline respectively. The synthetic scheme for D-APC spacer is shown in **Figure 3.34**.



Reagents and conditions : i. Z-OSu, aq NaOH; ii. Boc₂O, DMAP, *tert*-BuOH; iii. H₂, Pd/C, MeOH; iv. NaNO₂, 50 % AcOH, 0 °C; v. Zn, 50 % AcOH, 0 °C; vi. FmocCl, DIEA, CH₂Cl₂; vii. TFA, CH₂Cl₂; viii. PfpOTfa, DIEA, CH₂Cl₂.

Figure 3.34 A synthetic scheme for D-APC spacer.

The commercially available unnatural D-proline was the starting material for the D-APC spacer. Attempt to directly nitrosate the free acid followed by reduction of the *N*-nitroso-D-proline (**3.35a**) according to the literature [94] (**Figure 3.35**) gave poor results due to the difficulty in isolation of the highly polar products (**3.35b** and **63**). It was therefore chosen to work with carboxyl-protected derivatives instead.



Reagents and conditions : i. NaNO_2 , 3 M H_2SO_4 , 0 °C; ii. Zn, 50 % AcOH, 0 °C; iii. FmocOSu, NaHCO_3 , H_2O , MeCN;

Figure 3.35 An attempted synthetic scheme for D-APC spacer.

tert-Butyl group was selected as carbonyl protecting group because of its ease of removal and compatibility with the synthetic route chosen. However, synthesis of *tert*-butyl ester is not always simple. A survey of the literature suggests that the reaction of an acid, in this case *N*-nitroso-D-proline (**3.35a**) with *tert*-BuOH in the presence of DCC and DMAP was a possible synthetic route [113], but in our hands the results were not satisfactory. The other general method to convert carboxylic acids to esters was to use acid chloride. The reaction of (**3.35a**) with oxalyl chloride and catalytic amount of DMF followed by *tert*-BuOH was tried. The reaction was also unsuccessful and no ester product could be isolated. Consequently, it was decided to start from esterification of D-proline before nitrosation.

From the literature, *N*-Z proline can be readily changed to *N*-Z proline *tert*-butyl ester in high yield [92,113]. D-Proline was first protected with benzyloxy carbonyl group (Z) using Z-OSu under basic conditions to obtain *N*-Z D-proline (**48**) in high yield (90% and 99% for D-isomer and L-isomer respectively). The *tert*-butyl ester of Z-D-proline (**49**) was prepared according to the literature [92] by the reaction of (**48**) and *tert*-butanol in the presence of Boc_2O and catalytic amount of DMAP. Evolution of carbon dioxide was immediately observed and the reaction was completed in 1 h. *N*-Benzyloxycarbonyl-D-proline *tert*-butyl ester (**49**) was obtained in high yield after column chromatography (84 % and 87 % for D-isomer and L-isomer respectively). The reaction mechanism is explained in **Figure 3.36**.

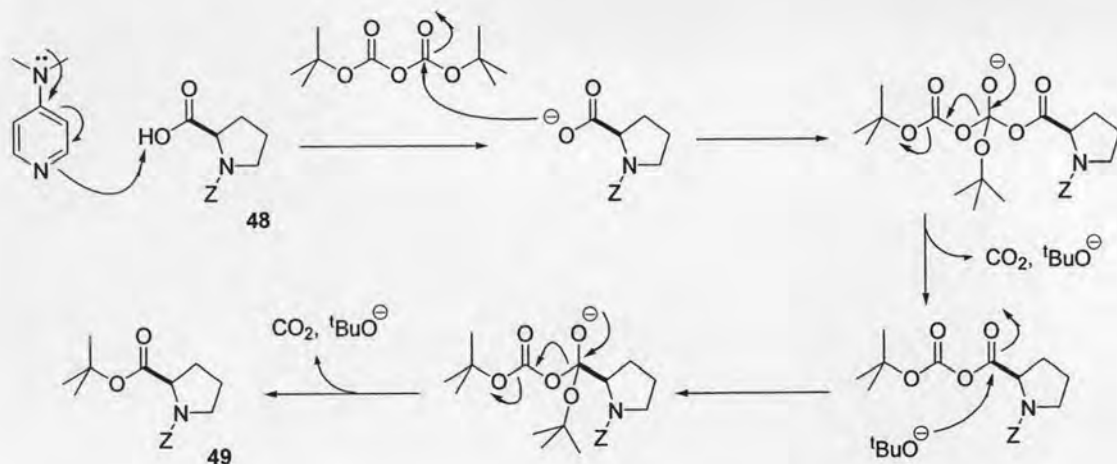


Figure 3.36 The reaction mechanism of *N*-*Z*-D-proline *tert*-butyl ester formation.

The identity of the protected D-proline (**49**) and (**57**) was confirmed by NMR and its optical purity was confirmed by comparison of the optical rotation with the value reported in the literature $\{[\alpha]_D^{25} = +51.1$ ($c=2.10$ g/100 mL, EtOH), for D-isomer and $[\alpha]_D^{25} = -54.3$ ($c=2.10$ g/100 mL, EtOH) for L-isomer, lit $[\alpha]_D^{25} = -54.2$ ($c=2.00$ g/100 mL, EtOH) for L-isomer [114]}. This indicated that racemization was not occurred during the protection steps. After that, the *Z* group of the protected D-proline (**49**) was cleaved by hydrogenolysis using palladium on charcoal catalyst under hydrogen atmosphere [93]. Both D- and L- proline *tert*-butyl esters (**50**) and (**58**) were obtained in high yield (86% and 79% for D-isomer and L-isomer respectively). Nitrosation of the D-proline *tert*-butyl ester (**50**) and the corresponding L-enantiomer (**58**) was successfully carried out using NaNO_2 in 50% acetic acid at 0 °C [94] to give the nitroso compound **51** and **59** in quantitative and 62% yield respectively. Next, the nitroso compounds were reduced by treatment with zinc in cold acetic acid [94]. The residual zinc was removed by filtration and conc. ammonia was added as previously described in the synthesis of the *N*-spacer. After extraction with dichloromethane, the hydrazines were obtained as yellow oil (82% and 84% yield for D-isomer and L-isomer respectively).

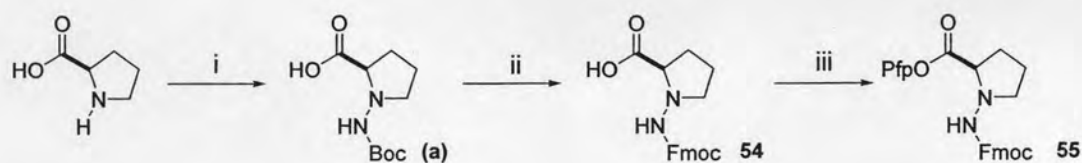
The hydrazine compounds **52** and **60** required Fmoc protection and Pfp-activation. This was carried out similarly to other monomers described previously. The reaction of hydrazines **52** and **60** with FmocCl in the presence of DIEA in dichloromethane afforded the protected hydrazine derivatives **53** and **61**, which were separated with difficulties from by-products *via* chromatography. The pure products

were obtained in only moderate yields (35% and 47% yield for D-isomer and L-isomer respectively). After treatment with TFA in dichloromethane to convert the *tert* butyl esters to the free acids **54** and **62**, they were activated by PfpOTfa/DIEA to give the D-APC and L-APC spacers ready for use in solid phase synthesis (47% and 42% yield from 2 steps for D-isomer and L-isomer respectively). Yields and physical properties of the D-APC and L-APC spacers and their intermediates were summarized in **Tables 3.7**.

Tables 3.7 The comparison detail of D-APC and L-APC.

Compound	D-isomer		L-isomer	
	% yield	$[\alpha]_D^{25}$	% yield	$[\alpha]_D^{25}$
Z-proline (48), (56)	99	+57.7	99	-63.9
Z-proline <i>tert</i> -butyl ester (49), (57)	93	+51.1	87	-54.3
Proline <i>tert</i> -butyl ester (50), (58)	86	+39.0	79	-37.3
<i>N</i> -nitroso proline <i>tert</i> -butyl ester (51), (59)	99	-	62	-
<i>N</i> -amino proline <i>tert</i> -butyl ester (52), (60)	89	-	84	-
<i>N</i> -Fmoc <i>N</i> -amino proline <i>tert</i> -butyl ester (53), (61)	35	+43.1	47	-39.4
<i>N</i> -Fmoc <i>N</i> -amino proline (54), (62)	47	-	42	-
APC monomer (55), (63)		+73.2		-73.8
Overall yield	11	-	7	-

In addition, the D-APC monomer has also been prepared *via* hydrazino acid using oxaziridine methodology [115-116]. This shortens the synthetic route from 8 to 3 steps (**Figure 3.37**).



Reagents and conditions : i. a) Et_4NOH , MeOH; b) *N*-Boc 2-cyanophenylloxaziridine, -15°C ; c) 2 N HCl; ii. a) TFA; b) FmocOSu, NaHCO_3 , H_2O , MeCN; iii. PfpOTfa, DIEA, CHCl_2 .

Figure 3.37 An attempted synthetic scheme for D-APC spacer.

According to this method, the starting amino acid D-proline was first converted into its tetrabutylammonium salt (3.38b) to increase the solubility in chloroform. The reaction with *N*-Boc 2-cyanophenylloxaziridine (3.38a) [117] turned out to be very fast and was completed within less than 1 h at -30°C . The excess 4-cyanobenzaldehyde spontaneously precipitated and was filtered off during the work up step. The aqueous layer was acidified and extracted with ethyl acetate to provide the compound (3.38c) in 87% yield. A possible reaction mechanism was shown in Figure 3.38.

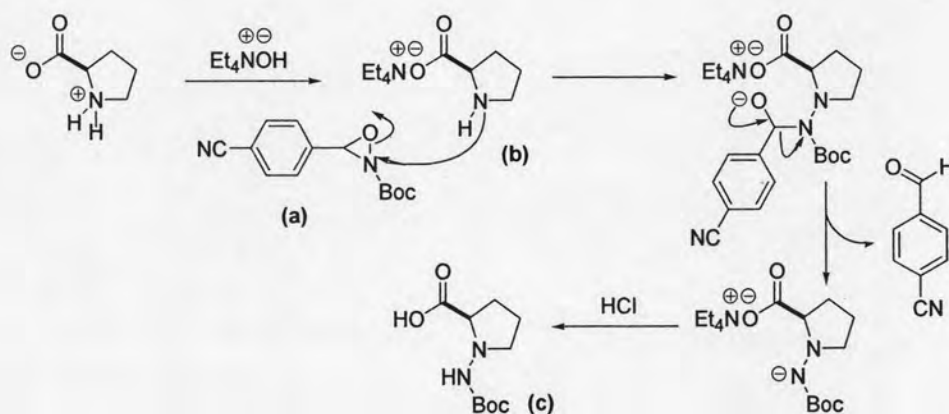


Figure 3.38 Mechanism of amination of proline by oxaziridine reagent.

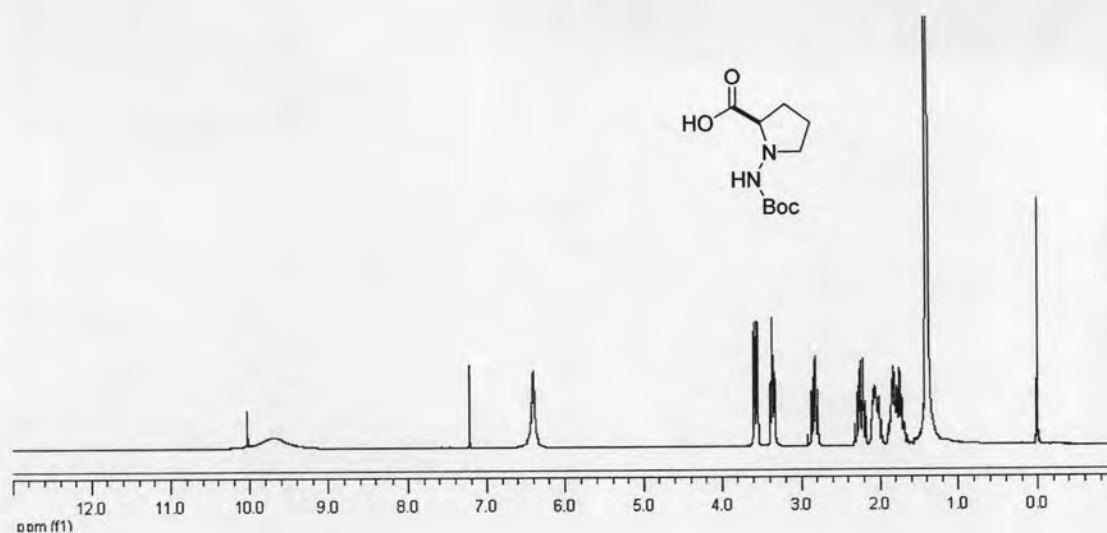


Figure 3.39 ^1H NMR of *N*-Boc hydrazino D-proline (**3.38c**).

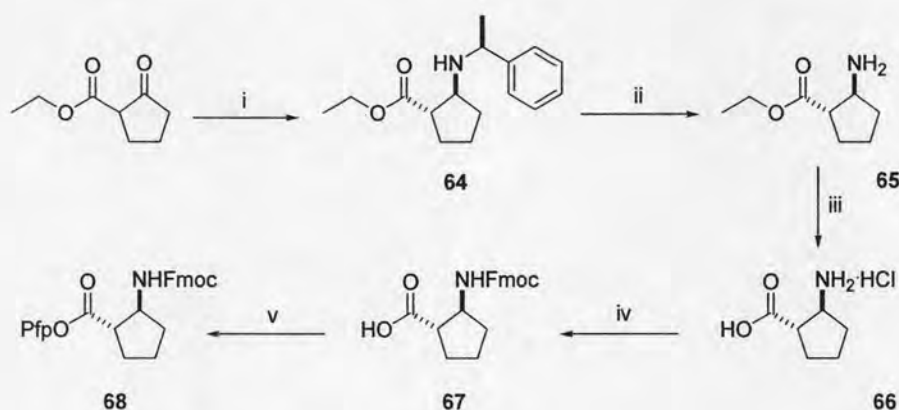
The *N*-Boc protecting group in the hydrazino acid (**3.38c**) was converted into Fmoc group. This was carried out by first treatment with TFA for 8 h. The reaction was flushed with a gentle stream of argon and the residue triturated with ether to obtain the free hydrazino acid as a white solid. Protection with Fmoc using FmocOSu and NaHCO_3 in H_2O and MeCN furnished the compound **54** which was activated with PfpOTfa/DIEA to Pfp ester (**55**) in 15 % overall yield from D-proline.

3.2.4 Synthesis of (1*S*,2*S*)-ACPC and (1*R*,2*R*)-ACPC spacer



Next cyclic β -amino acid spacers with two chiral stereogenic centers with *trans*-configuration were synthesized. These include *trans*-(1*S*,2*S*)-2-aminocyclopentanecarboxylic acid (**68**) [(1*S*,2*S*)-ACPC spacer] and *trans*-(1*R*,2*R*)-2-aminocyclopentanecarboxylic acid (**73**) [(1*R*,2*R*)-ACPC spacer]. Oligomers of these two β -amino acids were shown to have tendency to form a secondary structure or “foldamer” even when the oligomers were relatively short [35]. This might be an important factor for pre-organization of PNA to form duplex or complex with DNA. Synthesis of (1*S*,2*S*)-

ACPC was previously reported by Gellman [95] (**Figure 3.40**). Ethyl cyclopentanone-2-carboxylate was reacted with (*S*)-(-)- α -methylbenzylamine in glacial acetic acid to give an enamine intermediate. The enamine was stereoselectively reduced with sodium cyanoborohydride (NaBH_3CN) at 70 °C to give the (1*S*,2*S*)-*trans* β -amino ester (**64**) accompanied with others stereoisomers, which could be separated by column chromatography on silica in 21% yield.



Reagents and conditions : i. a) (*S*)-(-)- α -methylbenzylamine, glacial AcOH; b) NaBH_3CN , 70 °C; ii. H_2 , $\text{Pd}(\text{OH})_2\text{-C}$, MeOH; iii. 5% HCl, reflux; iv. FmocOSu, NaHCO_3 , H_2O , MeCN; v. PfpOH, EDC·HCl, CH_2Cl_2 .

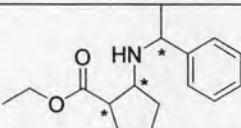
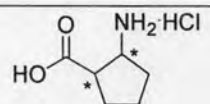
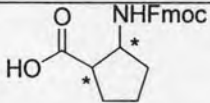
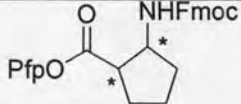
Figure 3.40 The synthetic scheme for (1*S*,2*S*)-ACPC spacer.

The configuration of compound **64** was confirmed by comparison of NMR spectrum and optical rotation value with that reported by Gellman. The (*S*)-methylbenzylamine auxiliary was removed by hydrogenation over a palladium-carbon catalyst in methanol to afford the free amine **65**. Hydrolysis of the ester in refluxing 5% HCl gave the amino acid hydrochloride **66** in 64% yield from compound **64**. Protection of the amino group with FmocOSu was accomplished in the same way as described for protection of the activated PNA monomers. This resulted in the free acid compound **67** in 63% yield. The ^1H NMR spectra of compound **67** showed the following important signals: 1.41-1.69 [CH_2 ring ACPC] 1.86-1.99 [CH_2 ring ACPC] 2.48-2.61 [CHCO_2H] 4.01-4.04 [CHNH] 4.19-4.28 [CH_2 and CH Fmoc] 7.29-7.47 [CH Ar Fmoc] 7.68 [CH Ar Fmoc] 7.85 [CH Ar Fmoc] which is in good agreement with the literature values [95]. The structure was further confirmed by comparing the

specific rotation value ($[\alpha]_D +36.4$, $c = 1.0$ in MeOH) with the value reported in the literature ($[\alpha]_D +36.3$, $c = 1.21$ in MeOH). The Fmoc free acid **67** was converted to the Pfp ester by reacting with PfpOH and EDC·HCl. The product **68** was obtained in 78% yield as a white solid. The identity of the product was confirmed by ^1H and ^{13}C NMR spectroscopy, which were fully consistent with the expected structure.

The (1*R*,2*R*)-ACPC spacer was similarly prepared but the chiral auxiliary was changed from (*S*)-(-)- α -methylbenzylamine to (*R*)-(+)- α -methylbenzylamine in the first step. This resulted in Ethyl (1*R*,2*R*)-2-[(1'*R*)-phenylethyl]-aminocyclopentane carboxylate (**69**) which was the precursor of (1*R*,2*R*)-ACPC spacer. Removal of the chiral auxiliary and acid hydrolysis gave the free amino acid hydrochloride salt (**71**) which was protected Fmoc and activated to the Pfp ester as usual for PNA monomers. The synthetic details and characterization data was demonstrated in **Tables 3.8** and **Section 2.3.6**.

Tables 3.8 The comparison detail of (1*S*,2*S*)-ACPC and (1*R*,2*R*)-ACPC.

Compound	(1 <i>S</i> ,2 <i>S</i>)-ACPC		(1 <i>R</i> ,2 <i>R</i>)-ACPC	
	% yield	$[\alpha]_D^{25}$	% yield	$[\alpha]_D^{25}$
	21	-	29	-
	64	-	70	-
	63	+36.4 ^a	64	-47.5 ^a
	95	+51.4 ^b	84	-46.5 ^c
Overall yield	8	-	11	-

^a the optical rotation were operated in MeOH ($c=1.00$ g/100 mL).

^b the optical rotations were measured in chloroform ($c=1.00$ g/100 mL).

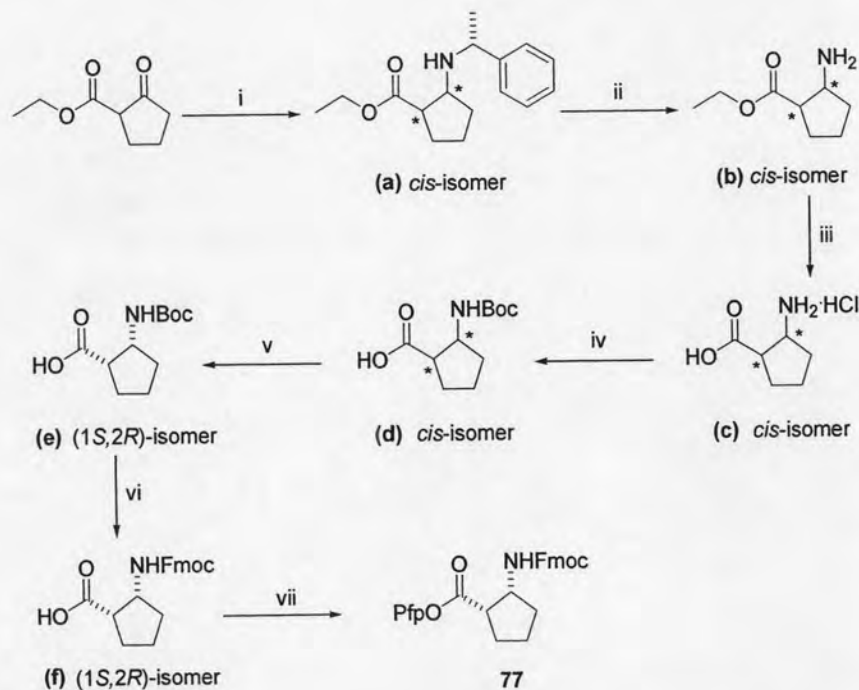
^c the optical rotations were measured in chloroform ($c=0.54$ g/100 mL).

Since the (1*S*,2*S*)-ACPC and (1*R*,2*R*)-ACPC spacers are enantiomers pair, therefore they should have identical ¹H and ¹³C NMR spectra, but opposite in optical rotation. Indeed the (1*R*,2*R*)-ACPC spacer shows the value of $[\alpha]_D^{25} = -46.5$ (*c* = 0.54 g/100 mL, CHCl₃) compared with $[\alpha]_D^{25} = +51.4$ (*c* = 1.00 g/100 mL, CHCl₃) for (1*S*,2*S*)-ACPC spacer. The NMR spectra of both compounds are shown in the next section (**Figure 3.45**).

3.2.5 Synthesis of (1*S*,2*R*)-ACPC and (1*R*,2*S*)-ACPC spacer



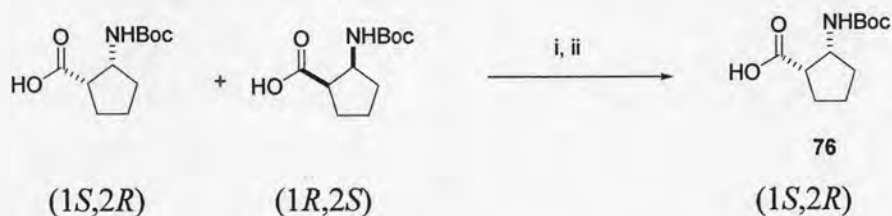
The *cis*-(1*S*,2*R*)-2-aminocyclopentanecarboxylic acid [(1*S*,2*R*)-ACPC spacer] and *cis*-(1*R*,2*S*)-2-aminocyclopentanecarboxylic acid [(1*R*,2*S*)-ACPC spacer] were stereoisomers of aminocyclopentanecarboxylic acid with *cis*-configuration. Similar to (1*S*,2*S*)-ACPC and (1*R*,2*R*)-ACPC, synthesis of these monomers started from ethyl cyclopentanone-2-carboxylate and methylbenzylamine as chiral auxiliaries. However, under slightly different reduction conditions, the *cis*-isomers may be obtained as the major products [96] as shown in **Figure 3.41**.



Reagents and conditions : i. a) (*R*)-(+)- α -methylbenzylamine, Na₂SO₄, toluene; b) NaHB(OAc)₃, AcOH, MeCN, 0 °C; ii. H₂, Pd(OH)₂-C, MeOH; iii. 5 % HCl, reflux; iv. Boc₂O, Na₂CO₃, *tert*-BuOH, H₂O; v. a) L-(-)-ephedrine; b) fractional recrystallization; c) NaHSO₄; vi. a) 2 N HCl, reflux; b) FmocOSu, NaHCO₃, H₂O, MeCN; vii. PfpOTfa, DIEA, CH₂Cl₂.

Figure 3.41 The proposed synthetic scheme for (1*S*,2*R*)-ACPC spacer.

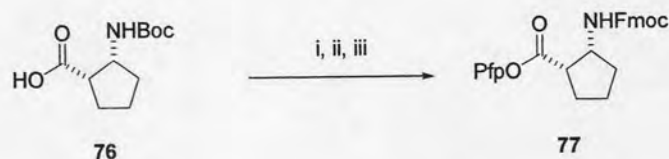
The enamine intermediate was stereoselectively reduced with sodium triacetoxyborohydride [NaHB(OAc)₃] to give a mixture of *cis*-isomer as the major product. In a typical procedure, a solution of sodium triacetoxyborohydride was prepared by addition of NaBH₄ to glacial acetic acid while keeping the temperature between 10-20 °C. After the hydrogen gas evolution had ceased (30 min) acetonitrile was added and the temperature was lowered to 0 °C (ice bath). The β -enamino ester was added in one portion and the reaction stirred for 1-3 h at 0 °C. After removal of the chiral auxiliary and hydrolyzing the ethyl ester to free carboxylic provided the product (**3.41c**) in the *cis*-configuration. However, this material was not optically pure and required further enrichment. The optically pure (1*S*,2*R*)-isomer of the *N*-Boc protected acid were obtained *via* fractional recrystallization with (-)-ephedrine in 37% recovery [118]. The optical rotation value of the *N*-Boc protected free acid was consistent with the literature value {[α]_D³⁰ +65.4 (*c*=1.28, MeOH), lit [α]_D²² +64.9 (*c*=1.3, MeOH) [138]} indicating that the resolution was successful.



Reagents and conditions : i. (-)-ephedrine then fractional crystallization (37% recovery) ii. aq. HCl (80%)

Figure 3.42 Enantiomeric enrichment of (1*S*,2*R*)-ACPC spacer.

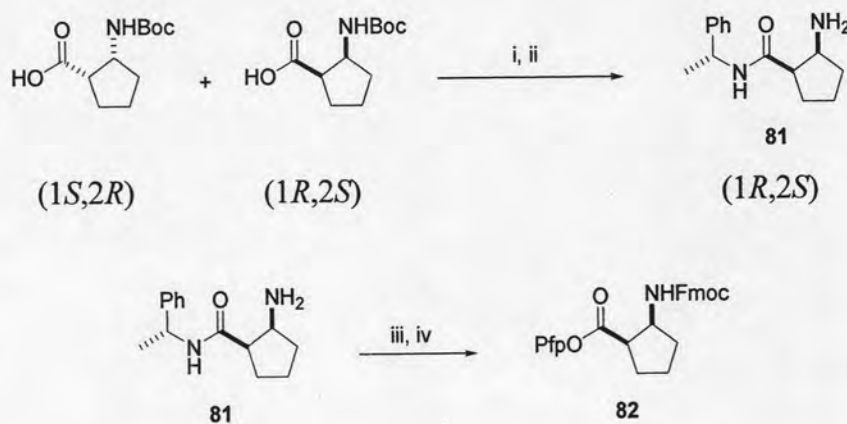
The *N*-Boc protected amino acid was deprotected by treatment with HCl. After that, the protection of Fmoc and activation with Pfp was performed to get the (1*S*,2*R*)-ACPC spacer (**77**) as shown in **Figure 3.42** and **3.43**.



Reagents and conditions : i. 2 N HCl, reflux (98%); ii. a) FmocOSu, NaHCO₃, H₂O, MeCN (98%); b) PfpOTfa, DIEA, CH₂Cl₂ (66%).

Figure 3.43 Preparation of the (1*S*,2*R*)-ACPC spacer.

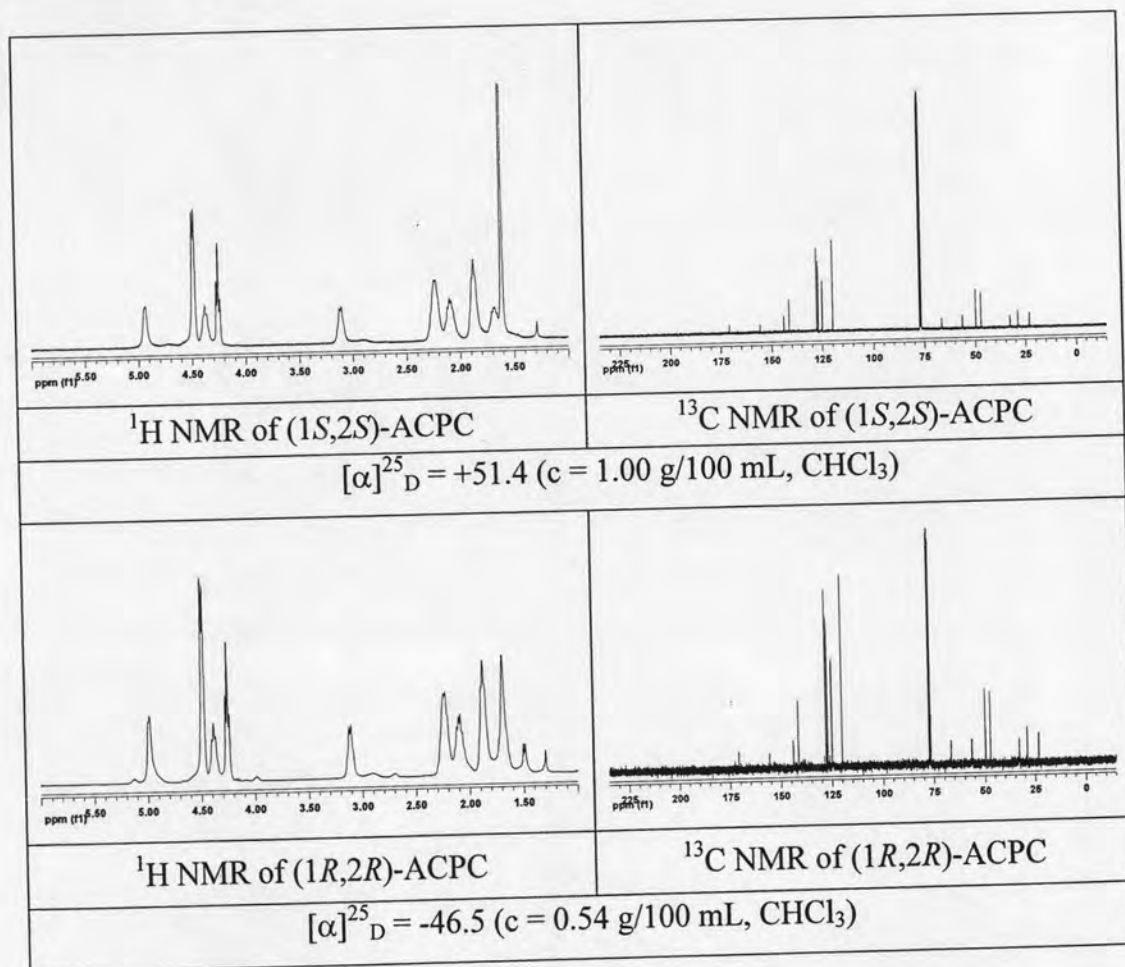
For the (1*R*,2*S*)-ACPC spacer, this monomer can be prepared in the same manner to (1*S*,2*R*)-ACPC spacer above by changing the chiral auxiliary from (*R*)-(+)- α -methylbenzylamine to (*S*)-(-)- α -methylbenzylamine in the first step. However, since (+)-ephedrine is not available, the enrichment step must be modified following a literature procedure [139]. The (1*R*,2*S*)-Boc free acid was coupled with (*R*)-(+)- α -methylbenzylamine using EDC·HCl in dichloromethane to obtain a mixture of diastereomeric pair, which were separated by column chromatography after removing the Boc group by TFA. The auxiliary group was hydrolyzed under acid hydrolysis. Fmoc protection and Pfp activation as usual afforded the (1*R*,2*S*)-ACPC spacer as shown below in the **Figure 3.44**.



Reagents and conditions : i. (*R*)-methylbenzylamine, DCC, CH₂Cl₂ (48%); ii. a) TFA b) aq Na₂CO₃ c) column chromatography (42%) iii. a) 2 N HCl, reflux; (98%) b) FmocOSu, NaHCO₃, H₂O, acetone; iv. PfpOTfa, DIEA, CH₂Cl₂ (78%)

Figure 3.44 The proposed synthetic scheme for (1*R*,2*S*)-ACPC spacer.

The NMR spectrum of the two *cis*-monomers were identical but were slightly different from their diastereomers [(1*S*,2*S*)-ACPC spacer and (1*R*,2*R*)-ACPC spacer] as shown in **Figure 3.45**. For example, the α -proton of (1*S*,2*S*)-ACPC and (1*R*,2*R*)-ACPC appeared as a broad multiplet at 3.11 ppm and 3.10 ppm respectively, while that of (1*S*,2*R*)-ACPC and (1*R*,2*S*)-ACPC isomers were a double doublet signal at 3.51 ppm and 3.50 ppm respectively. In addition, the optical rotation values of enantiomeric pairs were opposite.



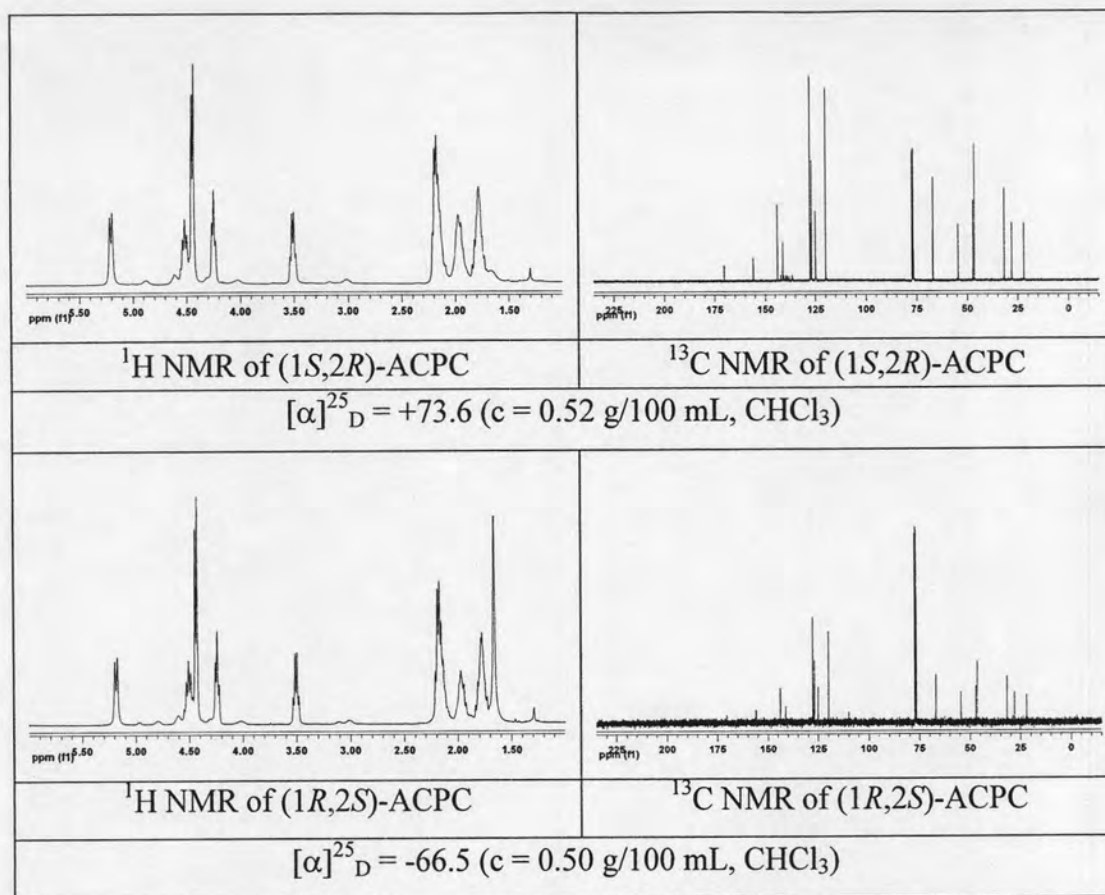


Figure 3.45 Comparison of NMR spectra of (1*S*,2*S*)-ACPC, (1*R*,2*R*)-ACPC, (1*S*,2*R*)-ACPC and (1*R*,2*S*)-ACPC spacers.

In summary, all three types of β -amino acid spacers consisting of totally eight compounds were successfully synthesized in the form of Fmoc/Pfp ester. The structures were confirmed by NMR spectra as well as elemental analysis (or HRMS) and optical rotation (for chiral compounds). The details of synthesis and characterization data were summarized in **Table 3.9**.

Table 3.9 The percent yield, optical rotation values and CHN or HRMS analysis of all spacers.

Spacer	Yield	$[\alpha]^{25}_D$	Calcd. CHN	Found CHN
<i>O</i> -spacer (42)	25% ^a	-	502.0690 ^c	502.0147 ^c
Spacer	Yield	$[\alpha]^{25}_D$	Calcd. CHN	Found CHN
<i>N</i> -Spacer (47)	12% ^b	-	C 58.54 % H 3.48 % N 5.69 % (515.1006) ^c	C 58.51 % H 3.46 % N 5.69 % (515.0425) ^c
D-APC (55)	11% ^c	+73.2	C 60.20 % H 3.69 % N 5.40 %	C 60.20 % H 3.72 % N 5.30 %
L-APC (63)	7% ^c	-73.8	C 60.20 % H 3.69 % N 5.40 %	C 60.10 % H 3.36 % N 5.26 %
(1 <i>S</i> ,2 <i>S</i>)-ACPC (68)	8% ^d	+51.4	C 62.93 % H 3.86 % N 2.75 %	C 62.93 % H 3.86 % N 2.75 %
(1 <i>R</i> ,2 <i>R</i>)-ACPC (73)	7% ^d	-46.5	C 62.93 % H 3.86 % N 2.75 %	C 62.93 % H 3.85 % N 2.75 %
(1 <i>S</i> ,2 <i>R</i>)-ACPC (77)	14% ^d	+73.6	C 62.93 % H 3.86 % N 2.75 %	C 62.79 % H 3.87 % N 2.51 %
(1 <i>R</i> ,2 <i>S</i>)-ACPC (82)	18% ^d	-66.5	C 62.93 % H 3.86 % N 2.75 %	C 62.68 % H 3.92 % N 2.67 %

a: Calculated from chloro acetic acid (4 steps), **b:** Calculated from *tert*-butyl chloro acetate (6 steps), **c:** Calculated from D-proline or L-proline (8 steps), **d:** Calculated from ethyl cyclopentanone-2-carboxylate (5-7 steps), **e:** $[M+Na]^+$

3.3 Synthesis of PNA oligomers

3.3.1 Standard procedure of solid phase peptide synthesis

A pyrrolidine monomer containing a nucleobase and a β -amino acid spacer was coupled together *via* a peptide bond to become one subunit of PNA. By coupling repeated on a solid support, PNAs of desired sequence were obtained.

Bruce Merrifield developed the principle of solid phase chemistry in 1963 [119], the method based on the idea that peptide chain could be lengthened in a stepwise process while it was attached at one end by a covalent bond to a solid supporting particle such as polystyrene resin. The process involves simple washing and filtration steps hence resulted in operational simplicity, fast reaction, minimized product loss, producing higher-yield (milligram levels of material) and higher-purity peptides. The synthetic peptides are usually extended from C (carboxyl) terminus to N (amino) terminus through a series of coupling cycles. The peptide chain was released from the support after the desired sequence had been assembled.

In this work, the microscale synthesis of PNA was carried out manually in a custom-made Pasteur pipette as described in **Section 2.3.1**. TentaGel [120] resin has been used extensively for PNA synthesis. It contains a polyethylene glycol (PEG) grafted on polystyrene resin by a benzylic ether bond and a moderately acid labile Rink amide (RAM) linker [121] (**Figure 3.46**). This linker is stable to piperidine which is used in Fmoc SPPS and can be easily cleaved with 95% TFA to provide peptide amides. In addition, the amino linker of RAM resin allows easy coupling with active esters such as Pfp ester to form amide bonds giving higher loading efficiency compared to resins containing *p*-benzyloxybenzyl alcohol linker such as Wang resin [122]. TentaGel resin with Rink amide linker was a commercially products available from NovaBiochem (NoyaSyn TGR) or Fluka (Tentagel S-RAM).

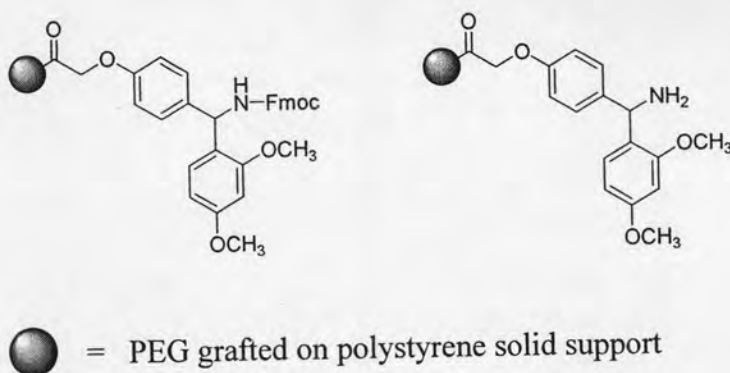


Figure 3.46 TentaGel S RAM Fmoc resin and TentaGel S RAM resin.

The TentaGel-type resin was chosen as the support for PNA synthesis because of its good swelling ability in many solvents, especially in *N,N*-dimethylformamide (DMF) which is the only solvent used for Fmoc-SPPS in this study. The swelling property of the solid support will determine how the reactant can access reactive sites on the solid support which has a direct consequence on the synthesis efficiency.

Synthesis of PNA (**P1**) consists of three important steps as follows.

i) Deprotection step: removal of the Fmoc protecting group from the amine group of the growing PNA oligomer, which is accomplished by 20% piperidine in DMF.

ii) Coupling step: the pyrrolidine monomer or β -amino acid spacer was alternately coupled by coupling reagent or activator to the chain end on the resin. This step was repeated until to give the required sequence.

iii) Capping step: the resin-bound amino group that had not been successfully coupled was capped by an acetyl group for stopping incomplete peptide chain from participation in the next cycle. Capping is carried out with a solution of 10 % Ac_2O /DIEA in DMF.

The synthesis cycle of PNA originally used in this study is exactly as described in the literature [123]. The details of which are shown in **Figure 3.47**.

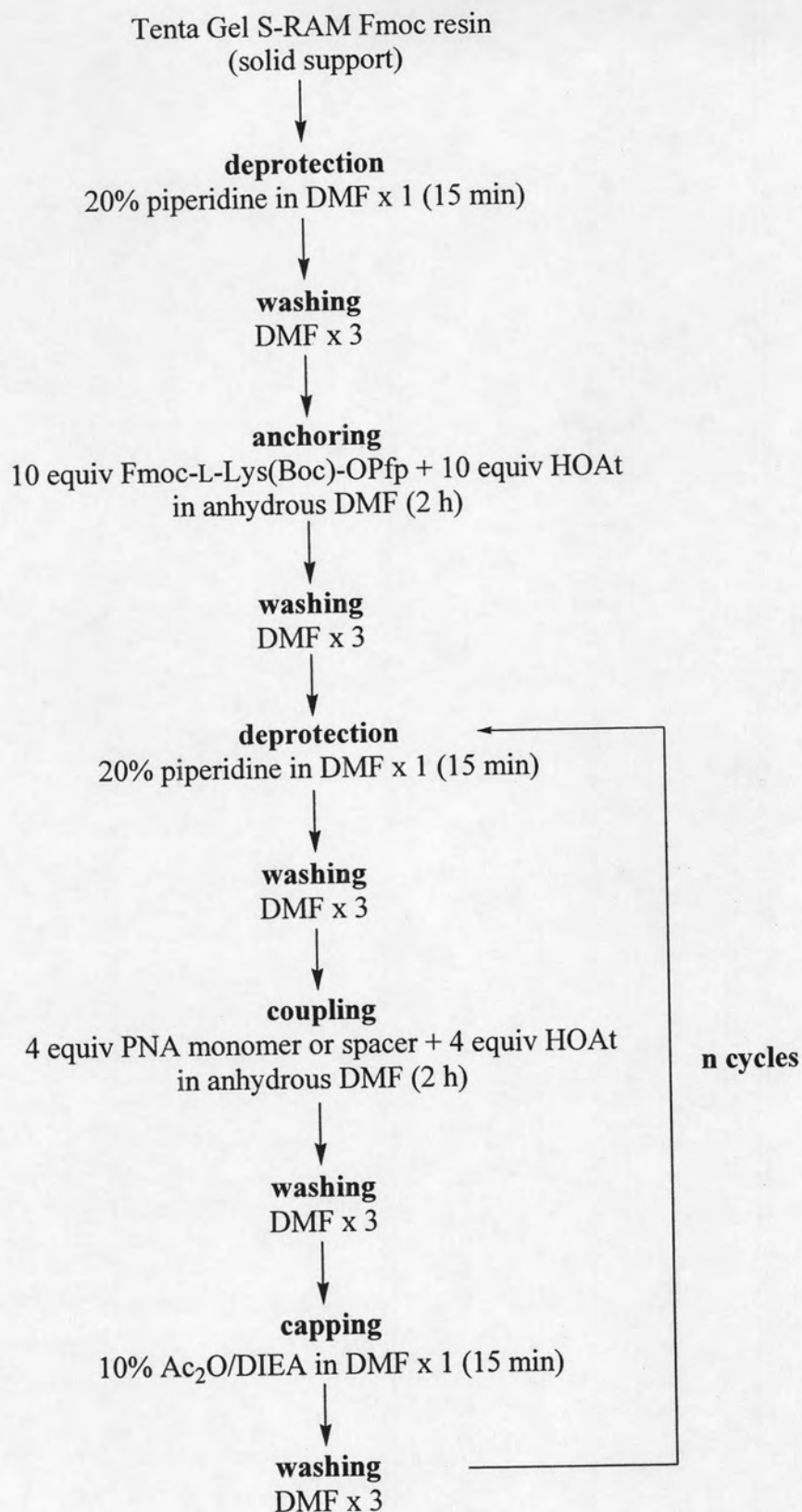


Figure 3.47 The original standard protocol for solid phase synthesis of PNA.

At the beginning, the resin in the SPPS column was swollen in anhydrous DMF for at least 30 min before the synthesis cycle started. In the next step, the TentaGel S-RAM resin which carry Fmoc group was deprotected by treatment with 20% piperidine in DMF for 15 min. For the NovaSyn TGR resin, which contains free NH_2 groups, this step can be skipped. The deprotected Fmoc group was liberated from the resin-bound peptide as the piperidine-dibenzofulvene adduct (**3.48b**) by an E_1CB -type mechanism *via* the stabilized dibenzocyclopentadienyl anion (**3.48a**) as shown in **Figure 3.48**.

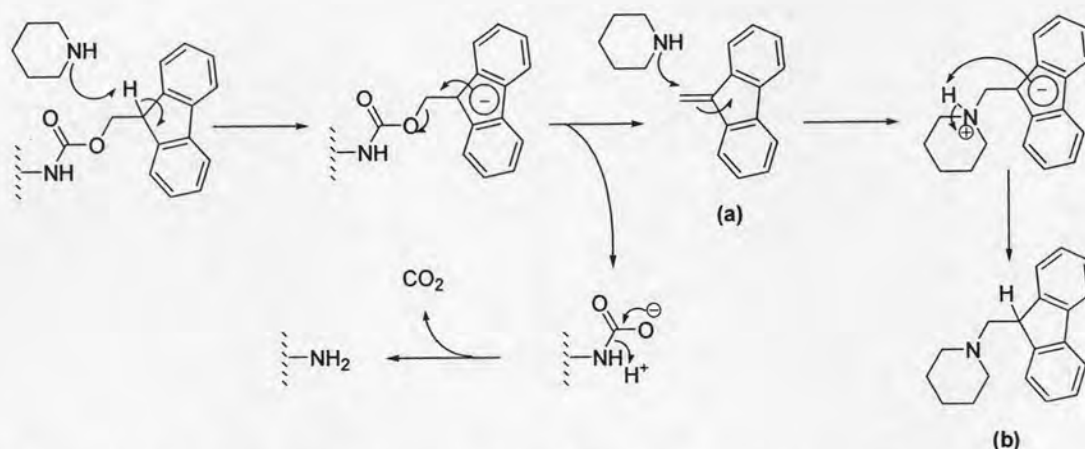


Figure 3.48 Mechanism for deprotection of Fmoc protecting group from resin bound peptide.

After the first deprotection, the resin was then anchored with Fmoc-Lys(Boc)-OPfp as the first amino acid residue. Attachment of lysine has been extensively employed in the literature [14,124]. It has been suggested that introducing a lysine at C-terminus of a PNA chain was necessary to prevent self aggregation of the PNA due to the repulsion of the lysine positively charged side chain. It also increased the solubility of the PNA in aqueous medium. In this study, attempts have been made to remove the lysine. This resulted in PNA which were not soluble in water, therefore we chose to follow the same practice. The coupling step of lysine residue was performed in the presence of 1-hydroxy-7-azabenzotriazole (HOAt) as an auxiliary nucleophile or “activator”. The role of the activator was to increase the reactivity of the Pfp ester by a transient formation of the highly reactive HOAt ester (**Figure 3.49**). It has been reported that HOAt is more reactive and provide less racimization than

HOBt and is now becoming the most popular additive for peptide coupling reactions [125-126].

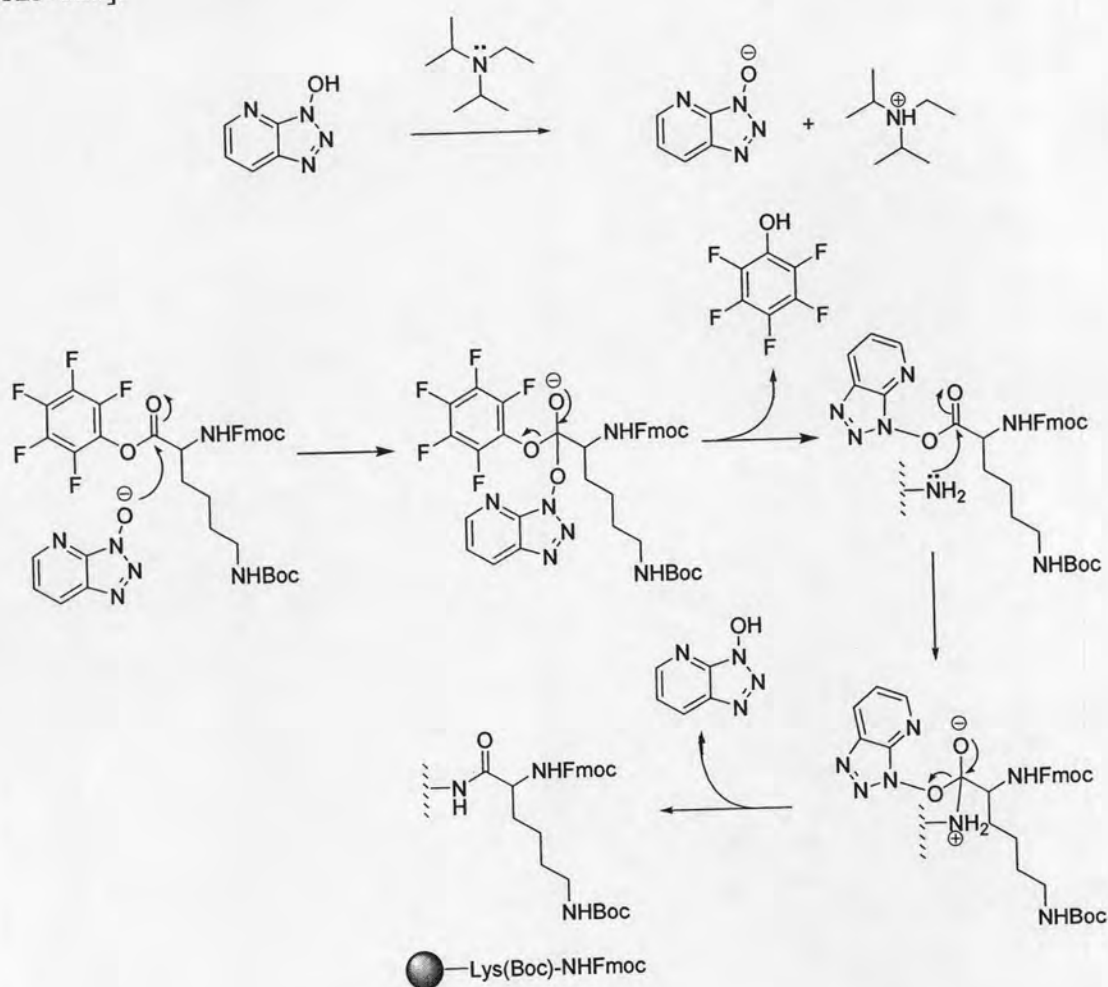


Figure 3.49 Mechanism for coupling of anchoring *via* HOAt.

It is noted that the equivalent of Fmoc-Lys(Boc)-OPfp in the coupling step was necessarily high due to the heterogeneous nature of SPPS. The reaction could not be completed at 1:1 stoichiometry between the reactant and the resin-bound intermediate within a reasonable time scale. Similar to lysine loading, other pyrrolidine monomers and spacers were generally used in excess (4 equivalents) and at a high concentration (~ 0.1 M) to compromise between the cost of the monomers and the coupling efficiency. After the first attachment of lysine to the resin, the Fmoc deprotection step was repeated to free up the amino group, which was alternately coupled with the activated pyrrolidine monomers and spacer. In some cases, attempts have been made to synthesize the PNA using Fmoc acid pyrrolidine free acids, which was activated *in situ* with HATU in the presence of DIEA (2 equiv), instead of active

Pfp ester. The comparative efficiency of free acid and Pfp ester was demonstrated in the **Table 3.11** in **Section 3.3.3**. The reaction mechanism of this amide formation mediated by HATU is demonstrated in **Figure 3.50**.

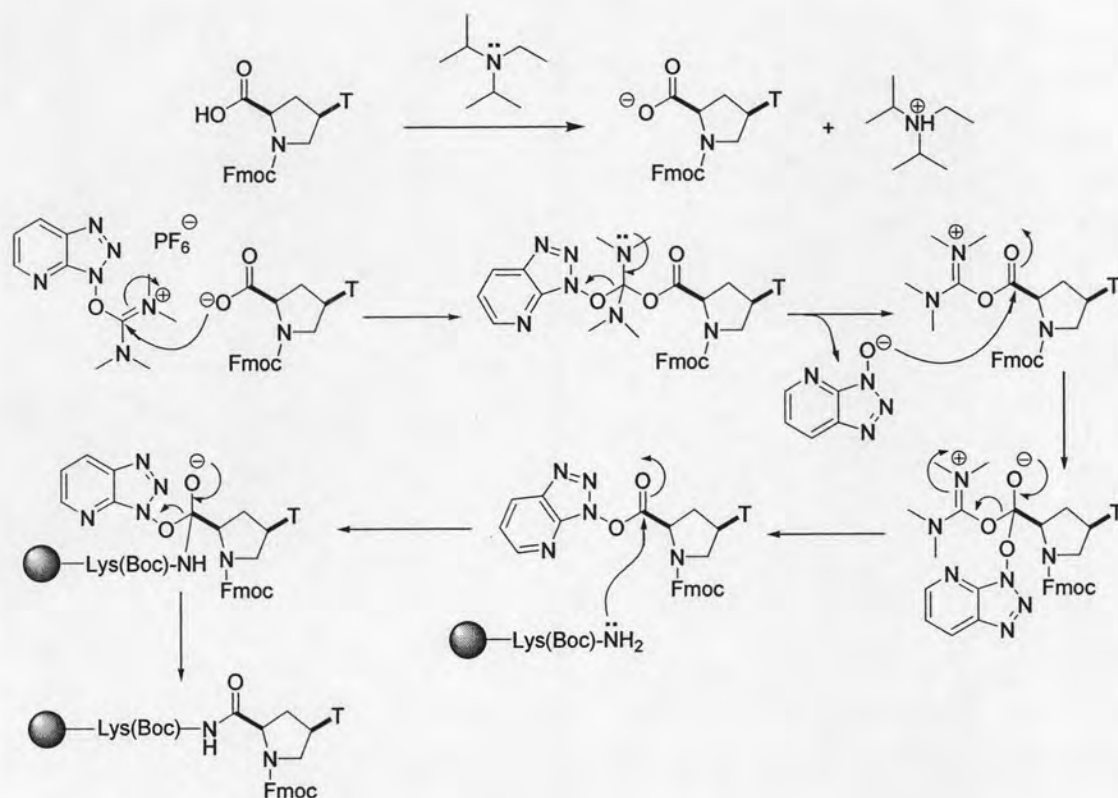


Figure 3.50 Mechanism for coupling of thymine Fmoc acid *via* HATU.

An extensive washing with DMF was performed after each step to remove the excess reagent. After the coupling reaction, unreacted amino groups were capped by addition of 10% Ac₂O/DIEA in DMF to stop the incomplete peptide chains from growing. The coupling efficiency can be monitored by measurement of the absorbance of dibenzofulvene-piperidine adduct released upon deprotection at 264 nm. Then the synthesis cycle was repeated until the growing peptide chain was extended up to the desired length (typically 5 to 10 bases). The coupling efficiency in each step was calculated from UV-absorption and a typical example is shown in **Table 3.10**.

Table 3.10 UV-absorption data and percent coupling efficiency in the synthesis of *cis*-D/D-APC Fmoc-T₅-LysNH₂ (**P1**).

Cycle No.	Monomer	Code	OD ₂₆₄ ^b	%efficiency
1	Fmoc-Lys(Boc)-OPfp	Lys	-	-
2	Fmoc-D-Pro-(<i>cis</i> -4-T)-OH (21)	T1	1.960	100%
3	Fmoc-D-APC-OPfp (55)	X1	1.888	97%
4	Fmoc-D-Pro-(<i>cis</i> -4-T)-OH (21)	T2	1.515	80%
5	Fmoc-D-APC-OPfp (55)	X2	1.623	107%
6	Fmoc-D-Pro-(<i>cis</i> -4-T)-OH (21)	T3	1.271	78%
7	Fmoc-D-APC-OPfp (55)	X3	1.388	109%
8	Fmoc-D-Pro-(<i>cis</i> -4-T)-OH (21)	T4	1.220	88%
9	Fmoc-D-APC-OPfp (55)	X4	1.153	95%
10	Fmoc-D-Pro-(<i>cis</i> -4-T)-OH (21)	T5	0.970	84%
11	Fmoc-D-APC-OPfp (55)	X5	-	-
Overall coupling efficiency				50%
Average coupling efficiency/step				93%

a when T is thymine pyrrolidine monomer (**21**) and X is the spacer (**55**).

b all OD₂₆₄ were received from 100-fold dilution with absolute methanol.

After addition of the final residue was completed, the Fmoc group at the *N*-terminus may be retained or removed by treatment with 20% piperidine in DMF, depending on the overall efficiency of the coupling reaction. If the efficiency was low, the Fmoc group was used as a handle for reverse-phase HPLC purification because of the polarity difference between *N*-Fmoc PNA and NH₂-PNA. For adenine, cytosine and guanine-containing PNA sequences, the exocyclic amino protecting groups (benzoyl and isobutyryl) were removed by treatment with 1:1 ammonia/dioxane in a sealed test tube at 55 °C for 6 h prior to the cleavage from the resin [123]. In these cases, the Fmoc group must be first deprotected and the free amino terminus capped with acetic anhydride to increase the stability of the PNA. Finally, the PNA sequence was released from the resin by treatment with 95% trifluoroacetic acid to

give the peptide amide which was collected as crude after removing the volatile and precipitating with ether. The mechanism of the cleavage step is shown in **Figure 3.51**. The acid-labile Boc group at the side chain of lysine was also simultaneously cleaved by the action of TFA.

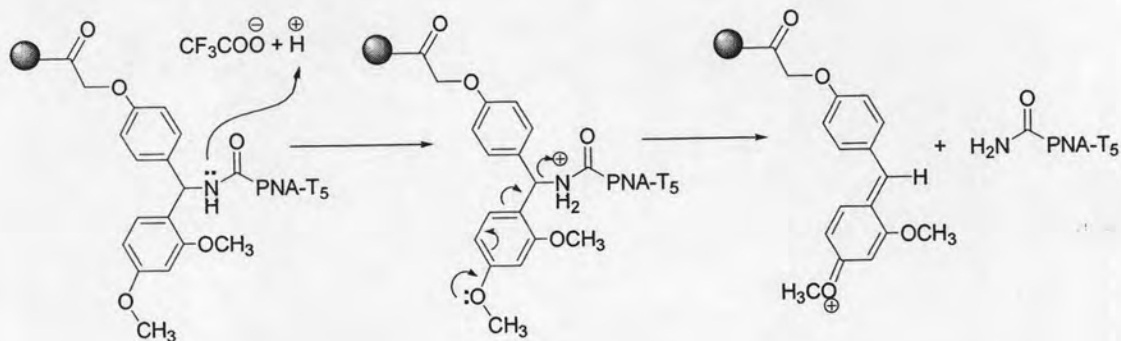
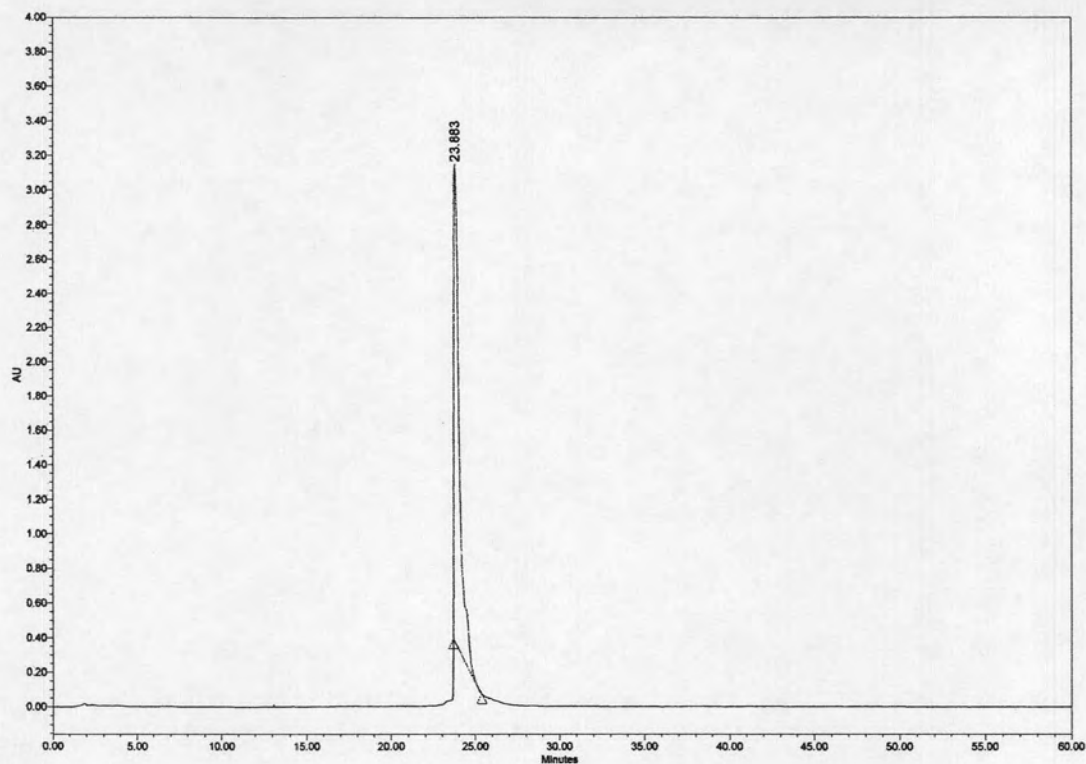
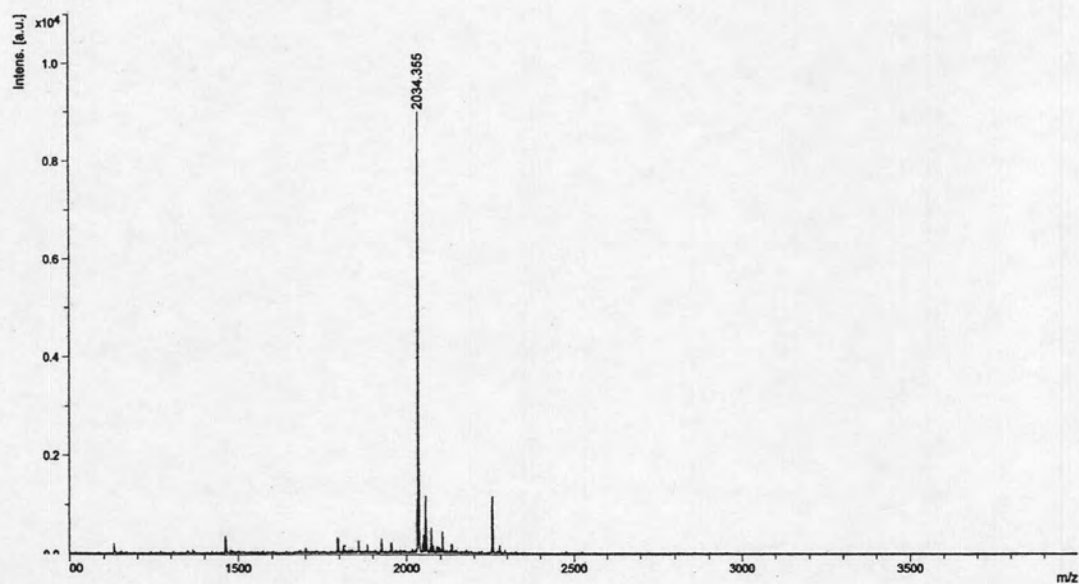


Figure 3.51 Mechanism for cleavage PNA from the resin in TFA

The PNA sequence was purified with C-18 reverse phase HPLC monitoring by UV-absorbance at 260 nm. And typical chromatogram is shown in **Figure 3.52a**. The collected fractions containing the major peak were combined and dried under vacuum centrifugation (speed rotavapor). The residue was redissolved in 150 μL of water and the concentration of the PNA was determined spectrophotometrically. The identity of the PNA was confirmed by MALDI-TOF mass spectrometry which showed the expected mass of the molecular ion $[\text{M}+\text{H}]^+$ or $[\text{M}+\text{Na}]^+$ as shown in **Figure 3.52b**. All hybridization studies were then conducted using this PNA solution.



(a)



(b)

Figure 3.52 (a) HPLC chromatogram using condition displayed in **Figure 2.2** and (b) MALDI-TOF MS of *cis*-D/D-APC Fmoc-T₅-LysNH₂, $M \cdot H^+$ (calcd) = 2035.996

3.3.2 Combined Solution-Solid Phase Synthesis of PNA

The above strategy for solid phase synthesis of PNA was quite lengthy because two monomers (pyrrolidine and spacer) must be coupled for each base sequence. Furthermore, it was oftenly observed that coupling of the activated pyrrolidine monomer onto the resin-bound amino group of the spacer was not always efficient. Therefore it was decided to attempt a segment SPPS by first coupling the pyrrolidine monomer to the spacer in solution using Boc strategy. Then the dipeptide will be oligomerized using Fmoc SPPS strategy.

The effort to synthesize PNA sequence *via* solution phase synthesis using Boc-chemistry was tried starting from the intermediate **15** and **45** as a model reaction as shown in **Figure 3.54**. The Boc group in the compound **15** was deprotected using methanolic HCl which was known to selectively remove the Boc group without touching the Dpm ester [127]. The HCl was generated from acetyl chloride (AcCl) and methanol (**Figure 3.53**). This active intermediate (**3.54a**) should be used immediately in the next coupling step to prevent self coupling between the pyrrolidine nitrogen and the protonated Dpm ester group.

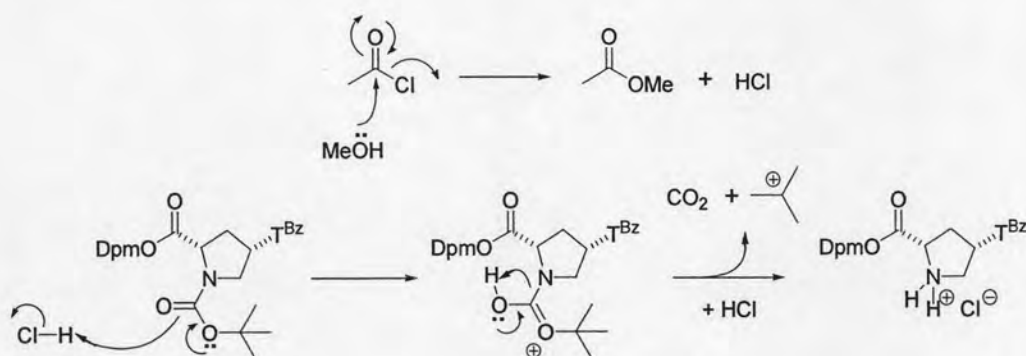
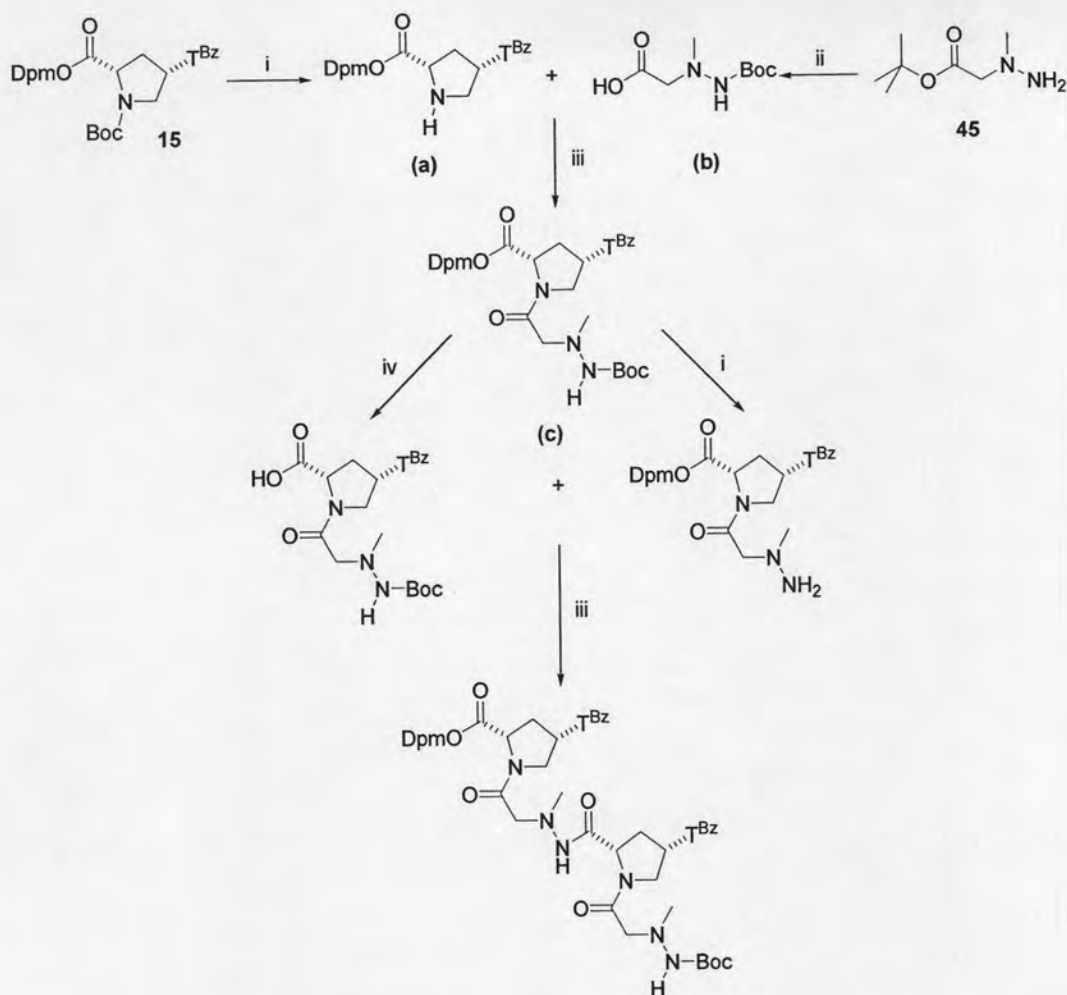


Figure 3.53 Proposed mechanism for deprotection of Boc group *via* AcCl/MeOH.

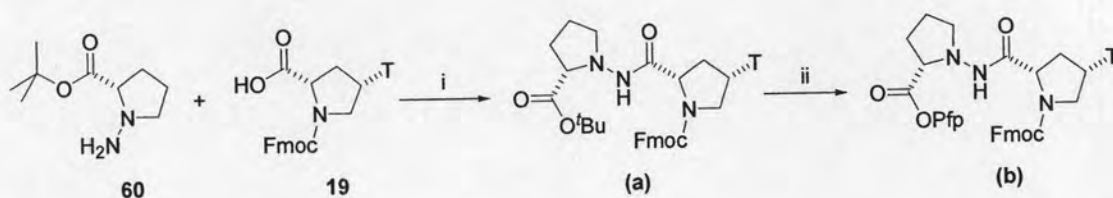


Reagents and conditions : i. AcCl, MeOH, 0 °C; ii. a) Boc₂O, Et₃N, CH₂Cl₂; b) NaOH, MeOH, H₂O; iii. DCC, HOBT, Et₃N, CH₂Cl₂, DMF; iv. C₆H₁₀, Pd-C, MeOH.

Figure 3.54 The proposed scheme for solution phase peptide synthesis.

For compound **45**, the amino group was protected with Boc group using Boc₂O, Et₃N in dichloromethane and then the *tert*-Butyl ester was removed by saponification to generate *N*-Boc β-amino acid (**3.53b**). The amide bond formation between (**3.53a**) and (**3.53b**) was performed using DCC, HOBT in the presence of Et₃N and dichloromethane. The progress of reaction was monitored by TLC, which showed more than six spots on TLC plate. The solution phase synthesis according to this plan was therefore abandoned because of the difficulty of preparation of starting material, non-reproducible results, formation of many by-products, and difficulties in purification.

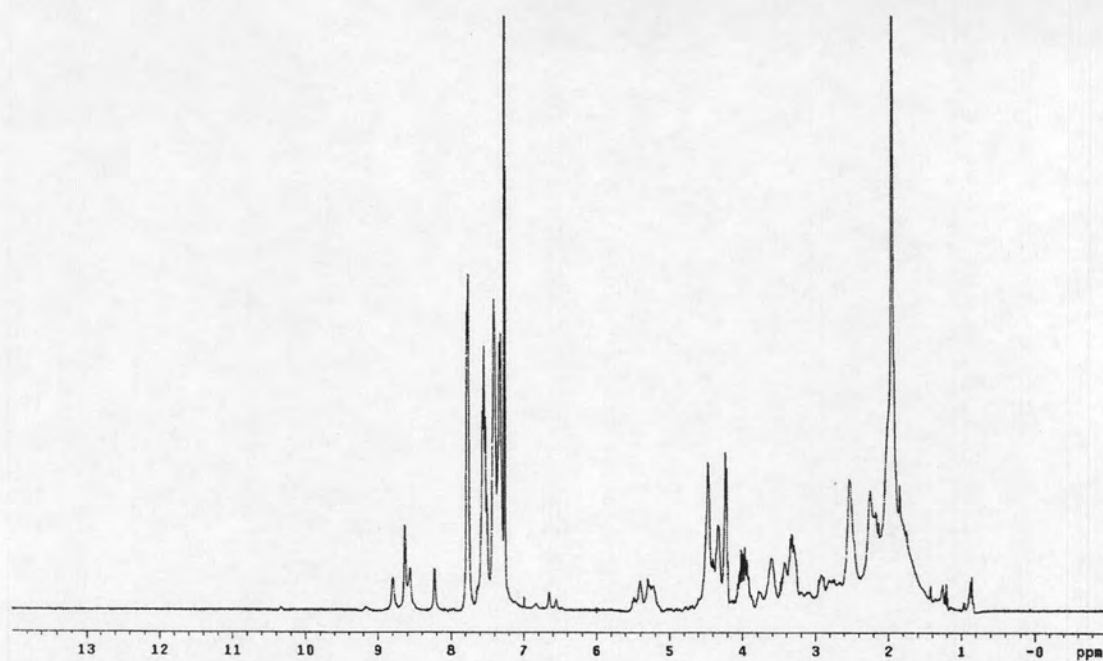
The Fmoc strategy of dipeptide was also considered starting from the coupling reaction of *cis*-L thymine Fmoc acid (**19**) with *N*-amino L-proline *tert*-butyl ester (**60**) to afford compound (**3.55a**). This protected dipeptide was treated with TFA in dichloromethane to remove *tert*-butyl group and then activated with Pfp as described previously to give a dipeptide derived from L-APC and pyrrolidinylyl thymine monomer as shown in **Figure 3.55**.



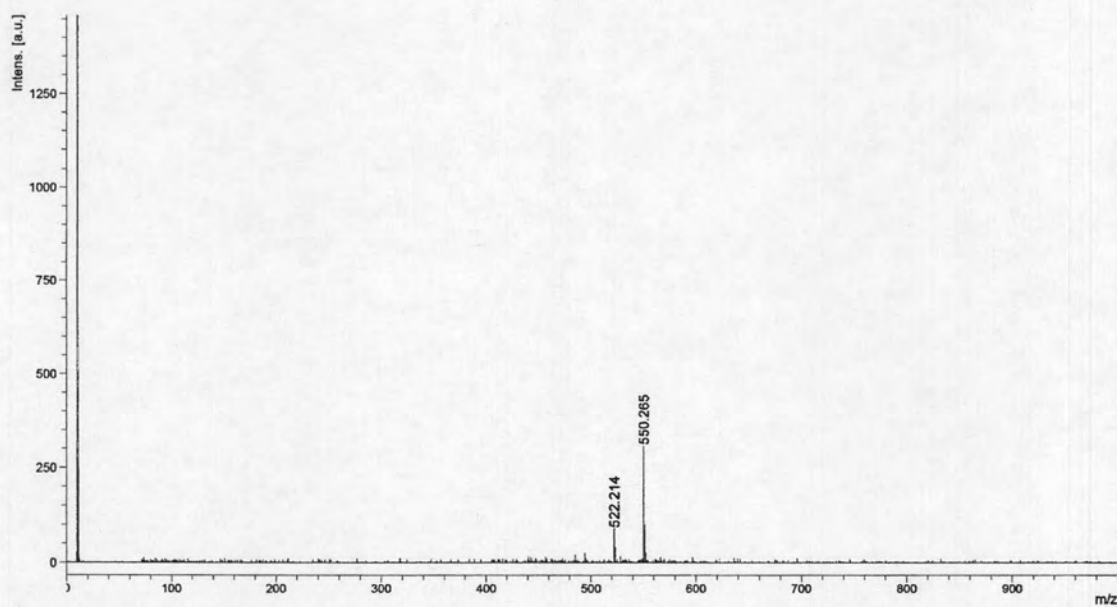
Reagents and conditions : i. EDC·HCl, HOBT, CH₂Cl₂; ii. a) TFA, CH₂Cl₂; b) PfpOH, EDC·HCl, DIEA, CH₂Cl₂.

Figure 3.55 The scheme for synthesis dipeptide (**3.55b**).

A similar dipeptide containing adenine was also synthesized. Both activated dipeptides showed expected MALDI-TOF spectra **Figure 3.56(b)** although their ¹H NMR spectra were rather complex, probably due to the formation of many possible rotamers (**Figure 3.56(b)**). Attempts to use these two dipeptides in the synthesis a PNA sequence Ac-T₄ATAT-LysNH₂ on solid phase were not successful as suggested by mass spectrometric analysis of the crude product formed (**Figure 3.57**).



(a)



(b)

Figure 3.56 (a) NMR spectrum and (b) MALDI-TOF MS of compound (3.55b).

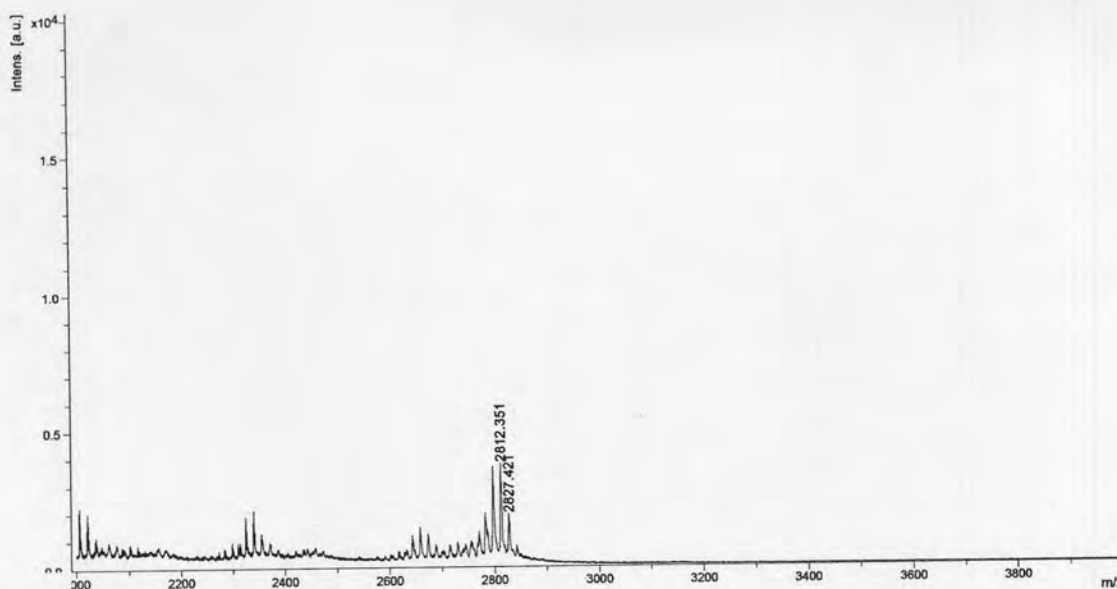


Figure 3.57 MALDI-TOF MS of Ac-TTTTATAT-LysNH₂ from dipeptide method, $M \cdot H^+$ (calcd) = 2872.988.

After several attempts, no satisfactory results were obtained from the combined solid-solution phase synthesis *via* dipeptide monomers. Therefore, we returned to alternative classical solid phase syntheses which generally give acceptable result for PNA synthesis.

3.3.3 Optimization of solid phase synthesis by varying coupling reagents

The original solid phase synthesis in this study was described by Vilaivan [123] as shown in **Figure 3.47** and an example of PNA synthesis using this condition was illustrated in **Table 3.10** in the previous section. Interestingly, percent coupling efficiency in each step of the synthesis *cis*-D/D-APC Fmoc-T₅-LysNH₂ (**P1**) was not reproducible. The figures were always low when Fmoc-D-Pro-(*cis*-4-T)-OPfp (**21**) was coupled to a resin-bound D-APC spacer (only 80-90%). It was therefore important to re-investigate the coupling conditions. Examples of percent efficiency in the coupling step of various pyrrolidine monomers and various spacers were demonstrated in **Table 3.11** and **Table 3.12**.

Table 3.11 Percent coupling efficiency of pyrrolidine monomer to D-APC spacer in the synthesis of PNA *cis*-D, *trans*-D, *cis*-L, *trans*-L, /D-APC Fmoc-T₅-LysNH₂.

PNA	Conditions ^c	% efficiency					
		1	2	3	4	5	Avg.
<i>cis</i> -D-T ^a	HATU/DIEA	100	80	78	88	84	86.0
<i>trans</i> -D-T ^a	HATU/DIEA	100	98	88	91	90	93.4
<i>cis</i> -L-T ^a	HATU/DIEA	100	90	81	86	88	89.0
<i>trans</i> -L-T ^a	HATU/DIEA	100	93	86	83	91	90.6
<i>cis</i> -D-T ^b	HOAt	100	95	94	96	94	95.8
<i>cis</i> -D-A ^{Bz b}	HOAt	100	95	100	95	97	97.4
<i>cis</i> -D-C ^{Bz b}	HOAt	100	101	103	96	95	99.0

^a Fmoc acid as a starting material. ^b Pfp ester as a starting material. ^c the coupling step was operated in 4 equiv of amino acid in DMF and coupling time was 2 h.

From the **Table 3.11**, the percent efficiency of couplings using Fmoc acid monomers in the presence of HATU/DIEA were around 86.0-90.6%, while that using Pfp ester in the presence of HOAt were around 95.8-99.0%. These suggested that Pfp ester was more superior to Fmoc acids. For β -amino acid spacers, the Pfp esters were use in all SPPS as shown in **Table 3.15**.

Table 3.12 Percent coupling efficiency of the coupling of β -amino acid spacers to thymine pyrrolidine monomer in the synthesis of *cis*-D PNA and various spacers of Fmoc/H-T₅-LysNH₂ sequences.

PNA	Condition ^a	% efficiency					
		1	2	3	4	5	Avg.
D-APC	HOAt	96	107	109	95	- ^b	106.4
L-APC	HOAt	97	100	99	98	- ^b	98.5
(1 <i>S</i> ,2 <i>S</i>)-ACPC	HOAt	95	109	100	113	97	102.8
(1 <i>R</i> ,2 <i>R</i>)-ACPC	HOAt	100	95	102	113	- ^b	102.3
(1 <i>S</i> ,2 <i>R</i>)-ACPC	HOAt	96	103	95	98	- ^b	98.0
(1 <i>R</i> ,2 <i>S</i>)-ACPC	HOAt	100	97	96	93	95	96.2
<i>N</i> -spacer	HOAt	78	102	105	75	- ^b	90.0
<i>O</i> -spacer	HOAt	91	19	-	-	-	Failed

a The coupling step was operated in 4 equiv of amino acid in DMF and coupling time was 2 h.

b The last coupling step was not measured percent efficiency due to keeping Fmoc group for purification step as described above.

The average percent efficiency of the coupling step of β -amino acid spacer was in the range of 90.0-106.4%. In some cases, percent efficiencies >100% was observed, which were still within the experimental limit. For the *O*-spacer, an unexpectedly low coupling efficiency was observed; therefore the PNA containing *O*-spacer could not be synthesized. The protocol of solid phase of PNA using through this study was shown in **Table 3.13**.

Table 3.13 The optimized protocol for solid phase synthesis of PNA.

Cycle	Step	Reagent	Time	Comment
A1	Deprotection	20 % piperidine in DMF	15 min	Fmoc removal
B	Washing	DMF×3		
Extra	Anchoring	Fmoc-L-Lys(Boc)-OPfp ^a HOAt ^a in DMF	2 h	Attachment of Lysine
B	Washing	DMF×3		
A2	Deprotection	20 % piperidine in DMF	15 min	Fmoc removal
B	Washing	DMF×3		
C ^c	Coupling	PNA monomer ^b or spacer ^b HOAt ^b in DMF	30 min	Extension of oligomer
B	Washing	DMF×3		
D	Capping	10 % Ac ₂ O/DIEA in DMF	15 min	Acetylation of uncoupled oligomer
B	Washing	DMF×3		
Return to cycle A2 → B → C → B → D → B and repeat this cycle as desired.				

a 10 eq loading in 30 μ L DMF; **b** 4 eq loading in 30 μ L DMF; **c** DIC/HOAt was used instead of HOAt for PNA monomer Fmoc acid.

The protocol for PNA syntheses allowed straightforward access to almost any sequences of PNA with the base length between 5-10 bases. A complete synthesis cycle for a decamer PNA can be readily performed in a few days (excluding purification). The coupling efficiency data of all PNA synthesized in this work was shown in **Table 3.14**.

Table 3.14 Quantitative analyses showing the efficiency of peptide synthesis.

PNA	Sequence	Scale (μmol)	Percent efficiency	
			overall	average
P1	<i>cis</i> -D/D-APC Fmoc-T ₅ -LysNH ₂	4.0	49.5	92.4
P2	<i>trans</i> -D/D-APC Fmoc-T ₅ -LysNH ₂	4.0	75.5	96.9
P3	<i>trans</i> -L/D-APC Fmoc-T ₅ -LysNH ₂	4.0	61.0	94.6
P4	<i>cis</i> -L/D-APC Fmoc-T ₅ -LysNH ₂	4.0	55.9	93.7
P5	<i>cis</i> -D/L-APC Fmoc-T ₅ -LysNH ₂	4.0	56.7	93.8
P6	<i>cis</i> -D/(1 <i>S</i> ,2 <i>S</i>)-ACPC H-T ₅ -LysNH ₂	4.0	95.0	99.4
P7	<i>cis</i> -D/(1 <i>R</i> ,2 <i>R</i>)-ACPC H-T ₅ -LysNH ₂	4.0	55.5	93.6
P8	<i>cis</i> -D/(1 <i>S</i> ,2 <i>R</i>)-ACPC H-T ₅ -LysNH ₂	4.0	70.5	96.2
P9	<i>cis</i> -D/(1 <i>R</i> ,2 <i>S</i>)-ACPC H-T ₅ -LysNH ₂	2.5	90.6	99.0
P10	<i>cis</i> -D/ <i>N</i> -spacer Ac-T ₅ -LysNH ₂	1.0	71.2	96.3
P11	<i>cis</i> -D/ <i>O</i> -spacer Ac-T ₅ -LysNH ₂	1.0	failed	failed
P12	<i>cis</i> -D/D-APC Ac-A ₅ -LysNH ₂	2.5	93.1	99.3
P13	<i>cis</i> -D/D-APC Ac-T ₇ -LysNH ₂	4.0 (split into 4 reactions)	60.0	95.8
P14	<i>cis</i> -D/D-APC Ac-T ₃ AT ₃ -LysNH ₂		64.4	96.7
P15	<i>cis</i> -D/D-APC Ac-T ₃ CT ₃ -LysNH ₂		72.5	97.5
P16	<i>cis</i> -D/D-APC Ac-T ₃ GT ₃ -LysNH ₂		39.1	93.5
P17	<i>cis</i> -D/D-APC Ac-T ₉ -LysNH ₂	1.0	52.8	96.5
P18	<i>cis</i> -D/D-APC Ac-T ₄ AT ₄ -LysNH ₂	1.0	57.4	97.0
P19	<i>cis</i> -D/D-APC Ac-T ₄ CT ₄ -LysNH ₂	1.0	54.8	96.7
P20	<i>cis</i> -D/D-APC Ac-T ₄ GT ₄ -LysNH ₂	1.0	54.9	96.7
P21	<i>cis</i> -D/D-APC Ac-T ₄ ATAT-LysNH ₂	1.0	60.0	96.8
P22	<i>cis</i> -D/D-APC Ac-TATAT ₄ -LysNH ₂	1.0	54.8	96.3
P23	<i>cis</i> -D/D-APC Ac-T ₄ ATA-Lys(FAM) NH ₂	4.0	30.0	91.7
P24	<i>cis</i> -D/D-APC Ac-Ser-T ₉ -Lys(F)-Ser- NH ₂	1.0	48.0	96.6

PNA	Sequence	Scale (μmol)	Percent efficiency	
			overall	average
P25	<i>cis</i> -D/D-APC Ac-Ser- Lys(F)-T ₉ - Ser NH ₂	1.0	45.6	96.3
P26	<i>cis</i> -D/(1 <i>S</i> ,2 <i>S</i>)-ACPC H-T ₁₀ -LysNH ₂	4.0	66.0	97.8

The successfully synthesized PNA were purified by reverse-phase HPLC and characterized by MALDI-TOF mass spectrometer as shown in **Table 3.15**.

Table 3.15 Characterization data of PNA sequences.

PNA	t_R	$M \cdot H^+$ (found)	$M \cdot H^+$ (calcd)	% error
P1	22.283 ^a	2036.989	2035.996	0.049
P2	23.230 ^a	2036.197	2035.996	0.010
P3	22.264 ^a	2034.423	2035.996	0.077
P4	23.032 ^a	2036.003	2035.996	0.001
P5	21.715 ^a	2035.356	2035.996	0.031
P6	17.450 ^a	1809.032	1808.996	0.002
P7	27.202 ^b	1807.871	1808.996	0.062
P8	27.917 ^b	1807.900	1808.996	0.061
P9	18.401 ^a	1806.381	1808.996	0.145
P10	21.215 ^a	1723.760	1725.536	0.103
P11	failed	failed	1660.376	failed
P12	20.674 ^a	1899.507	1899.998	0.026
P13	20.664 ^a	2520.605	2521.618	0.040
P14	26.215 ^c	2532.827	2530.638	0.086
P15	26.537 ^c	2506.112	2506.608	0.020
P16	22.314 ^c	2547.717	2546.638	0.042
P17	21.701 ^a	3188.306	3188.308	0.000
P18	21.898 ^c	3196.980	3197.318	0.011
P19	22.112 ^c	3173.013	3173.298	0.009
P20	22.126 ^c	3213.138	3213.318	0.006
P21	21.875 ^c	2874.024	2872.988	0.036
P22	22.236 ^c	2872.222	2872.988	0.027

PNA	t_R	M·H ⁺ (found)	M·H ⁺ (calcd)	% error
P23	nd ^d	2902.076	2913.718	0.399
P24	nd ^d	3737.655	3722.688	0.402
P25	nd ^d	3722.487	3722.688	0.005
P26	25.868	3467.838	3469.757	0.055

Condition for reverse-phase HPLC: **a:** C-18 column 3 μ particle size 4.6 x 50 mm; gradient system of 0.01% TFA in acetonitrile/water 10:90 to 90:10 in 25 min; hold time 5 min; flow rate 0.5 mL/min. **b:** C-18 column 5 μ particle size 4.6 x 250 mm; gradient system of 0.01% TFA in acetonitrile/water 10:90 to 90:10 in 25 min. **c:** C-18 column 3 μ particle size 4.6 x 50 mm; gradient system of 0.01% TFA in acetonitrile/water 0:100 to 90:10 in 25 min. **d:** purified by gel electrophoresis due to the excess of fluorescein is difficult to separate (see appendix **Figure B-21** and **B-22**)

3.4 Binding Properties of PNA

3.4.1 Hybridization of various PNA systems with DNA

The preliminary technique used for determining the formation of PNA·DNA hybrids in this study was a UV-titration [128]. Oligonucleotides exhibit a strong UV absorption maxima, λ_{max} , at approximately 260 nm and a molar extinction coefficient, ϵ , in the order of 10^4 ($\text{dm}^3 \text{mol}^{-1} \text{cm}^{-1}$). This absorption arises from complex electronic transitions in the purine and pyrimidine components. The intensity is a function of the base composition, the salt concentration and its pH, and the state of base-pairing interaction present. The last interaction is the most important because it enables detection of base pairing. In general, base-base stacking results in a decrease in ϵ which is known as hypochromism [129]. The hypochromism can be observed in DNA·DNA duplex including DNA·PNA complex. Dissociate of the duplex into single stranded oligonucleotides, e.g. by heating, results in increasing of the absorption called hyperchromicity which can be conveniently monitored at 260 nm (**Figure 3.58**)

Hyperchromicity of DNA during Helix-Coil Transition

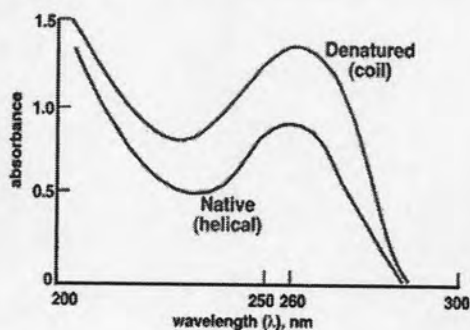


Figure 3.58 Typical UV absorption curves for equimolar base concentrations of single stranded (random coil) oligonucleotides and double helical DNA [130].

From this principle, the stoichiometry of the PNA·DNA complex was determined by UV titration. Adding the DNA titrant to the solution of the PNA analyte in phosphate buffer (10 mM, pH 7.0) in several aliquots (5 μ L of titrant) and the UV absorbance at 260 nm was measured after each addition.

3.4.1.1 Comparison between pyrrolidinyl diastereomers

Recent preliminary work from this laboratory suggested that PNA with *cis*-D proline and D-APC spacer can bind with DNA [28,123,]. It is therefore interesting to study the effect of the configuration of both the pyrrolidine ring and of the spacer. Interactions of PNA containing all four possible thymine pyrrolidine monomers and D-APC spacers will be studied in this section. The UV-titration experiment was carried out in the same way as described in **Section 3.4.1** and the UV titration curves were shown in **Figure 3.59**.

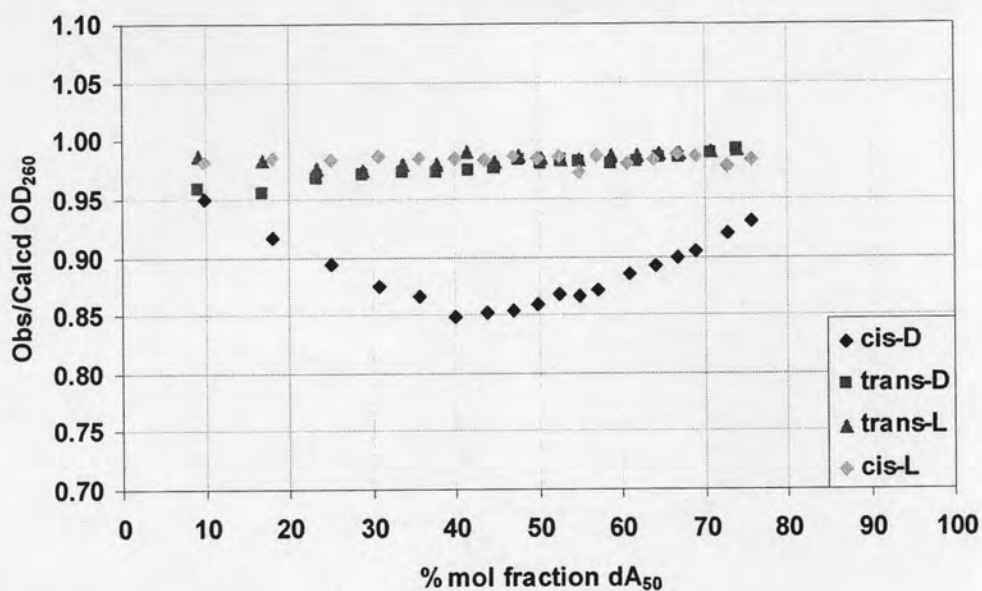
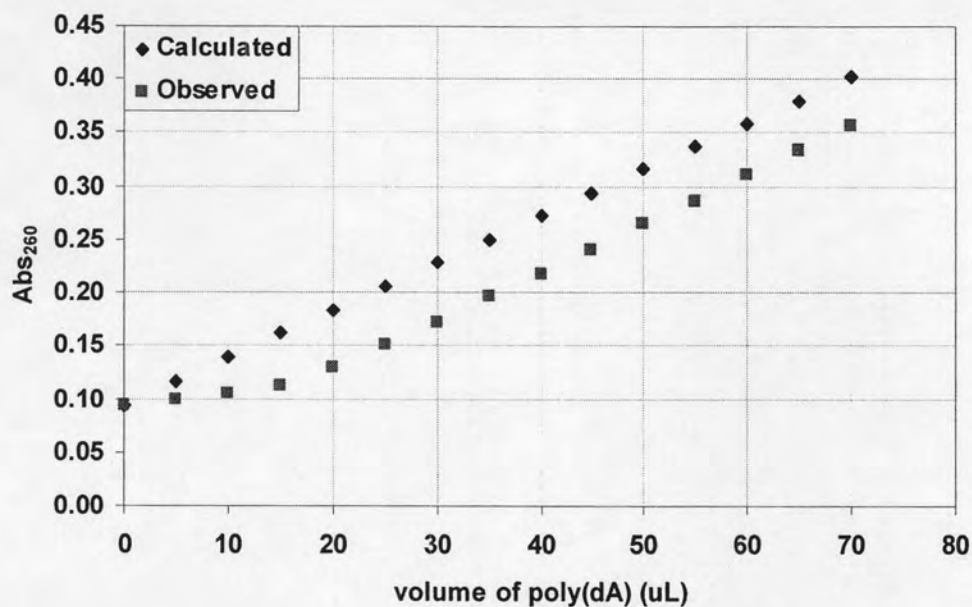


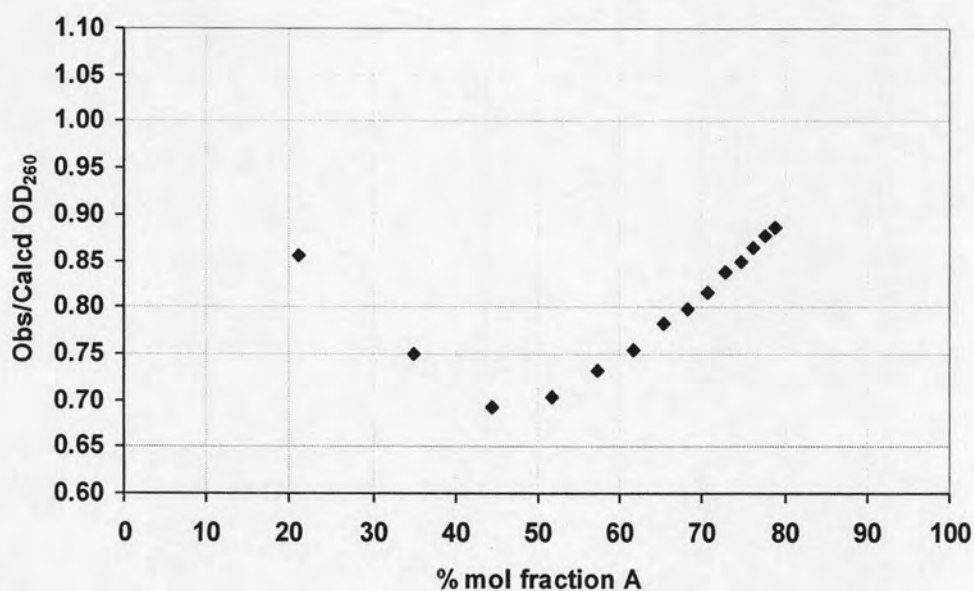
Figure 3.59 Comparison of UV-titration experiments between PNA (**P1**), (**P2**), (**P3**) and (**P4**) and dA₅₀.

For *trans*-D/D-APC Fmoc-T₅-LysNH₂ (**P2**), *trans*-L/D-APC Fmoc-T₅-LysNH₂ (**P3**) and *cis*-L/D-APC Fmoc-T₅-LysNH₂ (**P4**), the observed UV absorbance at 260 nm were identical within experimental limit to the calculated value, indicating that no interaction between these PNA and dA₅₀. Only the *cis*-D isomer, which possess the same configuration as the deoxyribose in natural DNA showed the hypochromicity therefore this system will be the model for other hybridization study between PNA and DNA such as melting temperature and fluorescent experiment.

The PNA *cis*-D/D-APC H-T₁₀-LysNH₂ which was synthesized previously by Dr. Tirayut Vilaivan was selected as a model for further titration study with DNA.



(a)

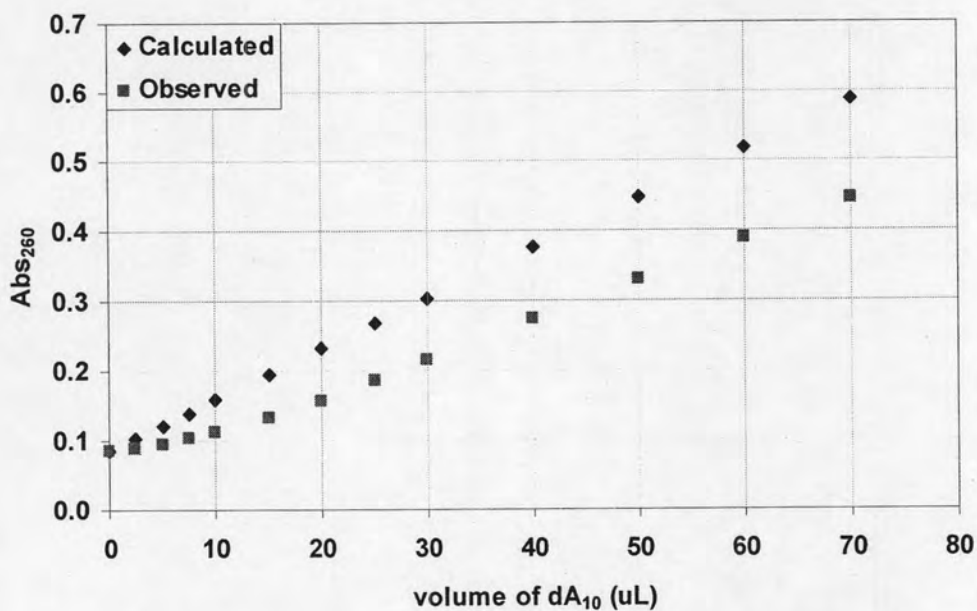


(b)

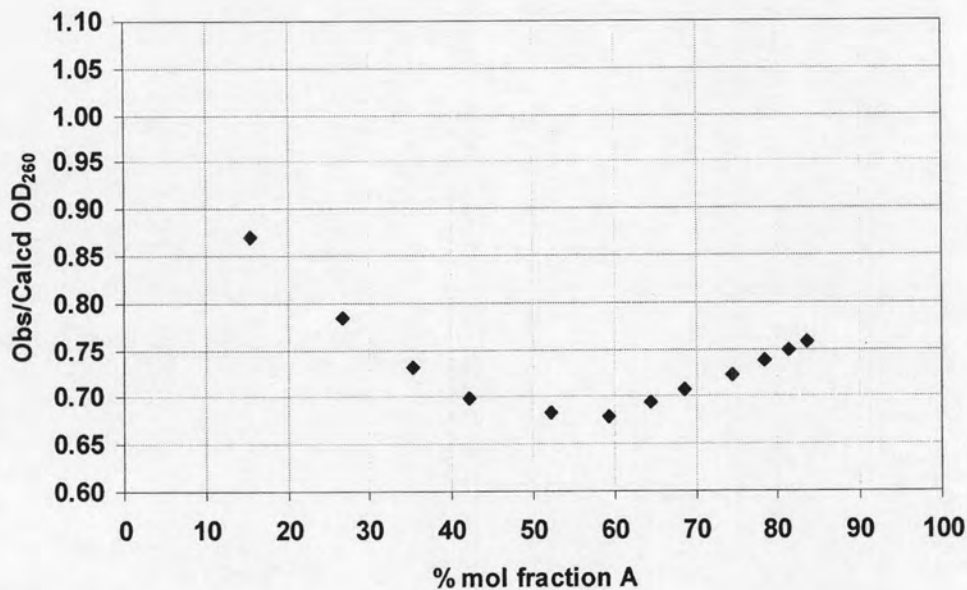
Figure 3.60 UV titration plot of poly(dA) and *cis*-D/D-APC H-T₁₀-LysNH₂. (a) a plot between Abs₂₆₀ and volume of poly(dA). (b) a plot between the ratio of observed Abs₂₆₀/calculated Abs₂₆₀ and % mole of poly(dA).

A significant deviation of the observed UV absorbance at 260 nm from the calculated value due to hypochromism was noted when *cis*-D/D-APC H-T₁₀-LysNH₂ as analyte was titrated with poly(dA) (**Figure 3.60a**). The ratio of observed and

calculated value at 260 nm was plotted against percent mole fraction of poly(dA). The result showed an inflection point around 50%, which indicated the formation of 1:1 PNA·DNA complex (**Figure 3.60b**). The results were confirmed using an exactly complementary DNA, dA₁₀, as a titrant instead of poly(dA). The UV-titration results between *cis*-D/D-APC H-T₁₀-LysNH₂ and dA₁₀ were shown in **Figure 3.61**.



(a)



(b)

Figure 3.61 UV titration plot of dA_{10} and *cis*-D/D-APC H-T₁₀-LysNH₂ (a) a plot between Abs₂₆₀ and volume of dA_{10} . (b) a plot between the ratio of observed Abs₂₆₀/calculated Abs₂₆₀ and % mole of dA_{10} .

The results were in good agreement with the previous titration experiment, confirming that the *cis*-D/D-APC PNA can form 1:1 hybrid with complementary DNA.

3.4.1.2 Comparison between β -amino acid spacers

From the previous experiment, it was found that with D-APC spacer, only *cis*-D pyrrolidiny PNA can bind with DNA. The binding of PNA pentamer containing *cis*-D thymine pyrrolidine monomer with various β -amino acid spacers with DNA was next studied by UV titration. The L-APC spacer was compared to D-APC spacer as shown in **Figure 3.62** (UV titration curves of all experiments may be found in the appendixes).

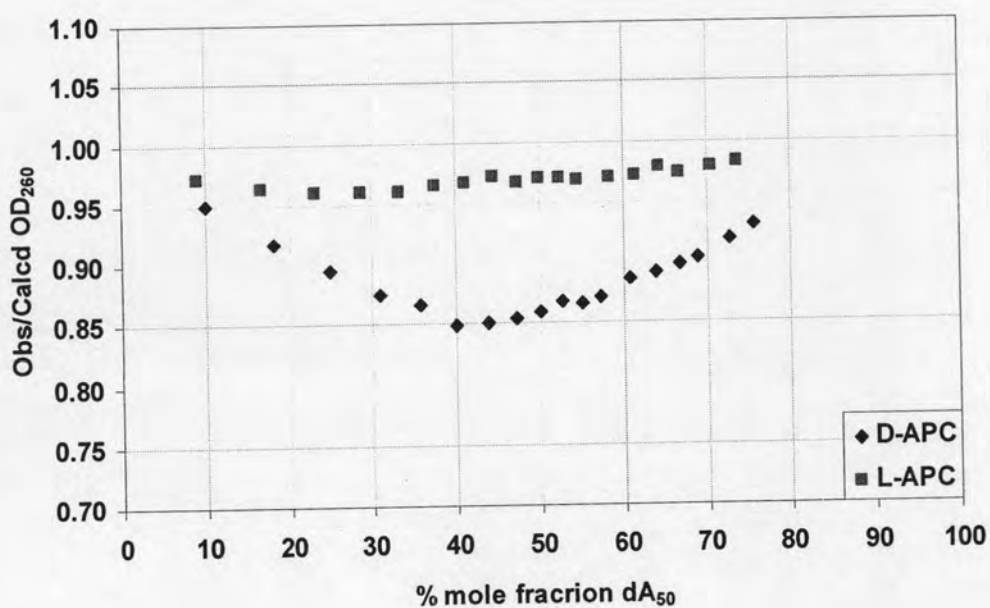


Figure 3.62 Comparison of UV-titration between PNA (P1) and (P5) with dA_{50} .

For *cis*-D/L-APC Fmoc-T₅-LysNH₂ (**P5**), the observed UV absorbance at 260 nm was identical with the calculated value indicating no interaction between PNA (**P5**) and dA₅₀. Furthermore, the ratio of observed and calculated value at 260 nm against percent mole fraction of dA₅₀ was linear which is in sharp contrast with *cis*-D/D-APC Fmoc-T₅-LysNH₂ (**P1**). These results suggested that the PNA (**P5**) did not bind to its complementary DNA by base-base pairing. The only difference between these two monomers is the configuration of the α -carbon of the spacer. This indicated that stereochemistry of the spacer is an important factor for binding properties of PNA·DNA duplex. From this behavior, it was expected to observe DNA-binding properties in PNA carrying (1*S*,2*S*)-ACPC and (1*S*,2*R*)-ACPC spacers which have the same *S*-configuration at the α -position as D-APC. The four T₅ PNA with ACPC-spacers were titrated with dA₅₀ and the results shown in **Figure 3.63**.

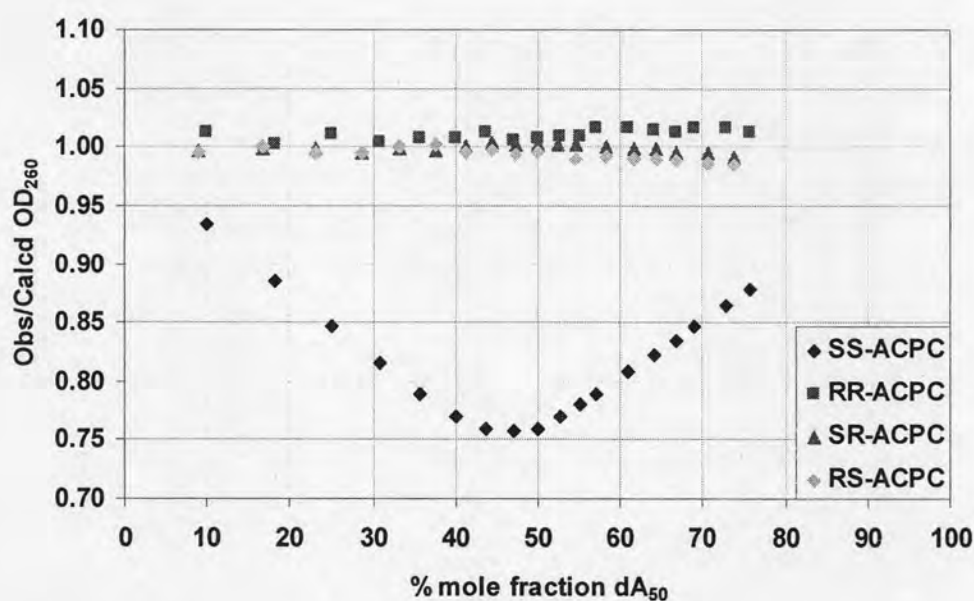
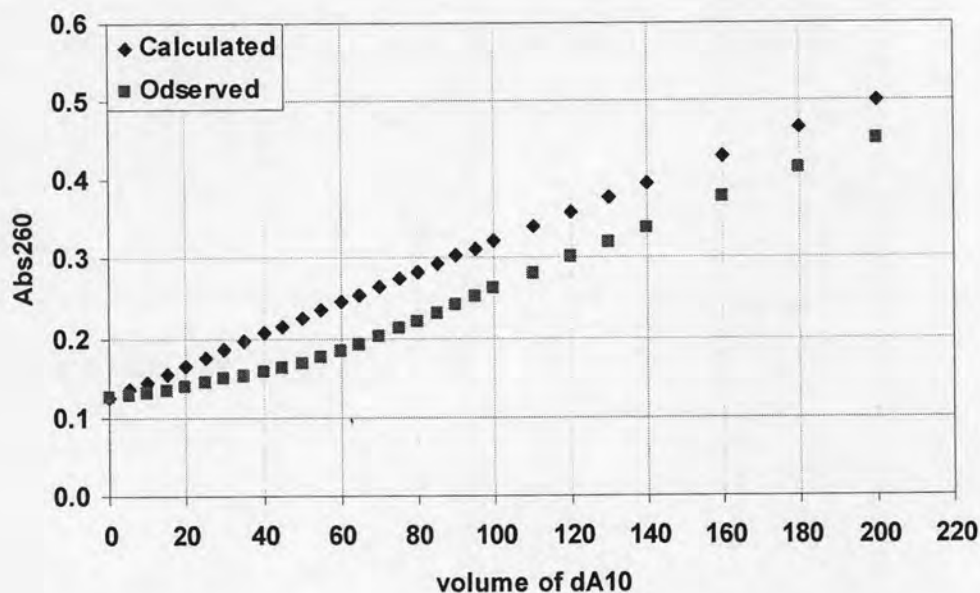


Figure 3.63 Comparison of UV-titration between PNA (**P6**), (**P7**), (**P8**) and (**P9**) with dA₅₀.

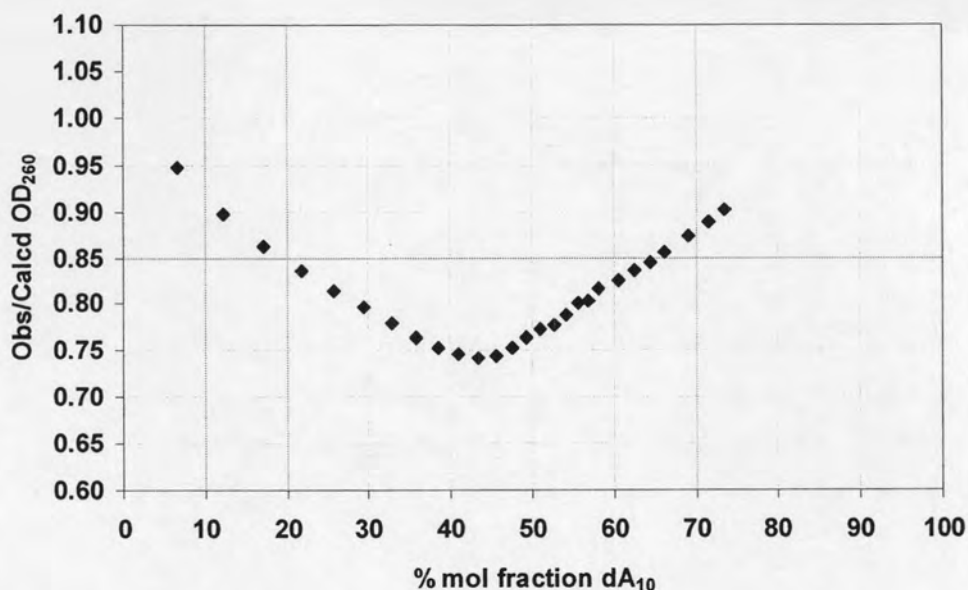
A significant hypochromism was observed when *cis*-D/(1*S*,2*S*)-ACPC H-T₅-LysNH₂ (**P6**) was titrated with dA₅₀ (**Figure 3.63**). Again, the position of the inflection point suggested the formation of 1:1 PNA·DNA complex as observed in the D-APC PNA (**P1**). Interestingly that the hypochromism in the case of PNA (**P6**) with (1*S*,2*S*)-ACPC spacer was much more pronounced when compared to the PNA (**P1**)

with D-APC spacer. This might be due to the higher stability of (P6)·DNA duplex compared to (P1)·DNA. This hypothesis has been supported by T_m experiment in the next section. On the other hand, the PNA *cis*-D/(1*S*,2*R*)-ACPC H-T₅-LysNH₂ (P8), which has the same *S*-configuration of the carboxyl group as (P1) and (P6) did not show any hypochromism. This suggested that the configuration of the β -amino group also affect the stability of the duplex. For the other two PNAs, namely *cis*-D/(1*R*,2*R*)-ACPC H-T₅-LysNH₂ (P7) and *cis*-D/(1*R*,2*S*)-ACPC H-T₅-LysNH₂ (P9), no hyperchromism was observed indicating that there was no interaction between these PNA and dA₅₀. These results lead to the conclusion that the configurations of the β -amino acid spacer must be essentially fixed for optimal binding. It should be noted that the amino group in D-APC spacer, although would not be stereogenic in solution due to the rapid inversion of nitrogen atom, it might adopt a *trans*-configuration relative to the alpha-position. According to this argument, the configuration of D-APC PNA (P1) should therefore identical to the (1*S*,2*S*)-ACPC PNA (P6). It is therefore concluded that the configurations of (1*S*,2*S*)-ACPC and D-APC are optimal, or at least the best compared to the other three alternative configurations, to allow stable complexation between PNA and DNA [132].

Titration of *cis*-D/(1*S*,2*S*)-ACPC H-T₁₀-LysNH₂ (P26) was also performed with dA₁₀. The results are shown in Figure 3.64.



(a)



(b)

Figure 3.64 UV titration plot of dA₁₀ and *cis*-D/(1*S*,2*S*)-ACPC H-T₁₀-LysNH₂ (**P7**).

(a) a plot between Abs₂₆₀ and volume of dA₁₀. (b) a plot between the ratio of observed Abs₂₆₀/calculated Abs₂₆₀ and % mole of dA₁₀. Condition : [PNA] = 2.41 mM (constant), [DNA] = 85.1 μM 10 mM sodium phosphate buffer, pH 7.0, 25 °C.

The stoichiometry of complex formation between this PNA this was also studied by Job's plot [134]. In the experiment ten solutions were prepared with varying mole fractions of (**P26**) and dA₁₀ from 100:0 to 0:100, keeping the total moles of PNA and DNA constant. The lowest absorbance at 260 nm appeared at 1:1 ratio of PNA:DNA as shown in **Figure 3.66**. This is in good agreement with the UV titration experiment above.

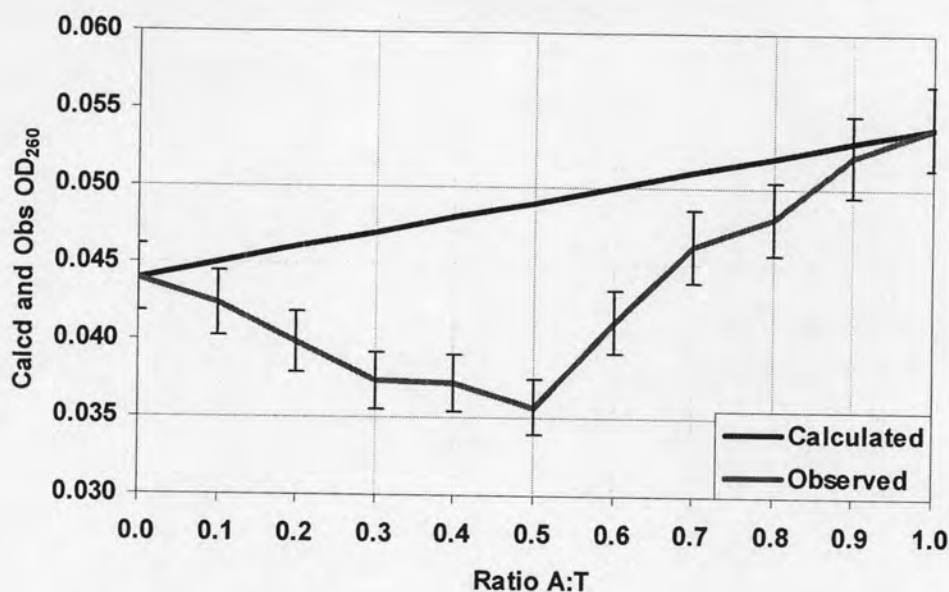


Figure 3.65 Job plot of dA_{50} and *cis*-D/(1*S*,2*S*)-ACPC H-T₁₀-LysNH₂ (P26). [PNA+DNA] = 1.1 μ M of each ratio, Conditions: 10 mM sodium phosphate buffer, pH 7.0, 25 °C.

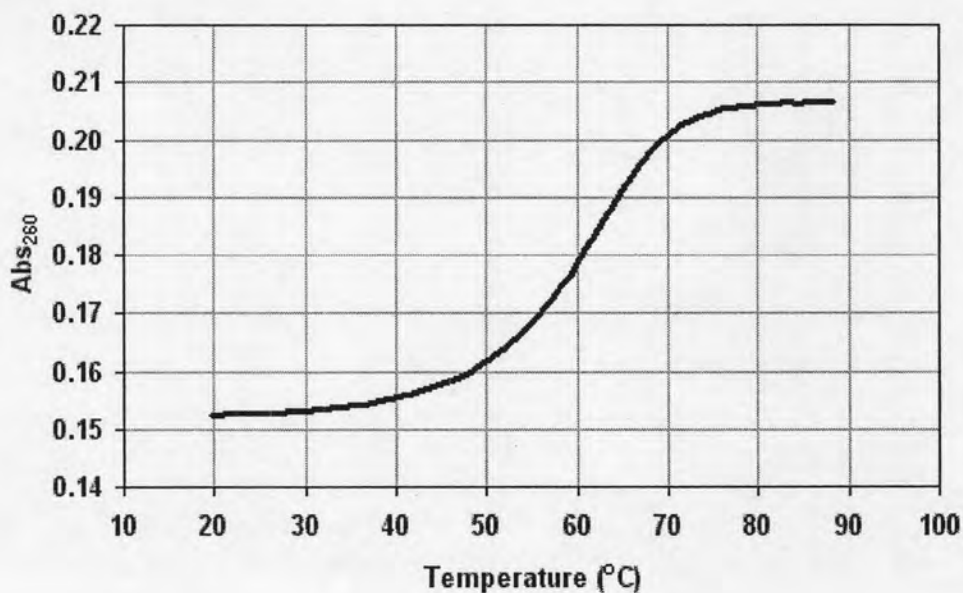
After this discovery, the *cis*-D/(1*S*,2*S*)-ACPC PNA system has already been the subject of intensive investigation by another member of this group, Dr. Choladda Srisuwannaket [111,135]. As a result, the *cis*-D/D-APC PNA will be the main focus of this work.

3.4.2 T_m experiments

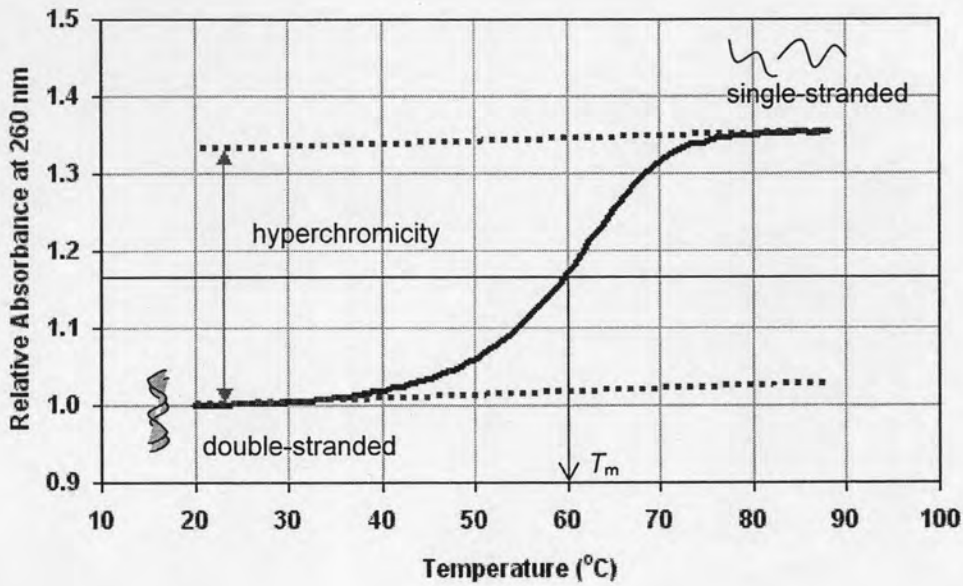
3.4.2.1 Selected *cis*-D/D-APC and *cis*-D/(1*S*,2*S*)-ACPC PNA systems

The principal technique used for determining the formation and stability of PNA·DNA hybrids is thermal denaturation or melting temperature (T_m) measurement. Two strands of nucleic acid in a duplex are held together by hydrogen bonding and are also stabilized by additional hydrophobic, π - π and dipole-dipole interaction between the stacked base pairs. At high temperature, the DNA duplex separates into two single stranded DNA (DNA denaturation). This will be accompanied by

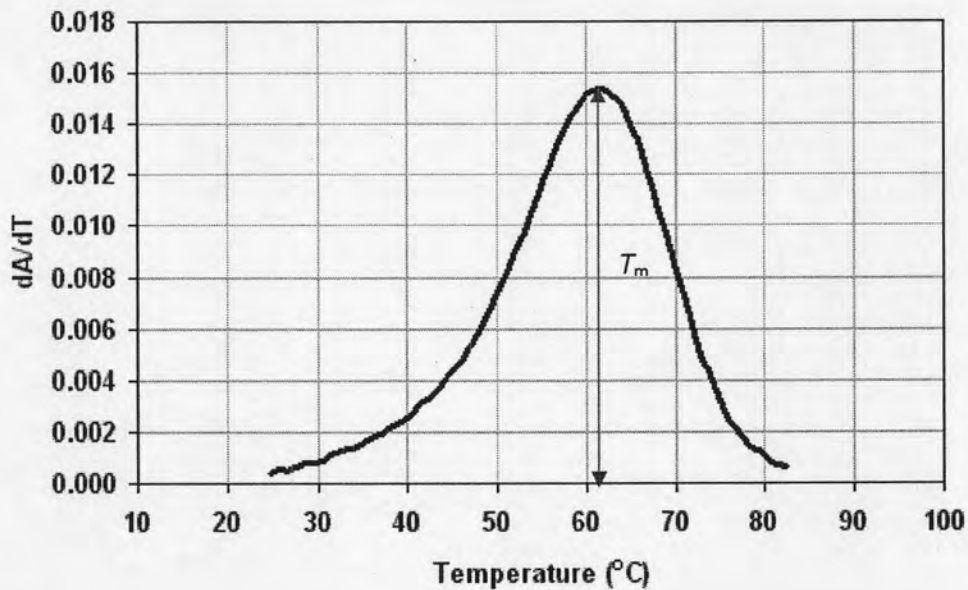
separation and unstacking of adjacent base pairs, resulting in a slight increase (10-20%) in the UV absorption of the nucleobase (hyperchromism). Measurement of the absorbance of a DNA complex at 260 nm while slowly increasing the temperature provides a convenient mean to observe denaturation of the complex. In a thermal denaturation experiment, the polynucleotide absorbance typically changes very slowly at first, and then rapidly rises to a maximum value (**Figure 3.66**). The temperature at which 50% of all duplexes are separated is called "melting temperature" (T_m). This value provides information on the stability of the duplex structure. Stable duplexes melt at a higher melting temperature than less stable duplexes. It should be noted that the melting process occurs abruptly within only 10-20 °C range. This is a result of cooperativity between base-base interactions. Once the input energy is sufficient to breach the first hydrogen-bonded base pair, the dissociation continues until the two strands completely separate.



(a)



(b)



(c)

Figure 3.66 The change of UV absorbance in a typical thermal denaturation experiment of a DNA duplex. (a) real melting temperature (b) relative melting temperature or normalized melting temperature (c) first derivative plot.

The raw data from a typical T_m experiment is shown in **Figure 3.66a**. The normalized absorbance scale (**Figure 3.66b**) is preferred in comparison between

different T_m curves. To calculate the correct melting temperature, first derivative between ΔAbs and ΔT was plot against temperature (**Figure 3.66c**). The temperature giving the maximum of this first derivative plot indicated the melting temperature.

In a preliminary experiment, the T_m of D-APC PNA bearing the four pyrrolidine isomers: *cis*-D, *trans*-D, *trans*-L, *cis*-L/D-APC Fmoc-T₅-LysNH₂ with dA₅₀ were measured (**Figure 3.67**).

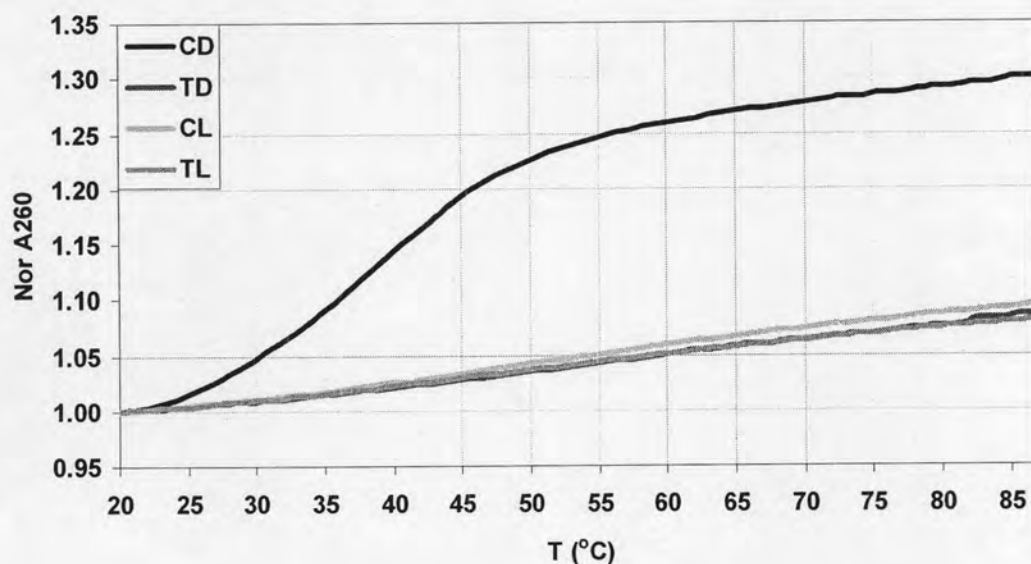


Figure 3.67 T_m curves of PNA *cis*-D, *trans*-D, *trans*-L, *cis*-L/D-APC Fmoc-TTTT-LysNH₂ with d(A₅₀): Condition PNA:DNA = 1:1, [PNA] = 1 μ M, 10 mM sodium phosphate buffer, pH 7.0, heating rate 1.0 $^{\circ}$ C/min.

The T_m values indicated that only the *cis*-D/D-APC Fmoc-T₅-LysNH₂ (P1)·d(A₅₀) hybrid can form the hybrid with d(A₅₀) (**Table 3.16**). This is in complete agreement with the UV titration experiment above. The T_m value for this particular PNA is estimated to be 38.7 $^{\circ}$ C which is more stable than the corresponding DNA·DNA hybrid (T_m = 21 $^{\circ}$ C) [136].

Table 3.16 T_m experiment between *cis*-D, *trans*-D, *trans*-L and *cis*-L/D-APC Fmoc- T_5 -LysNH₂ with dA₅₀.

PNA	dA ₅₀	
	T_m (°C)	% Hyperchromicity
<i>cis</i> -D (P1)	38.7	30 %
<i>trans</i> -D (P2)	< 20.0	-
<i>trans</i> -L (P3)	< 20.0	-
<i>cis</i> -L (P4)	< 20.0	-

Condition PNA:DNA = 1:1, [PNA] = 1 μ M, 10 mM sodium phosphate buffer, pH 7.0, heating rate 1.0 °C/min.

The T_m experiment to examine the various spacers on *cis*-D pyrrolidiny PNA was next carried out using the same thymine pentamer sequences. T_m of hybrids between the PNA sequences (P5), (P6), (P7), (P8) or (P9) and dA₅₀ were measured. The results are shown in Table 3.17. Only PNA (P6) can form the hybrid at 48.4 °C with moderate 19% hyperchromicity shift. This result was not unexpected since earlier UV-titration experiments had suggested that only the PNA (P6) with *cis*-D/(1*S*,2*S*)-ACPC skeleton could bind with DNA.

Table 3.17 T_m experiment between *cis*-D T_5 with various spacer L-APC, (1*S*,2*S*)-ACPC, (1*R*,2*R*)-ACPC, (1*S*,2*R*)-ACPC and (1*R*,2*S*)-ACPC with dA₅₀.

<i>cis</i> -D T_5 with spacers	dA ₅₀	
	T_m (°C)	% Hyperchromicity
L-APC (P5)	< 20.0	-
(1 <i>S</i> ,2 <i>S</i>)-ACPC (P6)	48.4	19 %
(1 <i>R</i> ,2 <i>R</i>)-ACPC (P7)	< 20.0	-
(1 <i>S</i> ,2 <i>R</i>)-ACPC (P8)	< 20.0	-
(1 <i>R</i> ,2 <i>S</i>)-ACPC (P9)	< 20.0	-

Condition PNA:DNA = 1:1, [PNA] = 1 μ M, 10 mM sodium phosphate buffer, pH 7.0, heating rate 1.0 °C/min.



To investigate the relationship between the base length and T_m of PNA·DNA hybrids, the melting curves of equimolar mixtures between selected PNA containing thymine and complementary DNA with different numbers of base pairs, $n = 5, 7, 9$ were obtained. Apart from $n = 5$, the melting lower than 26.0 °C was observed, All are much higher than the corresponding DNA·DNA duplexes with the same length. An increase in T_m of roughly 10 °C per number of additional base pair was observed as shown in **Table 3.18**. In these cases, multiple PNAs should bind simultaneously on the DNA strand and may be cooperatively stabilized by additional interstrand base-base stacking.

Table 3.18 T_m experiment between *cis*-D/D-APC Fmoc-T₅-LysNH₂, Ac-T₇-LysNH₂ and Ac-T₉-LysNH₂ with dA₅, dA₇ and dA₉. Condition PNA:DNA = 1:1, [PNA] = 1 μM, 10 mM sodium phosphate buffer, pH 7.0, heating rate 1.0 °C/min.

Length	PNA T _n with dA _n	
	T_m (°C)	% Hyperchromicity
n = 5 (P1)	< 26.0	-
n = 7 (P13)	49.3	14%
n = 9 (P17)	70.0	39%
n = 10	> 85.0	nd

The effect of pH to stability of the hybrid was also investigated. The T_m value at low pH (pH 6.0) is similar to the values at pH = 7.0 whereas T_m value is slightly decreased under higher pH condition (pH 8.0) (**Table 3.19**). This might be explained in terms of protonation of the ring nitrogen in the D-APC spacer and also of the nitrogen at the side chain of lysine at low pH to form positive charges which can interact electrostatically with the phosphate backbone of the DNA. At high pH, these amino groups became neutral; therefore this secondary stabilization (in addition to the usual base pairing) is absent.

Table 3.19 T_m experiment between *cis*-D/D-APC Ac-T₉-LysNH₂ with dA₉ at pH 6.0, 7.0 and 8.0. Condition PNA:DNA = 1:1, [PNA] = 1 μM, 10 mM sodium phosphate buffer, heating rate 1.0 °C/min.

pH	PNA (P17) with dA ₉	
	T_m (°C)	% Hyperchromicity
pH 6.0	71.0	40%
pH 7.0	69.0	39%
pH 8.0	67.3	37%

The effect of ionic strength was also studied. Different concentration of NaCl had relatively little effect on T_m of PNA·DNA hybrids (**Table 3.20**). In DNA, the T_m of duplex usually increases with the cation concentration. This is because these ions electrostatically shield the anionic phosphate groups from repelling each other. However, since PNA is uncharged, only a slight change in T_m was observed at higher salt concentration. Interestingly, the change in T_m is in the opposite direction to that of DNA·DNA hybrid but similar to Nielsen's PNA·DNA hybrid. It has been suggested that the counter ion released upon helix formation rather than counterion uptake as in the case DNA·DNA is the contributing factor to this destabilization of PNA·DNA duplex at high salt concentration [131].

Table 3.20 T_m experiment between *cis*-D/D-APC Ac-T₉-LysNH₂ with dA₉ at concentration of NaCl 10 mM, 100 mM, 1000 mM and 2000 mM. Condition PNA:DNA = 1:1, [PNA] = 1 μM, 10 mM sodium phosphate buffer, heating rate 1.0 °C/min.

NaCl concentration	PNA (P17) with dA ₉	
	T_m (°C)	% Hyperchromicity
10 mM	69.4	38%
100 mM	66.5	36%
1000 mM	63.7	36%
2000 mM	61.8	35%

3.4.2.2 Selectivity of DNA recognition by D-APC-PNA

Initially, the *cis*-D/(1*S*,2*S*)-ACPC PNA system was also investigated the stability and selectivity. PNA H-T₁₀-LysNH₂ was hybridized with DNA 5'-AAAAXAAAAA-3' (when X = T, A, C and G) to form perfect and single mismatch and DNA 5'-AAATATAAAA-3' as a double mismatch PNA·DNA hybrids. The *T_m* values obtained are shown in **Table 3.21**.

Table 3.21 *T_m* values of PNA *cis*-D/(1*S*,2*S*)-ACPC Ac-T₁₀-LysNH₂ with DNA 5'-AAAAXAAAAA-3' (when X = T, A, C and G) and DNA 5'-AAATATAAAA-3'. Condition PNA:DNA = 1:1, [PNA] = 1 μM, 10 mM sodium phosphate buffer, pH 7.0, heating rate 1.0 °C/min.

PNA	<i>T_m</i> with DNA (°C) ^a				
	dA ₁₀	dA ₄ TA ₅	dA ₄ CA ₅	dA ₄ GA ₅	dA ₃ TATA ₄
T ₁₀ (P26)	> 85.1	66.1 (36)	66.3 (33)	60.3 (26)	33.1 (19)
<i>aeg</i> PNA	72	-	-	59	-

a % hyperchromicity display in the parenthesis

The *T_m* value of a *cis*-D/(1*S*,2*S*)-ACPC Ac-T₁₀-LysNH₂ with dA₁₀ was estimated to be >85.1 °C [132]. This indicates that the *cis*-D/(1*S*,2*S*)-ACPC Ac-T₁₀-LysNH₂·dA₁₀ hybrid is much more stable than the corresponding DNA·DNA hybrid (*T_m* = 21 °C) [136]. The presence of a single mismatch base in the DNA strand resulted in lowering of the *T_m* values of the complex by 19-25 °C. Two mismatch bases lowered the *T_m* further to 32 °C as shown in **Table 3.21**. The corresponding *T_m* data for *aeg*PNA [133] with the same *cis*-D/(1*S*,2*S*)-ACPC Ac-T₁₀-LysNH₂ sequence is also included for comparison. This indicated high sequence specificity in DNA recognition by PNA.

Next, in order to investigate the base-pairing specificity in more details, four degenerate sequences of heptameric PNA were designed in order to investigate the stringency of base recognition by the *cis*-D/D-APC PNA system. The PNA sequences studied were *cis*-D/D-APC Ac-TTTXTTT-LysNH₂ when X = T, A, C and G. These

sequences derived from replacement of one thymine base in the T₇ sequence with A, C and G respectively. The difference of T_m of the hybrids formed between these PNA and complementary or single-mismatched DNA will provide indication on how well these PNA can differentiate between perfect match and single mismatch interactions. These PNA sequences were hybridized with degenerate heptamer DNA 5'-AAAYAAA-3' sequences (when Y = T, A, C and G) resulting in the formation of 16 possible distinct hybrids. These symmetrical sequences should be able to form hybrids regardless of the preferred orientation of PNA·DNA binding. The T_m experiment was performed under the same condition as described in Section 3.4.2 and T_m values of these experiments shown in Appendix and Table 3.22.

Table 3.22 T_m values of PNA *cis*-D/D-APC Ac-TTXXTTT-LysNH₂ (when X = T, A, C and G) with DNA 5'-AAAYAAA-3' (when Y = T, A, C and G). Condition PNA:DNA = 1:1, [PNA] = 1 μM, 10 mM sodium phosphate buffer, pH 7.0, heating rate 1.0 °C/min.

PNA	T_m with DNA (°C)			
	d(A ₃ <u>A</u> A ₃)	d(A ₃ <u>T</u> A ₃)	d(A ₃ <u>G</u> A ₃)	d(A ₃ <u>C</u> A ₃)
T ₃ <u>T</u> T ₃ (P13)	53.2 (24)	26.7 (10)	< 20.0	< 20.0
T ₃ <u>A</u> T ₃ (P14)	< 20.0	36.6 (19)	< 20.0	< 20.0
T ₃ <u>C</u> T ₃ (P15)	< 20.0	< 20.0	< 20.0	nd
T ₃ <u>G</u> T ₃ (P16)	< 20.0	< 20.0	< 20.0	26.8 (8)

% hyperchromicity display in the parenthesis

In Table 3.22, the T_m values displayed in bold digits are for the perfect match hybrids, while the others contain a single mismatch in the middle position of the sequences. Gratifyingly, only the hybrids formed from perfect match PNA and DNA possessed the highest T_m values. Furthermore, in three out of four cases the T_m values were higher than the corresponding DNA·DNA hybrids (18-20 °C). The hybrid formed between the PNA Ac-T₇-LysNH₂ (P13) and DNA 5'-A₇-3' gave the highest T_m of 53.2 °C. Other perfect match PNA·DNA hybrids exhibited decreased T_m values (53.2 °C for X = A, Y = T, <25 °C for X = C, Y = G and 26.8 °C for X = G, Y = C).

Unexpectedly, no melting was observed with the complementary C·G and G·C base pairs. It was proposed that the T_m was too low to be detected despite the fact that in DNA·DNA hybrid, the C·G and G·C base pairs are more stable than T·A and A·T base pairs. In all but one cases when there is a mismatched, no melting was observed. In the case where the T_m was observed for the mismatched pair, the T_m was much lower than that of the perfect match by 26 °C indicating that the PNA system should be powerful in discriminating between matched and mismatched DNA sequences.

Increasing the T_m of the hybrids was expected to provide more useful information regarding to the binding specificity and will confirm that recognition of G in DNA by C in PNA is also possible. Longer PNA sequences Ac-TTTTXXXXT-LysNH₂ (P17-P20) were therefore synthesized and hybridized with the degenerate DNA nonamer 5'-AAAAYAAAA-3' as described above. The stability of the 16 hybrids was determined again by T_m measurement as described above. The results are shown in **Table 3.23**.

Table 3.23 T_m values of PNA *cis*-D/D-APC Ac-TTTTXXXXT-LysNH₂ (when X = T, A, C and G) with DNA 5'-AAAAYAAAA-3' (when Y = T, A, C and G). Condition PNA:DNA = 1:1, [PNA] = 1 μM, 10 mM sodium phosphate buffer, pH 7.0, heating rate 1.0 °C/min.

PNA	T_m with DNA (°C)			
	d(A ₄ <u>A</u> A ₄)	d(A ₄ <u>T</u> A ₄)	d(A ₄ <u>G</u> A ₄)	d(A ₄ <u>C</u> A ₄)
T ₄ <u>T</u> T ₄ (P17)	68.8 (40)	43.4 (26)	35.5 (25)	43.4 (32)
T ₄ <u>A</u> T ₄ (P18)	35.6 (25)	60.0 (32)	25.8 (8)	34.7 (23)
T ₄ <u>C</u> T ₄ (P19)	33.8 (22)	26.1 (9)	46.7 (24)	26.3 (7)
T ₄ <u>G</u> T ₄ (P20)	27.8 (14)	32.7 (19)	26.0 (7)	56.4 (29)

% hyperchromicity display in the parenthesis.

Data in **Tables 3.23** and **Tables 3.24** clearly indicated that the nonamer PNA can differentiate between the complementary and single mismatched DNA. The pair of PNA Ac-T₉-LysNH₂ and DNA 5'-A₉-3' still gave the highest T_m around 68.8 °C compared with others perfect match complementary (60.0 °C for X = A, Y = T, 46.7

°C for X = C, Y = G and 56.4 °C for X = G, Y = C). A single mismatch at the central positions in the DNA strands caused a drop in T_m of 13-34 °C as shown in **Table 3.24**. Interestingly, in the single mismatch case, when purine base is present on the DNA and/or PNA sequence, it leads to the high ΔT_m such as entry 3 compare with entry 2, 4 and entry 7 compare with entry 5, 8 and entry 13, 15 compare with entry 14.

Table 3.24 T_m values and ΔT_m of PNA *cis*-D/D-APC Ac-TTTTXXXXT-LysNH₂ (when X = T, A, C and G) with DNA 5'-AAAAYAAAA-3' (when Y = T, A, C and G).

Entry	X in PNA	Y in DNA	T_m (°C)	ΔT_m (°C)
<u>1</u>	<u>T</u>	<u>A</u>	68.8	0.0
2	T	T	43.4	-25.4
3	T	G	35.5	-33.3
4	T	C	43.4	-25.4
5	A	A	35.6	-24.4
<u>6</u>	<u>A</u>	<u>T</u>	60.0	0.0
7	A	G	25.8	-34.2
8	A	C	34.7	-25.3
9	C	A	33.8	-12.9
10	C	T	26.1	-20.6
<u>11</u>	<u>C</u>	<u>G</u>	46.7	0.0
12	C	C	26.3	-20.4
13	G	A	27.8	-28.6
14	G	T	32.7	-23.7
15	G	G	26.0	-30.4
<u>16</u>	<u>G</u>	<u>C</u>	56.4	0.0

In addition, percent hyperchromicity for the mismatch hybrids was also significantly decreased (about 24-40% for perfect match, and <10-32% for single mismatch) indicating a less favorable base stacking. It is therefore concluded that *cis*-D/D-APC PNA system can form hybrid with complementary DNA in a highly sequence-specific manner. Furthermore the outcome confirmed that recognition

between C and G bases in PNA and DNA still followed Watson-Crick base pairing rules. However, the presence of C·G and G·C base pairs resulted in less stable complex compared to T·A and A·T base pairs. This behavior is opposite with the natural DNA and other PNA systems. At present, no satisfactory explanation is yet available. Nevertheless, both the decreases in T_m and hyperchromicity for mismatched hybrids clearly indicated that the base pairing in PNA and DNA follows the normal Watson-Crick base-pairing specificity.

Table 3.25 T_m values of PNA *cis*-D/D-APC Ac-TTTT \underline{X} TTTT-LysNH₂ (when X = T, A, C and G) with RNA 5'-AAAAYAAAA-3' (when Y = U, A, C and G). Condition PNA:RNA = 1:1, [PNA] = 1 μ M, 10 mM sodium phosphate buffer, pH 7.0, heating rate 1.0 $^{\circ}$ C/min.

PNA	T_m with RNA ($^{\circ}$ C)			
	r(A ₄ <u>A</u> A ₄)	r(A ₄ <u>U</u> A ₄)	r(A ₄ <u>G</u> A ₄)	r(A ₄ <u>C</u> A ₄)
T ₄ <u>T</u> T ₄ (P17)	26.2 (7)	<20.0	<20.0	<20.0
T ₄ <u>A</u> T ₄ (P18)	<20.0	25.1 (5)	<20.0	<20.0
T ₄ <u>C</u> T ₄ (P19)	<20.0	<20.0	<20.0	<20.0
T ₄ <u>G</u> T ₄ (P20)	<20.0	<20.0	<20.0	24.8 (11)

% hyperchromicity display in the parenthesis.

Furthermore, the T_m experiments with other nucleic acid were investigated. The same PNA sequences as in **Table 3.23** were mixed with the complementary and single mismatched RNA. The pair of PNA Ac-T₉-LysNH₂ and RNA 5'-A₉-3' still gave the highest T_m around 26.2 $^{\circ}$ C compared with others perfect match complementary (25.1 $^{\circ}$ C for X = A, Y = U, <20.0 $^{\circ}$ C for X = C, Y = G and 24.8 $^{\circ}$ C for X = G, Y = C). A single mismatch at the central positions in the RNA strands caused a drop in T_m to <20.0 $^{\circ}$ C. However, the ΔT_m of the pair of perfect complementary matched when compared between DNA and RNA were 42.6 $^{\circ}$ C (for X = T, Y = A), 34.9 $^{\circ}$ C (for X = T, Y = A), >26.7 $^{\circ}$ C (for X = C, Y = G) and 31.6 $^{\circ}$ C (for X = G, Y = C) respectively. These results indicated the high sequence specificity in DNA recognition over RNA.

3.4.3 Other experiments

Polyacrylamide gel electrophoresis technique was also used to investigate the binding properties of these new PNA. The fluorescently labeled DNA (FdA₁₀) used as a probe with complementary sequence to the PNA was kindly provided by Prof. Gordon Lowe (University of Oxford, UK). The PNA sequences studied were as follow: *cis*-L/*N*-spacer H-T₁₀-LysNH₂ (**P-G1**), *cis*-D/*N*-spacer H-T₁₀-LysNH₂ (**P-G2**), *cis*-L/*L*-APC H-T₆-LysNH₂ (**P-G3**), *cis*-D/*D*-APC H-T₆-LysNH₂ (**P-G4**) and *cis*-D/*D*-APC H-T₁₀-LysNH₂ (**P-G5**). The resulting gel photograph is presented in **Figure 3.68**. In lane 1 and 2, (**P-G1**) and (**P-G2**) were the series of *N*-spacer PNA showed the negative results similar to (**P-G3**) (lane 4) which bearing L-APC spacer. For (**P-G4**) and (**P-G5**), these sequences were different in length (6 and 10 bases respectively). Surprisingly, (**P-G4**) (lane 5) showed a negative result. A possible explanation is that the PNA is too short to form a stable hybrid with DNA under the electrophoresis conditions. While the presence of a new fluorescent band with longer PNA sequence (**P-G5**) (lane 7) clearly indicated the interaction between (**P-G5**) and FdA₁₀.

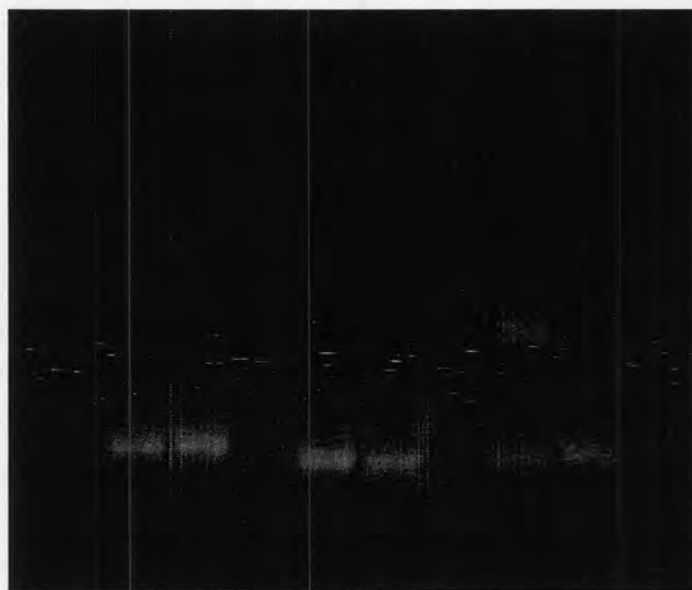
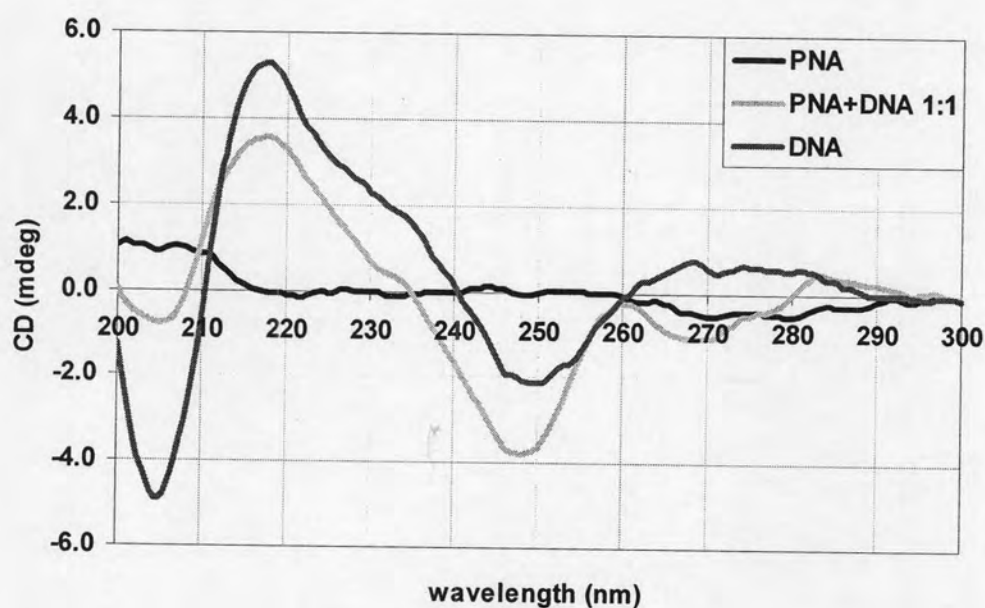
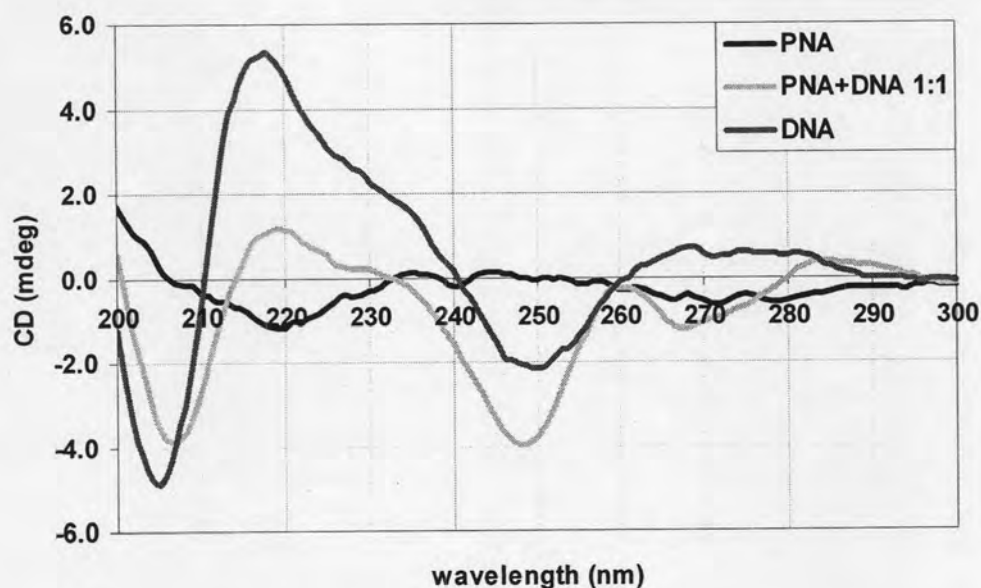


Figure 3.68 Gel hybridization experiment: Lane 1: (**P-G1**)+FdA₁₀, Lane 2: (**P-G2**)+FdA₁₀, Lane 4: (**P-G3**)+FdA₁₀, Lane 5: (**P-G4**)+FdA₁₀, Lane 7: (**P-G5**)+FdA₁₀, Lane 8: FdA₁₀. Condition: 15% polyacrylamide gel in 90 mM TBE buffer pH 8.3 at a constant DC voltage of 100 V.

The binding properties of both *cis*-D/D-APC and *cis*-D/(1*S*,2*S*)-ACPC PNA were also studied by circular dichroism (CD). The CD spectra of the *cis*-D/D-APC H-T₁₀-LysNH₂ and *cis*-D/(1*S*,2*S*)-ACPC H-T₁₀-LysNH₂ (**P26**) with dA₁₀ were measured (**Figure 3.69**). The CD signal of the 1:1 hybrid formed between *cis*-D/D-APC H-T₁₀-LysNH₂ and dA₁₀ showed negative bands at 205, 247, and 268 nm and positive bands at 217, 283 nm and CD signal of the 1:1 hybrid formed between (**P26**) and dA₁₀ showed negative bands at 205, 247, and 268 nm and positive bands at 217, 283 nm which are similar to those of the duplex formed between poly(dT) and poly(dA) [131].



(a)



(b)

Figure 3.69 A CD titration plot of (a) *cis*-D/D-APC H-T₁₀-LysNH₂ with dA₁₀ and (b) *cis*-D/(1*S*,2*S*)-ACPC H-T₁₀-LysNH₂ (P26) with dA₁₀. Condition: concentration of PNA was constant at 11.1 μM, 10 mM sodium phosphate buffer, pH 7.0, 20 °C. The titrant used in this experiment was dA₁₀ (958.4 μM).

3.4.4 Directional preference of PNA·DNA hybrid

In the previous section, only symmetrical PNA sequences were studied therefore it was not possible to get the information about the direction of binding. Similar to DNA, PNA·DNA duplexes have two possible orientations in hybridization. In DNA, the antiparallel binding defined as when the 5' end of the first DNA sequence is directed to 3' end of the other sequence, while parallel binding defined as 5' end directed to the 5' end. For our PNA system, the definition of antiparallel binding is the 3' end of the DNA sequence is oriented toward the *N*-terminal of the PNA. The opposite binding, parallel orientation when the 5' end of the DNA sequence is oriented toward the *N*-terminal of the PNA as shown in **Figure 3.70**.

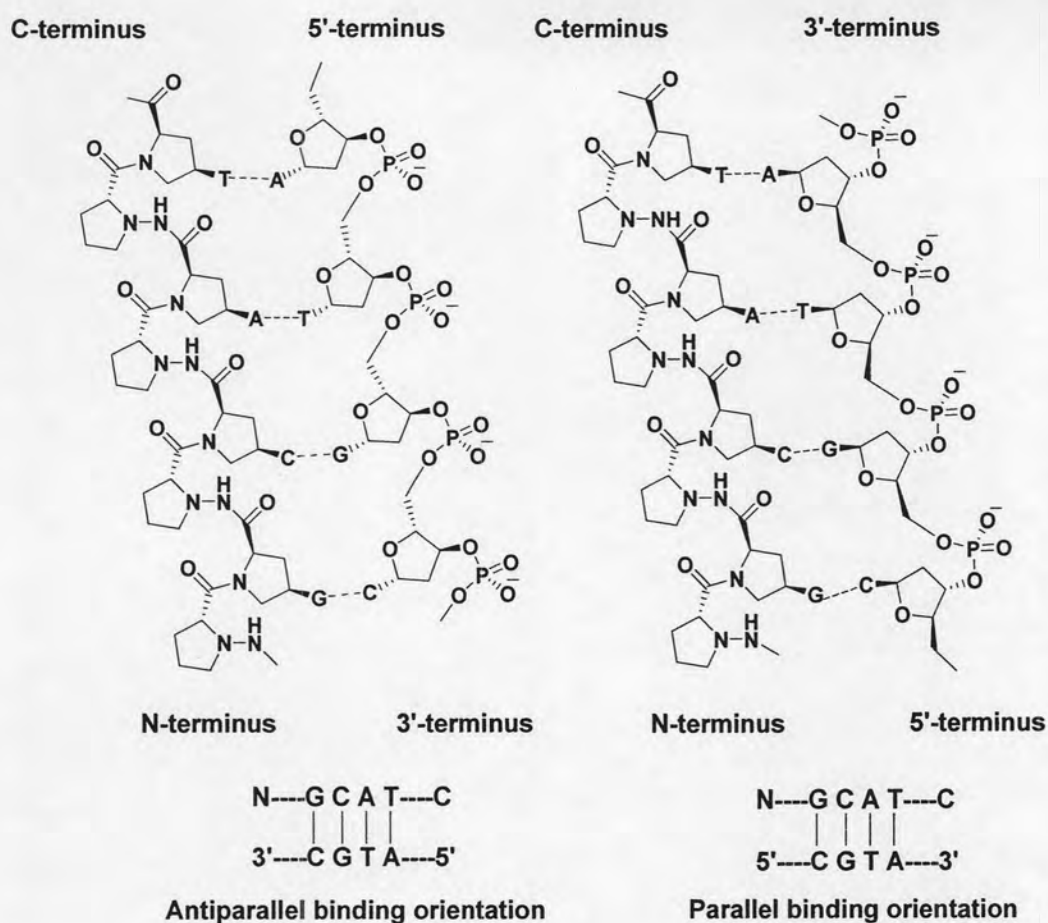


Figure 3.70 Definition of parallel and antiparallel orientations in PNA·DNA hybrids.

In order to investigate the relative orientation of each component in a PNA·DNA hybrid, two unsymmetrical *cis*-D/D-APC PNA octamer sequences containing T and A were synthesized. These include *cis*-D/D-APC Ac-TTTTATAT-LysNH₂ (**P21**) and Ac-TATATTTT-LysNH₂ (**P22**). The cross T_m experiments of (**P21**) and (**P22**) with complementary DNA 5'-AAAATATA-3' and 5'-ATATAAAA-3', resulting in antiparallel and parallel hybrids of both sequences, were carried out. The results are as shown in **Table 3.26**.

Table 3.26 T_m experiment of *cis*-D/D-APC Ac-TATATTTT-LysNH₂ (**P22**) and *cis*-D/D-APC Ac-TTTTATAT-LysNH₂ (**P21**) with antiparallel and parallel complementary DNA. Condition PNA:DNA = 1:1, [PNA] = 1 μ M, 10 mM sodium phosphate buffer, pH 7.0, heating rate 1.0 $^{\circ}$ C/min.

PNA	T_m with DNA ($^{\circ}$ C)		
	AAAATATA	ATATAAAA	ΔT_m
TATATTTT (P22)	49.1 (24) ^a	34.9 (18) ^b	14.2
TTTTATAT (P21)	< 30.0 (6) ^b	55.2 (31) ^a	24.2

% hyperchromicity display in the parenthesis **a** antiparallel hybrids **b** parallel hybrids

The antiparallel hybrid PNA (**P22**)-d(AAAATATA) showed a T_m value of 49.1 $^{\circ}$ C, while the parallel hybrid PNA (**P22**) \cdot d(ATATAAAA) showed a T_m value of 34.9 $^{\circ}$ C under identical conditions and ΔT_m value of 14.2 $^{\circ}$ C was observed. The same result occurred with PNA (**P21**) which showed a T_m value of antiparallel hybrid at 55.2 $^{\circ}$ C, while the parallel hybrid showed a T_m value of <30.0 $^{\circ}$ C under identical conditions and ΔT_m value of >25.2 $^{\circ}$ C was observed. However, a curve of parallel hybrids was still observed around 35 $^{\circ}$ C for the parallel hybrid between (**P22**) \cdot d(AAAATATA) which may be derived from two possibilities. First, the parallel duplex could indeed form but it was less stable than antiparallel duplex. Second, an overlap antiparallel binding mode as shown in **Figure 3.71** might also be possible.

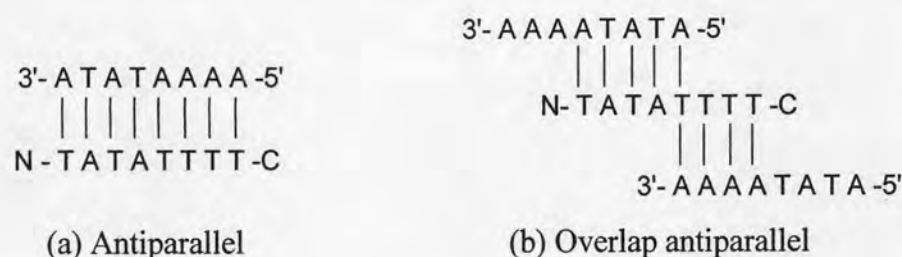


Figure 3.71 Binding model of PNA (**P22**) (a) antiparallel binding (b) overlap antiparallel with parallel DNA sequences.

To further confirm the preference for antiparallel hybrid formation, the same experiment was also carried out with a CG-capped DNA GCG-AAAATATA-CGC

and GCG-ATATAAAA-CGC to prevent the undesired overlap antiparallel hybrid as shown in **Table 3.27**.

Table 3.27 T_m experiment of *cis*-D/D-APC Ac-TATATTTT-LysNH₂ and Ac-TATATTTT-LysNH₂ with antiparallel and parallel complementary DNA including CG-cap. Condition PNA:DNA = 1:1, [PNA] = 1 μ M, 10 mM sodium phosphate buffer, pH 7.0, heating rate 1.0 $^{\circ}$ C/min.

PNA	T_m with DNA ($^{\circ}$ C)		
	GCG-AAAATATA-CGC	GCG-ATATAAAA-CGC	ΔT_m
TATATTTT (P22)	58.9 (21) ^a	39.0 (12) ^b	19.9
TTTTATAT (P21)	< 30.0 (7) ^b	65.4 (19) ^a	35.4

% hyperchromicity display in the parenthesis **a** antiparallel hybrids **b** parallel hybrids

The antiparallel hybrid PNA (P22)·d(GCGAAAATATACGC) showed a higher T_m value of 58.9 $^{\circ}$ C compared to 49.1 $^{\circ}$ C of the previous experiment. The parallel hybrid PNA (P22)·d(GCGAAAATATACGC) showed a T_m value of 39.0 $^{\circ}$ C compared to 34.9 $^{\circ}$ C under identical conditions and a ΔT_m value of 19.9 $^{\circ}$ C was observed. Similar results were obtained with PNA (P21) which showed a T_m value of the antiparallel hybrid at 65.4 $^{\circ}$ C, which is higher than T_m value of 55.2 $^{\circ}$ C from the previous experiment. The parallel hybrid showed a T_m value of < 30.0 $^{\circ}$ C under identical conditions and ΔT_m value up to 35.4 $^{\circ}$ C was observed. This last experiment confirmed the higher stability of antiparallel over parallel hybrids. This indicates that the antiparallel orientation is strongly preferred in hybridization of *cis*-D/D-APC and DNA.

Prof. Supot Hannongbua and Dr. Parawan Chiuchay have performed a preliminary investigation of the binding energy by Molecular Dynamics (MD) Simulation in gas phase [137]. They found that the binding energy of antiparallel duplex is preferred over parallel duplex with the free energies for the antiparallel and parallel hybrids of -287.9 ± 8.7 and -137.9 ± 9.1 kcal/mole respectively. The models of their studies were shown below in **Figure 3.72**. The models can thus nicely explain the experimental result.

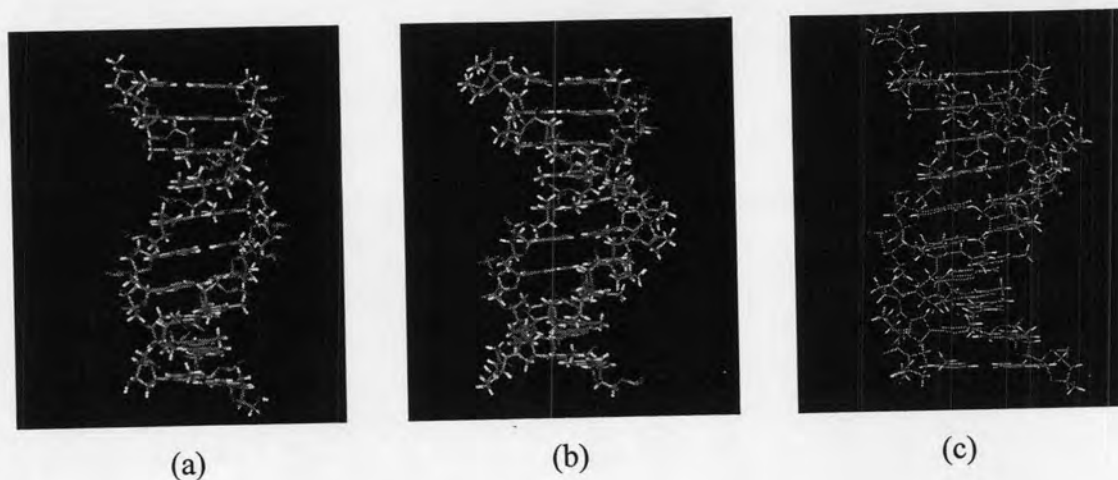


Figure 3.72 Model of (a) DNA·DNA strand (b) PNA·DNA parallel form and (c) PNA·DNA antiparallel form.

3.4.5 Fluorescent experiment

Fluorescence is defined as the emission of radiation given out as a molecule returns to its ground state from an excited electronic state and fluorescence can be investigated by the analysis of changes in the emission. The emission from oligonucleotides is very weak at room temperature. As a result, synthetic fluorophores can be introduced earlier into an oligonucleotides or PNA by specific covalent or non-covalent addition, which has become very important in the application of fluorescence energy transfer (FRET) to the study of nucleic acids.

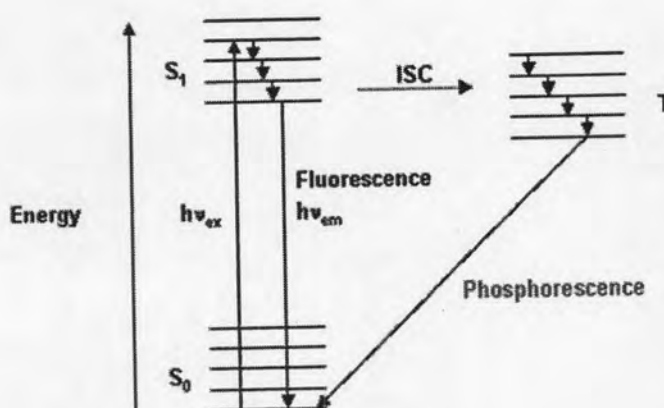


Figure 3.73 A simplified Jablonski diagram illustrating the principles of fluorescence and phosphorescence.

FRET is a spectroscopic process by which energy is passed non-radiatively between molecules over long distances (10-100 Å). The non-radiative transfer of excited-state energy from a fluorescence donor molecule to an unexcited acceptor molecule *via* dipole-dipole coupling between the donor and the acceptor. The rate of this energy transfer depends on the spectral properties of the donor and acceptor, their relative dipole orientations and the distance. In general, the donor molecule is a fluorophore which has an absorption maximum at a shorter wavelength, can be excited selectively, and transfer the energy of an adsorbed photon non-radiatively to an acceptor molecule. The acceptor usually has an excitation λ_{\max} at the longer wavelength and with significant absorption overlap with the fluorescence emission envelop of donor. The result is that the energy of a photon absorbed by donor can be lost by fluorescence photon emission from donor or by radiationless transition to acceptor leading to photon emission from acceptor at a longer wavelength (other quenching processes are also possible) (Figure 3.74).

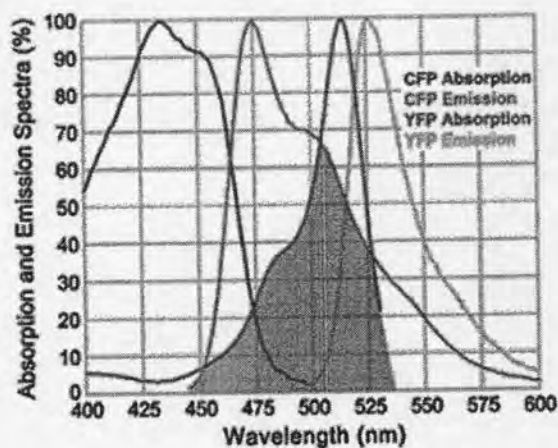


Figure 3.74 The diagram of absorption and emission spectra of the donor (purple and magenta) and the acceptor (green and yellow) at any wavelength. The overlap absorption between emission of the donor and absorption of the acceptor shown in green area.

The fluorophore, FAM (5-carboxy fluorescein), as a donor was introduced to the PNA sequence *cis*-D/D-APC Ac-T₄ATA-Lys-NH₂ (**P23**) at the amino group of the side chain of lysine residue. The FAM fluorophore has λ_{\max} at 520 nm, which overlap along with methyl red group (MeR), therefore the methyl red moiety was attached to

the duplex DNA probe as shown in **Figure 3.75**. The duplex DNA probes were designed for investigate the direction of binding of PNA·DNA hybrid as antiparallel and parallel probe. The reasons for using the duplex probe instead of single stranded probe is for prevent an undesired overlap interaction as described in **Section 3.4.4**.

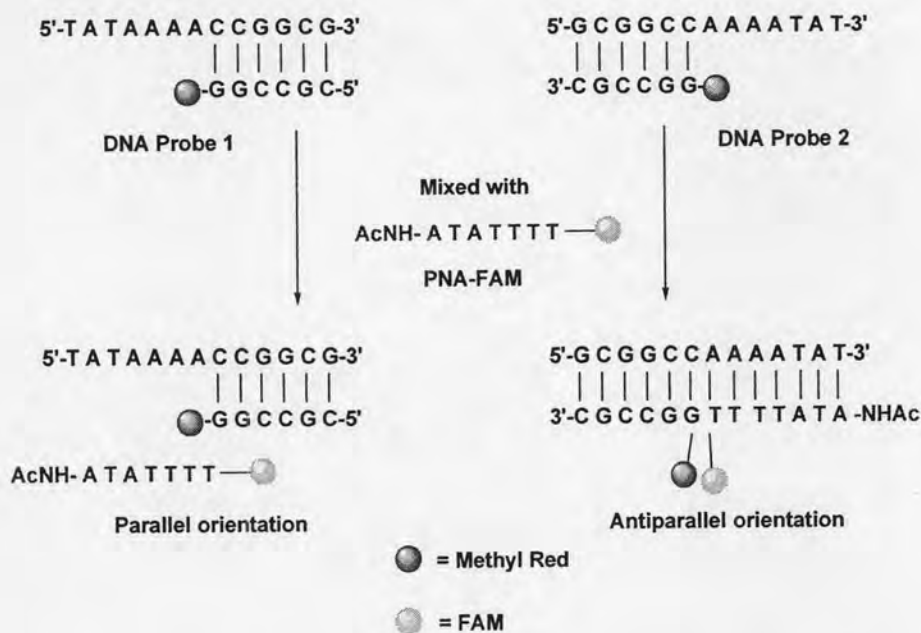
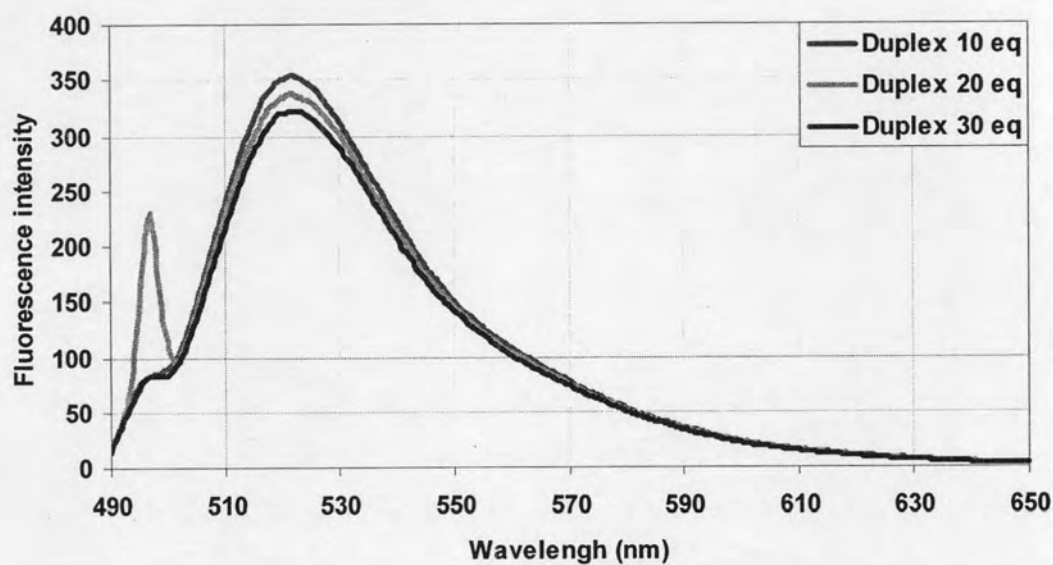


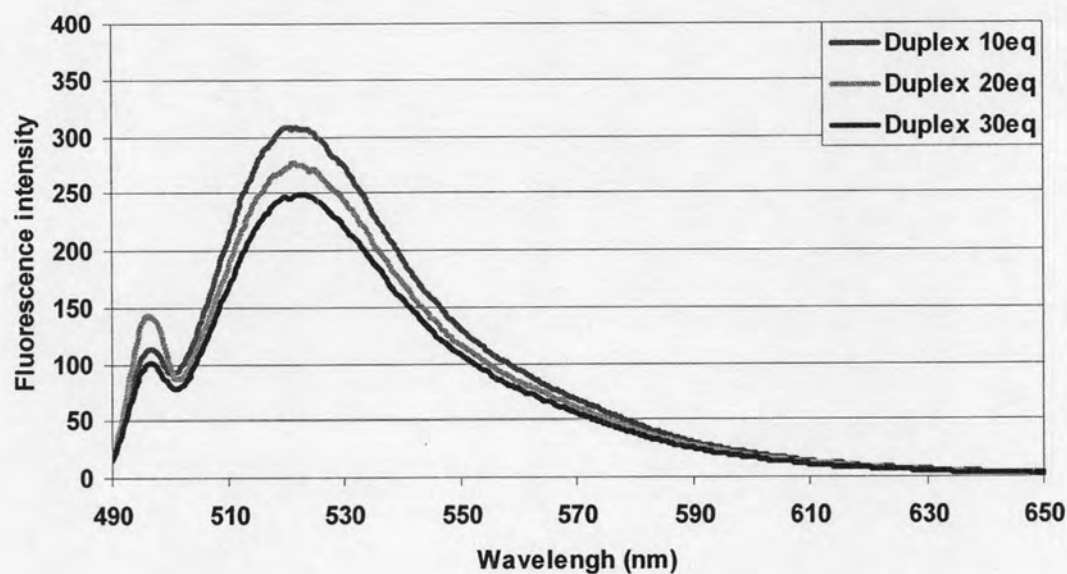
Figure 3.75 The duplex DNA probes for parallel and antiparallel binding with *cis*-D/D-APC Ac-T₄ATA-Lys(FAM)-NH₂ (**P23**).

This part of dissertation was studied at University of Southampton (UK) under guidance of Prof. Tom Brown as part of collaboration under Royal Golden Jubilee (RGJ PhD) program. The PNA sequences were synthesized as usual and after cleavage from resin, the crude PNA was dissolved in 0.5 M NaHCO₃ solution (50 μL) pH 9.0 and 5-carboxy fluorescein succinimidyl ester (1 mg) in DMSO (50 μL) was added to the crude PNA. The reaction was kept in the dark at rt for 24 h, then filtered through sephadex (NAP-10 column) G-25 medium for desalting and buffer exchange and purified by reverse phase HPLC. The fluorescence intensity measurement of this sequence with two DNA probes was operated, the DNA probe was added to the PNA solution in phosphate buffered (10 mM, pH 7.0) in three aliquots (10, 20 and 30 eq) and the fluorescence intensity of FAM was measured after each addition. The decrease of the intensity was observed at the selected wavelength (520 nm) as shown in **Figure 3.76**, the intensity decreases around 8% and 19% for parallel and

antiparallel binding. As a result, it can be explained that the MeR group in DNA probe will have the proper distance with the FAM group in PNA sequence provided the FRET phenomenon between these fluorophore. The FAM group releases the non-radiative energy to the quencher, consequently the drop of intensity was observed.



(a)



(b)

Figure 3.76 The fluorescence measurement of PNA (P23) and DNA probes (a) parallel binding (b) antiparallel binding.

Both the data from T_m and fluorescence experiments strongly suggested that the *cis*-D/D-APC PNA system favors forming antiparallel hybrid with DNA.